EUROPEAN ORGANISATION FOR NUCLEAR RESEARCH (CERN)

Submitted to: JHEP

CERN-EP-2016-271
13th December 2016

arXiv:1612.03636v1 [hep-ex] 12 Dec 2016

Measurements of top-quark pair to Z-boson cross-section ratios at $\sqrt{s} = 13, 8, 7$ TeV with the ATLAS detector

The ATLAS Collaboration

Ratios of top-quark pair to Z-boson cross sections measured from proton–proton collisions at the LHC centre-of-mass energies of $\sqrt{s} = 13$ TeV, 8 TeV, and 7 TeV are presented by the ATLAS Collaboration. Single ratios, at a given $\sqrt{s}$ for the two processes and at different $\sqrt{s}$ for each process, as well as double ratios of the two processes at different $\sqrt{s}$, are evaluated. The ratios are constructed using previously published ATLAS measurements of the $t\bar{t}$ and Z-boson production cross sections, corrected to a common phase space where required, and a new analysis of $Z \to \ell^+\ell^-$ where $\ell = e, \mu$ at $\sqrt{s} = 13$ TeV performed with data collected in 2015 with an integrated luminosity of 3.2 fb^{-1}. Correlations of systematic uncertainties are taken into account when evaluating the uncertainties in the ratios. The correlation model is also used to evaluate the combined cross section of the $Z \to e^+e^-$ and the $Z \to \mu^+\mu^-$ channels for each $\sqrt{s}$ value. The results are compared to calculations performed at next-to-next-to-leading-order accuracy using recent sets of parton distribution functions. The data demonstrate significant power to constrain the gluon distribution function for the Bjorken-x values near 0.1 and the light-quark sea for $x < 0.02$.

© 2016 CERN for the benefit of the ATLAS Collaboration.
Reproduction of this article or parts of it is allowed as specified in the CC-BY-4.0 license.

Contents

1 Introduction **3**

2 ATLAS detector **4**

3 Theoretical predictions **5**
3.1 Z-boson cross-section predictions 5
3.2 $t\bar{t}$ cross-section predictions 6
3.3 Predictions of ratios of cross sections 6

4 Analysis of $Z \to \ell^+\ell^-$ at $\sqrt{s} = 13$ TeV **8**
4.1 Data set and simulated event samples 8
4.2 Event selection 9
4.3 Background processes 10
4.4 Cross-section measurement and estimation of the systematic uncertainties 10
4.5 Cross-section results 11

5 Analysis of ratios **12**
5.1 Methodology 12
5.2 Inputs to the ratios 14
5.3 Correlation model 16
5.4 Results 18
5.4.1 Single ratios at a given $\sqrt{s}$ 18
5.4.2 Single ratios at different $\sqrt{s}$ 19
5.4.3 Double ratios 21
5.4.4 Correlated cross-section measurements 22
5.5 Quantitative comparison with predictions 23

6 Conclusion **28**

Appendix **30**

A Predictions involving Z-boson total cross sections **30**

B Acceptance factors and results in the Z-boson total phase space **31**

C Tables of results **31**

1 Introduction

Precision measurements of top-quark-pair [1–7] and Z-boson [8–15] production by the ATLAS [16] and CMS [17] collaborations at the CERN Large Hadron Collider (LHC) [18] provide important tests of the Standard Model (SM). The experimental precision of such measurements has reached the few-percent level in the case of the total $t\bar{t}$ production cross section, $\sigma_{t\bar{t}}^{\text{tot}}$, and the sub-percent level for the Z-boson production cross section with subsequent $Z \to \ell^+\ell^-$ decay within the fiducial region defined by the detector acceptance, σ_Z^{fid}. This experimental precision is complemented by an accurate determination of the proton–proton, pp, collision luminosity, which has reached a precision of approximately 2% [19, 20]. These measurements are compared with theoretical predictions performed at next-to-next-to-leading-order (NNLO) and next-to-next-to-leading-log (NNLL) accuracy in quantum chromodynamics (QCD) for $\sigma_{t\bar{t}}^{\text{tot}}$ [21–27] and at NNLO QCD plus next-to-leading-order (NLO) electroweak (EW) accuracy for σ_Z^{fid} [28–35]. Quantitative comparisons to the predictions can be used to impose constraints on a number of Standard Model parameters such as the parton distribution functions (PDF), the strong coupling constant (α_S) and the top-quark mass (m_t).

Further tests may be performed by examining the centre-of-mass-energy ($\sqrt{s}$) dependence of the cross sections. Top-quark-pair and Z-boson production at various $\sqrt{s}$ values sample different Bjorken-x regions, with higher energies sampling smaller average x. This dependence leads to a strong increase of the gluon-fusion-dominated $t\bar{t}$ production cross section with $\sqrt{s}$ while the increase of the $q\bar{q}$-dominated Z-boson production cross section is more moderate. However, the luminosity uncertainties associated with such measurements are dominated by effects uncorrelated between different centre-of-mass energies and data-taking periods, thereby limiting the precision with which cross sections measured at different $\sqrt{s}$ values can be directly compared.

The luminosity uncertainties as well as some of the experimental uncertainties can cancel when ratios of cross sections are evaluated. The predictions of the ratios of Z-boson production cross sections at different centre-of-mass energies are only moderately affected by PDF uncertainties, opening the possibility to use such measurements to cross-normalise other measurements made at different $\sqrt{s}$ values or in different running periods, as well as providing cross-checks on the corresponding integrated-luminosity ratios and their uncertainties.

Given that the $t\bar{t}$ and Z-boson production dynamics are driven to a large extent by different PDFs, the ratio of these cross sections at a given centre-of-mass energy has a significant sensitivity to the gluon-to-quark PDF ratio [36, 37]. Double ratios of $t\bar{t}$ to Z-boson cross sections, i.e. the ratio of the ratio of the two processes at two energies, provide sensitive tests of the Standard Model predictions which do not depend significantly on the determination of the luminosity.

This paper reports an evaluation of single ratios and double ratios of the $t\bar{t}$ and Z-boson[1] production cross sections at $\sqrt{s} = 13, 8, 7$ TeV. Previously published ATLAS results for $t\bar{t}$ and Z-boson production at $\sqrt{s} = 7$ and 8 TeV [1, 9, 10] as well as for $t\bar{t}$ production at $\sqrt{s} = 13$ TeV [2] are used in the evaluation. For the ratios involving 13 TeV data, a new analysis of $Z \to \ell^+\ell^-$, where $\ell = e, \mu$, is performed using the data collected in 2015 with an integrated luminosity of 3.2 fb^{-1}. This measurement uses the same methodology as a previous measurement performed at 13 TeV [11] but is specifically designed to be fully synchronised with the corresponding $t\bar{t}$ selection at the same energy. A detailed evaluation of the correlations of the systematic uncertainties for the different ATLAS results for the two processes and three centre-of-mass energies is performed, resulting in significant cancellations of some of the uncertainties

[1] Throughout this paper, Z/γ^*-boson production is denoted simply by Z-boson production.

in the ratios. The correlation model is also used to evaluate the combined cross section times branching ratios of the $Z \to e^+e^-$ and the $Z \to \mu^+\mu^-$ channels for each $\sqrt{s}$ value, and the resulting measurements are reported together with the corresponding correlation matrix. The data are compared to the state-of-the-art calculations performed at the highest-available order in perturbative theory, using several of the modern PDF sets. A quantitative study of projected PDF uncertainties with the inclusion of these results shows that the ATLAS measurements presented in this paper can have a significant impact in constraining the gluon and light-quark sea distributions.

The paper is organised as follows. The ATLAS detector is described in Section 2 and the theoretical predictions for the cross sections and their ratios are summarised in Section 3. Section 4 describes the new measurement of the Z-boson production cross section times the branching ratio for $Z \to \ell^+\ell^-$ at $\sqrt{s} = 13$ TeV. The cross-section single and double ratios as well as the combined cross sections, including full correlation information, are evaluated and compared to theoretical predictions in Section 5, and the ability of these data to further constrain the PDF distributions is discussed. Section 6 summarises the results obtained in the paper. An Appendix contains additional predictions that use the total rather than fiducial Z-boson cross sections and also presents all experimental results in tabular form.

2 ATLAS detector

The ATLAS detector [16] at the LHC is a multi-purpose particle detector with a forward-backward symmetric cylindrical geometry and a near 4π coverage in solid angle.[2] It consists of an inner tracking detector, electromagnetic and hadronic calorimeters, and a muon spectrometer.

The inner detector is surrounded by a thin superconducting solenoid magnet and includes silicon detectors, which provide precision tracking in the pseudorapidity range $|\eta| < 2.5$, and a transition-radiation tracker providing additional tracking and electron identification information for $|\eta| < 2.0$. For the $\sqrt{s} = 13$ TeV data-taking period, the inner detector also includes a silicon-pixel insertable B-layer [38], providing an additional layer of tracking information close to the interaction point. A lead/liquid-argon (LAr) electromagnetic calorimeter covers the region $|\eta| < 3.2$. Hadronic calorimetry is provided by a steel/scintillator-tile calorimeter for $|\eta| < 1.7$ and two copper/LAr hadronic endcap calorimeters for $1.5 < |\eta| < 3.2$. The forward region is covered by additional coarser-granularity LAr calorimeters up to $|\eta| = 4.9$. The muon spectrometer consists of three large superconducting toroids each containing eight coils, precision tracking chambers covering the region $|\eta| < 2.7$, and separate trigger chambers up to $|\eta| = 2.4$.

For the data taken at 7 and 8 TeV, a three-level trigger system was used. The first-level trigger is implemented in hardware and uses a subset of the detector information. This is followed by two software-based trigger levels that together reduce the accepted event rate to approximately 400 Hz. For the data taken at 13 TeV, the trigger was changed [39] to a two-level system, using custom hardware followed by a software-based level which runs offline reconstruction software, reducing the event rate to approximately 1 kHz.

[2] ATLAS uses a right-handed coordinate system with its origin at the nominal interaction point (IP) in the centre of the detector and the z-axis along the beam pipe. The x-axis points from the IP to the centre of the LHC ring, and the y-axis points upwards. Cylindrical coordinates (r, ϕ) are used in the transverse plane, ϕ being the azimuthal angle around the z-axis. The pseudorapidity is defined in terms of the polar angle θ as $\eta = -\ln\tan(\theta/2)$ and the rapidity is given by $y = \frac{1}{2}\ln\left(\frac{E+p_z}{E-p_z}\right)$, where E is the jet/particle energy and p_z is the z-component of the jet/particle momentum.

The data used in this paper were collected by the ATLAS detector in 2011, 2012, and 2015 and correspond to total integrated luminosities of 4.6, 20.2, and 3.2 fb^{-1} at $\sqrt{s} = 7, 8$, and 13 TeV, respectively.

3 Theoretical predictions

In this section, predictions are presented at NNLO+NNLL accuracy for the production cross section of a top-quark pair and at NNLO accuracy for the production cross section of a Z boson times the branching ratio of the decay into a lepton pair of flavour $\ell^+\ell^- = e^+e^-$ or $\mu^+\mu^-$ within the dilepton invariant mass range $66 < m_{\ell\ell} < 116$ GeV. The total cross sections for these processes, denoted respectively by $\sigma_{t\bar{t}}^{\text{tot}}$ and σ_Z^{tot}, are calculated for the centre-of-mass energies $\sqrt{s} = 13, 8, 7$ TeV. Also presented are predictions at NNLO accuracy for the Z-boson production cross section times the same branching ratio within a fiducial region defined by the detector acceptance, $\sigma_Z^{\text{fid}} = \sigma_Z^{\text{tot}} \cdot A$, where the acceptance factor A is expressed as the fraction of decays satisfying the matching fiducial acceptance (geometric and kinematic requirements) at the Monte Carlo generator level. The Z-boson fiducial phase space is defined by the lepton transverse momentum $p_{\text{T}}^{\ell} > 25$ GeV, the lepton pseudorapidity $|\eta_\ell| < 2.5$, and $66 < m_{\ell\ell} < 116$ GeV. Predictions of top-quark-pair fiducial cross sections are not yet available at NNLO accuracy.

3.1 Z-boson cross-section predictions

Theoretical predictions of the fiducial and total Z-boson production cross sections times the branching ratio of the decay into a lepton pair $Z \to \ell^+\ell^-$ at $\sqrt{s} = 13, 8, 7$ TeV are computed using a version of DYNNLO 1.5 [28, 29] optimised for speed of computation, for both the central values and all variations reflecting systematic uncertainties, thereby providing NNLO QCD calculations. Electroweak corrections at NLO, calculated with FEWZ 3.1 [30–33], are calculated in the G_μ EW scheme [40]. The cross sections are calculated for Z-boson decays into leptons at Born level, i.e. before the decay leptons emit photons via final-state radiation, to match the definition of the cross sections measured in data. Thus, the following components are included: virtual QED and weak corrections, initial-state radiation (ISR), and interference between ISR and FSR [41]. The NNLO PDFs CT14 [42], NNPDF3.0 [43], MMHT14 [44], ABM12 [45], HERAPDF2.0 [46], and ATLAS-epWZ12 [47] are used in the comparisons to data. The CT14 PDF set is used as the baseline for the predictions.

The systematic uncertainties in the predictions are dominated by the knowledge of proton PDFs. These uncertainties are obtained from the sum in quadrature of the differences between predictions obtained with the central PDF values and those obtained using the variations (eigenvectors) of the respective PDF sets. Where appropriate, asymmetric uncertainties are determined using separate sums of negative and positive variations. The CT14 uncertainties are rescaled from 90% to 68% confidence level (CL). The uncertainties due to the strong coupling constant are estimated following the prescription given with the CT14 PDF, varying α_{S} by ± 0.001 to correspond to 68% CL. The QCD scale uncertainties are defined by the envelope of variations in which the renormalisation (μ_{R}) and factorisation (μ_{F}) scales are changed by factors of two with an additional constraint of $0.5 \leq \mu_{\text{R}}/\mu_{\text{F}} \leq 2$. The dynamic scale $m_{\ell\ell}$ is used as the central value for the Z-boson predictions. The limitations in the NNLO calculations, referred to as the "intrinsic" uncertainties, are estimated by comparing the predictions calculated with the optimised version of DYNNLO 1.5 to the ones obtained with FEWZ 3.1. For the total cross-section predictions, these differences are found to be $< 0.2\%$ and hence are negligible. For the fiducial cross-section predictions, these differences are larger due to a feature of the calculations involving leptons with symmetric p_{T}

	σ_Z^{fid}			$\sigma_{t\bar{t}}^{\text{tot}}$		
$\sqrt{s}$ [TeV]	13	8	7	13	8	7
Central value [pb]	744	486	432	842	259	182
Uncertainties [%]						
PDF	$^{+2.7}_{-3.4}$	$^{+2.5}_{-3.1}$	$^{+2.5}_{-3.0}$	$^{+2.6}_{-2.7}$	$^{+3.9}_{-3.4}$	$^{+4.4}_{-3.7}$
α_S	$^{+0.9}_{-1.1}$	$^{+1.0}_{-0.8}$	$^{+1.0}_{-0.7}$	$^{+1.9}_{-1.8}$	$^{+2.1}_{-2.1}$	$^{+2.2}_{-2.1}$
Scale	$^{+0.5}_{-0.8}$	$^{+0.5}_{-0.5}$	$^{+0.7}_{-0.3}$	$^{+2.4}_{-3.6}$	$^{+2.6}_{-3.5}$	$^{+2.6}_{-3.5}$
Intrinsic Z	$^{+0.7}_{-0.7}$	$^{+0.7}_{-0.7}$	$^{+0.7}_{-0.7}$	N/A	N/A	N/A
m_t	N/A	N/A	N/A	$^{+2.8}_{-2.7}$	$^{+3.0}_{-2.9}$	$^{+3.1}_{-3.0}$
Total	$^{+3.0}_{-3.7}$	$^{+2.8}_{-3.3}$	$^{+2.9}_{-3.2}$	$^{+5}_{-6}$	$^{+6}_{-6}$	$^{+6}_{-6}$

Table 1: Predictions of the fiducial cross section, σ_Z^{fid}, and the total cross section, $\sigma_{t\bar{t}}^{\text{tot}}$, at $\sqrt{s} = 13, 8, 7$ TeV using the CT14 PDF. The uncertainties, given in %, correspond to variations of: CT14 eigenvector set at 68% CL, α_S, QCD scale, intrinsic Z-boson prediction, and top-quark mass, as described in the text. The statistical uncertainties in the predictions are ≤ 1 pb for the Z boson and ≤ 0.1 pb for $t\bar{t}$ and are not given in the table. The notation N/A means "not applicable".

requirements, resulting in consistently larger values from FEWZ. The differences are calculated using the CT14 PDF to obtain the central value in both cases, and are approximately 0.7% at all three $\sqrt{s}$ values.

The predictions of the fiducial cross sections, together with their uncertainties, are given in Table 1 while the predictions of the total cross sections are given in Table 13 of Appendix A.

3.2 $t\bar{t}$ cross-section predictions

Theoretical predictions [21–26] of the total $t\bar{t}$ production cross sections at $\sqrt{s} = 13, 8, 7$ TeV are computed using Top++v2.0 [27] for the central values and for all variations reflecting systematic uncertainties, thereby providing NNLO+NNLL resummed QCD calculations. The systematic uncertainties in the predictions are performed as for those of the Z boson, with the following exceptions. Since there is no alternative calculation of the NNLO $t\bar{t}$ cross section available, no intrinsic uncertainty is assigned to its cross-section prediction. It was verified that the code Hathor v1.5 [48], which implements the exact NNLO $t\bar{t}$ cross sections, matches the results obtained with Top++v2.0. The $t\bar{t}$ production cross section also has a significant dependence on the value of the top-quark mass, m_t. A systematic uncertainty is assessed by varying the mass of the top quark by ± 1 GeV from the baseline value of 172.5 GeV used to obtain the central value of the predictions, resulting in an uncertainty in the cross section of approximately 3%. The predictions of the total cross sections, together with their uncertainties, are given in Table 1.

3.3 Predictions of ratios of cross sections

The Z-boson cross-section measurements made in a fiducial phase space require only a small extrapolation from the experimental phase space and hence benefit from significantly reduced theoretical uncertainties in comparison to the measurements extrapolated to the total phase space. For this reason, the

	$R^{\text{fid}}_{Z_i/Z_j}$			$R^{\text{tot}}_{t\bar{t}_i/t\bar{t}_j}$		
i/j	13/7	13/8	8/7	13/7	13/8	8/7
Central value	1.722	1.531	1.125	4.634	3.251	1.425
Uncertainties [%]						
PDF	$^{+1.0}_{-0.9}$	$^{+0.8}_{-0.7}$	$^{+0.22}_{-0.21}$	$^{+1.9}_{-2.3}$	$^{+1.4}_{-1.8}$	$^{+0.5}_{-0.6}$
α_S	$^{-0.1}_{-0.4}$	$^{-0.1}_{-0.3}$	$^{-0.1}_{-0.1}$	$^{-0.32}_{+0.29}$	$^{-0.25}_{+0.22}$	$^{-0.08}_{+0.07}$
Scale	$^{+0.03}_{-0.60}$	$^{+0.02}_{-0.29}$	$^{+0.02}_{-0.31}$	$^{+0.19}_{-0.26}$	$^{+0.13}_{-0.19}$	$^{+0.05}_{-0.07}$
m_t	N/A	N/A	N/A	$^{+0.29}_{-0.29}$	$^{+0.22}_{-0.22}$	$^{+0.07}_{-0.07}$
Total	$^{+1.0}_{-1.2}$	$^{+0.8}_{-0.8}$	$^{+0.22}_{-0.40}$	$^{+1.9}_{-2.4}$	$^{+1.4}_{-1.8}$	$^{+0.5}_{-0.6}$

Table 2: Predictions of the cross-section ratios $R^{\text{fid}}_{Z_i/Z_j}$ and $R^{\text{tot}}_{t\bar{t}_i/t\bar{t}_j}$ at the different $\sqrt{s}$ values where $i/j = 13/7, 13/8,$ and $8/7$ using the CT14 PDF. The uncertainties, given in %, correspond to variations of: CT14 eigenvector set at 68% CL, α_S, and QCD scale, as described in the text. The statistical uncertainties in the predictions are ≤ 0.002 for the Z process and ≤ 0.001 for the $t\bar{t}$ process and are not given in the table. The notation N/A means "not applicable".

Z-boson fiducial cross sections are primarily used in the measurements of the cross-section ratios. The predictions given in Table 1 are used to build cross-section ratios for

- a given process at the different $\sqrt{s}$: $R^{\text{fid}}_{Z_i/Z_j} = \sigma^{\text{fid}}_{Z(i\text{TeV})}/\sigma^{\text{fid}}_{Z(j\text{TeV})}$ and $R^{\text{tot}}_{t\bar{t}_i/t\bar{t}_j} = \sigma^{\text{tot}}_{t\bar{t}(i\text{TeV})}/\sigma^{\text{tot}}_{t\bar{t}(j\text{TeV})}$,
- different processes at the same $\sqrt{s}$: $R^{\text{tot/fid}}_{t\bar{t}/Z}(i\text{ TeV}) = \sigma^{\text{tot}}_{t\bar{t}(i\text{TeV})}/\sigma^{\text{fid}}_{Z(i\text{TeV})}$,
- different processes at the different $\sqrt{s}$: $R^{\text{tot/fid}}_{t\bar{t}/Z}(i/j) = \left[\sigma^{\text{tot}}_{t\bar{t}(i\text{TeV})}/\sigma^{\text{fid}}_{Z(i\text{TeV})}\right] / \left[\sigma^{\text{tot}}_{t\bar{t}(j\text{TeV})}/\sigma^{\text{fid}}_{Z(j\text{TeV})}\right]$ denoted in this paper as double ratios,

where $i, j = 13, 8, 7$. The first set of predictions is presented in Table 2 while the latter two are presented in Table 3. The corresponding ratios using the total Z-boson production cross sections rather than the fiducial ones are given in Tables 13 and 14 of Appendix A.

The choice of correlation model when combining the theoretical uncertainties in the ratios in not unique. For this paper, the treatment of the systematic uncertainties is taken as follows. The PDF uncertainties are considered as correlated, eigenvector by eigenvector, between predictions. The QCD scale uncertainties are treated as uncorrelated between processes but correlated, variation by variation, at the different $\sqrt{s}$ values for a given process. The α_S uncertainties are correlated between predictions. The Z-boson intrinsic and m_t uncertainties are both considered as correlated at the different $\sqrt{s}$ values within their respective processes. In the few cases where the coherent variation of a source of systematic uncertainty in the numerator and in the denominator of a ratio results in variations of the same sign, only the largest variation is added in the total uncertainty of the corresponding sign.

	$R^{\text{tot/fid}}_{t\bar{t}/Z}(i\text{ TeV})$			$R^{\text{tot/fid}}_{t\bar{t}/Z}(i/j)$		
i or i/j	13	8	7	13/7	13/8	8/7
Central value	1.132	0.533	0.421	2.691	2.124	1.267
Uncertainties [%]						
PDF	$^{+6}_{-5}$	$^{+7}_{-5}$	$^{+7}_{-5}$	$^{+1.5}_{-2.0}$	$^{+1.1}_{-1.6}$	$^{+0.4}_{-0.5}$
α_S	$^{+0.9}_{-0.8}$	$^{+1.1}_{-1.3}$	$^{+1.1}_{-1.5}$	$^{-0.22}_{+0.70}$	$^{-0.22}_{+0.50}$	$^{-0.00}_{+0.20}$
Scale	$^{+2.6}_{-3.6}$	$^{+2.6}_{-3.5}$	$^{+2.7}_{-3.6}$	$^{+0.62}_{-0.27}$	$^{+0.32}_{-0.20}$	$^{+0.31}_{-0.07}$
Intrinsic Z	$^{+0.7}_{-0.7}$	$^{+0.7}_{-0.7}$	$^{+0.7}_{-0.7}$	$^{+0.00}_{-0.00}$	$^{+0.00}_{-0.00}$	$^{+0.00}_{-0.00}$
m_t	$^{+2.8}_{-2.7}$	$^{+3.0}_{-2.9}$	$^{+3.1}_{-3.0}$	$^{+0.29}_{-0.29}$	$^{+0.22}_{-0.22}$	$^{+0.07}_{-0.07}$
Total	$^{+7}_{-7}$	$^{+8}_{-7}$	$^{+8}_{-7}$	$^{+1.8}_{-2.1}$	$^{+1.3}_{-1.6}$	$^{+0.5}_{-0.5}$

Table 3: Predictions of the cross-section ratios $R^{\text{tot/fid}}_{t\bar{t}/Z}(i\text{ TeV})$ and $R^{\text{tot/fid}}_{t\bar{t}/Z}(i/j)$ at the different $\sqrt{s}$ values where $i, j = 13, 8, 7$ using the CT14 PDF. The uncertainties, given in %, correspond to variations of: CT14 eigenvector set at 68% CL, α_S, QCD scale, intrinsic Z-boson prediction, and top-quark mass, as described in the text. The statistical uncertainties in the predictions are ≤ 0.001 for $R^{\text{tot/fid}}_{t\bar{t}/Z}(i\text{ TeV})$ and ≤ 0.003 for $R^{\text{tot/fid}}_{t\bar{t}/Z}(i/j)$ and are not given in the table.

4 Analysis of $Z \to \ell^+\ell^-$ at $\sqrt{s} = 13$ TeV

4.1 Data set and simulated event samples

The data sets used in this analysis of $Z \to \ell^+\ell^-$ at $\sqrt{s} = 13$ TeV were collected by the ATLAS detector during the period of August to November 2015. During this period, the LHC circulated 6.5 TeV proton beams with a 25 ns bunch spacing. The peak delivered instantaneous luminosity was $\mathcal{L} = 5 \times 10^{33}\,\text{cm}^{-2}\,\text{s}^{-1}$ and the mean number of pp interactions per bunch crossing (hard scattering and pile-up events) was $\langle\mu\rangle = 13$. The data set corresponds to a total integrated luminosity of 3.2 fb^{-1}.

Monte Carlo simulations are used to evaluate the selection efficiency for signal events and the contribution of several background processes to the analysed data set. All of the samples are processed with the GEANT4-based simulation [49] of the ATLAS detector [50].

Events containing a Z boson decaying to a lepton pair, $Z \to \ell^+\ell^-$ where $\ell = e, \mu, \tau$, and events from the leptonic decay of W bosons are generated with the POWHEG-Box v2 Monte Carlo program [51–55] interfaced to the PYTHIA 8.186 [56] parton shower model. The CT10 PDF set [57] is used in the matrix element and the AZNLO [58] set of generator-parameter values (tune) is used, with the CTEQ6L1 [59] PDF set, for the modelling of non-perturbative effects. The EvtGen v.1.2.0 program [60] is used for properties of the bottom and charm hadron decays, and PHOTOS++ version 3.52 [61, 62] is used for QED emissions from electroweak vertices and charged leptons. Samples of top-quark pairs are generated with the POWHEG-Box v2 generator, which uses the four-flavour scheme for the NLO matrix element calculations together with the fixed four-flavour PDF set CT10f4. The top-quark-spin correlations are preserved in these samples and the top-quark mass is set to 172.5 GeV. The parton shower, fragmentation, and underlying event are simulated using PYTHIA 6.428 [63] with the CTEQ6L1 PDF set and the corresponding Perugia 2012 tune (P2012) [64]. The EvtGen v1.2.0 program is used for properties of the bottom and charm hadron decays. Diboson processes are simulated using the SHERPA v2.1.1 generator [65]. Multiple

overlaid pp collisions are simulated with the soft QCD processes of Pythia v.8.186 using the A2 tune [66] and the MSTW2008LO PDF [67].

The Monte Carlo events are reweighted so that the μ distribution matches the one observed in the data. Correction factors are applied to the simulated events to account for the differences observed between the data and MC simulation in the trigger, identification, reconstruction, and isolation efficiencies for the selected electron and muon candidates. Electron-energy- and muon-momentum-calibration corrections are applied as well.

For the comparison to the data distributions, the signal MC simulations are normalised to the cross sections measured by this analysis. The remaining simulations are normalised to the predictions of the highest-order available QCD calculations, with uncertainties of 5% for the single-boson processes and 6% for the diboson and top-quark processes.

4.2 Event selection

The selections of electron and muon candidates from the decay of the Z boson are designed to be fully synchronised to the $t\bar{t}$ selection at 13 TeV [2] e.g. using the same lepton trigger, identification, and kinematical requirements on the same data set.

Candidate events are selected using triggers which require at least one electron or muon to exceed transverse momentum thresholds of $p_{\mathrm{T}} = 24\,\mathrm{GeV}$ or 20 GeV, respectively, with some isolation requirements for the muon trigger. To recover possible efficiency losses at high momenta, additional electron triggers with thresholds of $p_{\mathrm{T}} \geq 60\,\mathrm{GeV}$ and a muon trigger with a threshold of $p_{\mathrm{T}} = 50\,\mathrm{GeV}$ are included. Candidate events are required to have a primary vertex, defined as the vertex with the highest sum of track p_{T}^2, with at least two associated tracks with $p_{\mathrm{T}} > 400\,\mathrm{MeV}$.

Electron candidates are required to have $p_{\mathrm{T}} > 25\,\mathrm{GeV}$ and to pass "medium" likelihood-based identification requirements [68] optimised for the 2015 operating conditions, within the fiducial region $|\eta| < 2.47$, excluding candidates in the transition region between the barrel and endcap electromagnetic calorimeters, $1.37 < |\eta| < 1.52$. Muon candidates are considered for $|\eta| < 2.4$ with $p_{\mathrm{T}} > 25\,\mathrm{GeV}$ and must pass "medium" identification requirements [69] also optimised for the 2015 operating conditions. At least one of the lepton candidates is required to match the lepton that triggered the event. The electron and muon candidates must also satisfy p_{T}-dependent cone-based isolation requirements, using tracking detector and calorimeter information described in Refs. [70, 71], respectively. The isolation requirements are tuned so that the lepton-isolation efficiency is at least 90% for $p_{\mathrm{T}} > 25\,\mathrm{GeV}$, increasing to 99% at 60 GeV. Both the electron and muon tracks are required to be associated with the primary vertex, using constraints on the transverse impact-parameter significance, $|d_0|/\delta d_0$, where d_0 is the transverse impact parameter and δd_0 is its uncertainty, and on the longitudinal impact parameter, z_0, corrected for the reconstructed position of the primary vertex. The transverse impact-parameter significance is required to be less than five for electrons and three for muons, while the absolute value of the corrected z_0 multiplied by the sine of the track polar angle is required to be less than 0.5 mm.

Events containing a Z-boson candidate are chosen by requiring exactly two selected leptons of the same flavour but of opposite charge with an invariant mass of $66 < m_{\ell\ell} < 116\,\mathrm{GeV}$. A total of 1,367,026 candidates and 1,735,197 candidates pass all requirements in the electron and muon channels, respectively.

4.3 Background processes

Contributions from the single-boson ($W \to \ell\nu$ and $Z \to \tau^+\tau^-$), diboson, and top-quark-pair components of the background are estimated from the Monte Carlo samples described in Section 4.1. The $Z \to \tau^+\tau^-$ process with the subsequent leptonic decay of the τ is treated as a background.

Events involving semileptonic decays of heavy quarks, hadrons misidentified as leptons, and, in the case of the electron channel, electrons from photon conversions (all referred to collectively as "multijet" events) are a minor background in this analysis. The multijet background is estimated in both channels using data-driven methods. The transverse impact-parameter distribution d_0 times the value of the charge of the lepton, to take into account the direction of photon radiation, is used in a template fit in the region where the transverse impact-parameter requirement is inverted. The contribution of multijet events to the event selection in both channels is found to be $< 0.1\%$ and therefore is neglected in the calculation of the central value of the cross section but contributes 0.05% to the cross-section uncertainty.

The total background event rate contributing to the $Z \to \ell^+\ell^-$ selection in both channels is approximately 0.5%, dominated by $t\bar{t}$ production while the sum of all electroweak backgrounds is 0.2%.

4.4 Cross-section measurement and estimation of the systematic uncertainties

The methodology for the evaluation of the inclusive fiducial cross section is the same as in previous ATLAS publications [10, 11]. The fiducial production cross section of a Z boson times the branching ratio of the decay of the Z boson into a lepton pair of flavour $\ell^+\ell^- = e^+e^-$ or $\mu^+\mu^-$ can be expressed as a ratio of the numbers of background-subtracted data events N to the product of the integrated luminosity of the data $\mathcal{L}$ and a correction factor C:

$$\sigma_Z^{\text{fid}} = \frac{N}{\mathcal{L} \cdot C}. \tag{1}$$

The correction factor C is the ratio of the total number of simulated events which pass the final Z-boson selection requirements after reconstruction to the total number of simulated events within the fiducial acceptance defined in Section 3. This factor, defined at Born level, includes the efficiencies for triggering on, reconstructing, and identifying the Z-boson decay products within the acceptance, and also accounts for the slight difference between the fiducial and reconstructed phase spaces. The contribution from the $Z \to \tau^+\tau^-$ process with the subsequent leptonic decay of the τ is considered as a background and is not part of the fiducial definition. The total cross section, evaluated by extrapolating to the full phase space by use of the acceptance factor A ($\sigma_Z^{\text{tot}} = \sigma_Z^{\text{fid}}/A$), is further elaborated in Appendix B.

The experimental systematic uncertainties in the measurements of the cross section enter via the evaluation of the correction factor and the luminosity in the denominator of Eq. (1), as well as through the estimation of the background subtracted from the candidate events in its numerator.

The sources of systematic uncertainties in the correction factors C, summarised in Table 4, are as follows.

- *Trigger:* The lepton trigger efficiency is estimated in simulation, with a dedicated data-driven analysis performed to obtain the simulation-to-data trigger correction factors and the corresponding uncertainties.

- *Reconstruction, identification, and isolation:* The lepton selection efficiencies as determined from simulation are corrected with simulation-to-data correction factors and their associated uncertainties [68, 69].
- *Energy, momentum scale/resolution:* Uncertainties in the lepton calibrations [69] are assessed as they can cause a change of acceptance because of migration of events across the p_{T} threshold and $m_{\ell\ell}$ boundaries.
- *Charge identification:* Electron charge misidentification may occur when electrons radiate in the inner regions in the detector and the resulting photons subsequently convert and are reconstructed as high-p_{T} tracks. A particle with reconstructed charge opposite to the parent electron may then be accidentally associated with the energy deposit in the calorimeter. The effect of electrons having their charge misidentified is studied [11] using a control sample of $Z \to e^{+}e^{-}$ events in which both electrons are reconstructed with the same charge and is found to be well described by the Monte Carlo simulation, within the statistical uncertainty of the control sample. An uncertainty is assessed to cover any small residual differences between data and simulation. The probability of charge misidentification is negligible in the muon channel.
- *Pile-up:* Incorrect modelling of pile-up effects can lead to acceptance changes and is accounted for with dedicated studies.
- *PDF:* The impact of the PDF uncertainty is estimated by propagating NNPDF3.0 PDF variations to the correction factor.
- $p_T^{\ell\ell}$ *mismodelling:* Mismodelling in the simulation at high dilepton transverse momentum, $p_{\mathrm{T}}^{\ell\ell}$, has been studied in detail in the context of a $\sqrt{s}$ = 8 TeV Z-boson analysis [10]. The effect is estimated here by reweighting the simulated $p_{\mathrm{T}}^{\ell\ell}$ distribution to a fourth-order polynomial derived from a fit to the corresponding data distribution. It has a small impact on the measured fiducial cross section, as established in a previous Z-boson cross-section analysis at 13 TeV [11] and confirmed for this paper.

The systematic uncertainties from the background estimation contribute negligibly to the experimental cross-section uncertainty. The cross sections have a 2.1% uncertainty in the measurement of the integrated luminosity, which is derived, following a methodology similar to that detailed in Refs. [19, 20], from a preliminary calibration of the luminosity scale using a pair of x–y beam separation scans performed in August 2015. Finally, there exists an uncertainty related to knowledge of the beam energy, taken as 0.66% of the beam-energy value [72], and propagated to the cross section with the VRAP 0.9 program [73]. Apart from the determination of the luminosity, the dominant experimental systematic uncertainties in the cross-section evaluations are the lepton reconstruction and identification efficiencies.

4.5 Cross-section results

Distributions of the lepton η and p_{T}, and of the dilepton p_{T} and invariant mass after applying all selection criteria are shown in Figures 1 and 2. Good agreement between data and simulation is observed in the lepton η and in the dilepton invariant-mass distributions. As can be seen from the figure, agreement is also achieved in the lepton p_{T} distribution after reweighting the simulated dilepton transverse momentum, $p_{\mathrm{T}}^{\ell\ell}$, to the data, as explained in Section 4.4.

$\delta C/C$ [%]	$Z \to e^+e^-$	$Z \to \mu^+\mu^-$
Lepton trigger	< 0.1	0.1
Lepton reconstruction, identification	0.4	0.7
Lepton isolation	0.1	0.4
Lepton scale and resolution	0.2	0.1
Charge identification	0.1	–
Pile-up modelling	< 0.1	< 0.1
PDF	0.1	< 0.1
$p_{\mathrm{T}}^{\ell\ell}$ mismodelling	0.1	< 0.1
Total	0.5	0.8

Table 4: Relative systematic uncertainties, in %, in the correction factors C in the electron and muon channels.

	$Z \to e^+e^-$	$Z \to \mu^+\mu^-$
Events	$1,360,680 \pm 1170$ (stat) ± 760 (syst) ± 130 (lumi)	$1,727,700 \pm 1320$ (stat) ± 950 (syst) ± 160 (lumi)
C	0.554 ± 0.003 (tot)	0.706 ± 0.006 (tot)
σ_Z^{fid} [pb]	778 ± 1 (stat) ± 4 (syst) ± 5 (beam) ± 16 (lumi)	774 ± 1 (stat) ± 6 (syst) ± 5 (beam) ± 16 (lumi)

Table 5: The observed numbers of signal events after background subtraction are shown for the electron and muon channels along with the correction factors C and the Z-boson fiducial cross sections. The statistical, systematic, beam-energy, and luminosity uncertainties are quoted in that order except for the C factor where the total uncertainty is quoted.

All elements necessary to calculate the cross sections for Z-boson production and decay in the electron and muon channels with 3.2 fb^{-1} of data are summarised in Table 5. The measured fiducial cross sections are also presented in this table, along with their statistical, experimental systematic, luminosity, and beam-energy uncertainties, except for the C factor where the total uncertainty is quoted. The fiducial phase space for this measurement is presented in Section 3. These numbers are in agreement, within experimental systematic uncertainties, with the previous ATLAS measurement [11] of Z-boson production in the combined electron and muon channels in the same fiducial phase space and which uses an independent data set at $\sqrt{s} = 13$ TeV: 779 ± 3 (stat) ± 6 (syst) ± 16 (lumi) pb. The results are also compatible with the NNLO prediction shown in Section 3.1 of 744^{+22}_{-28} (tot) pb.

5 Analysis of ratios

5.1 Methodology

The following ratios are considered in this section: $R^{\mathrm{fid}}_{Z_i/Z_j}$, $R^{\mathrm{tot}}_{t\bar{t}_i/t\bar{t}_j}$, $R^{\mathrm{tot/fid}}_{t\bar{t}/Z}(i\text{ TeV})$, and $R^{\mathrm{tot/fid}}_{t\bar{t}/Z}(i/j)$ where $i, j = 13, 8, 7$ and $i \neq j$. The corresponding ratios using the Z-boson total cross section are reported in Appendix C. Ratios using fiducial $t\bar{t}$ cross sections are also reported in Appendix C, although there are no NNLO calculations available yet for $t\bar{t}$ production cross sections with requirements on the final-state leptons.

For the evaluation of the $t\bar{t}/Z$ ratios, $R_{t\bar{t}/Z}$, the Z-boson cross sections from the electron and muon channels

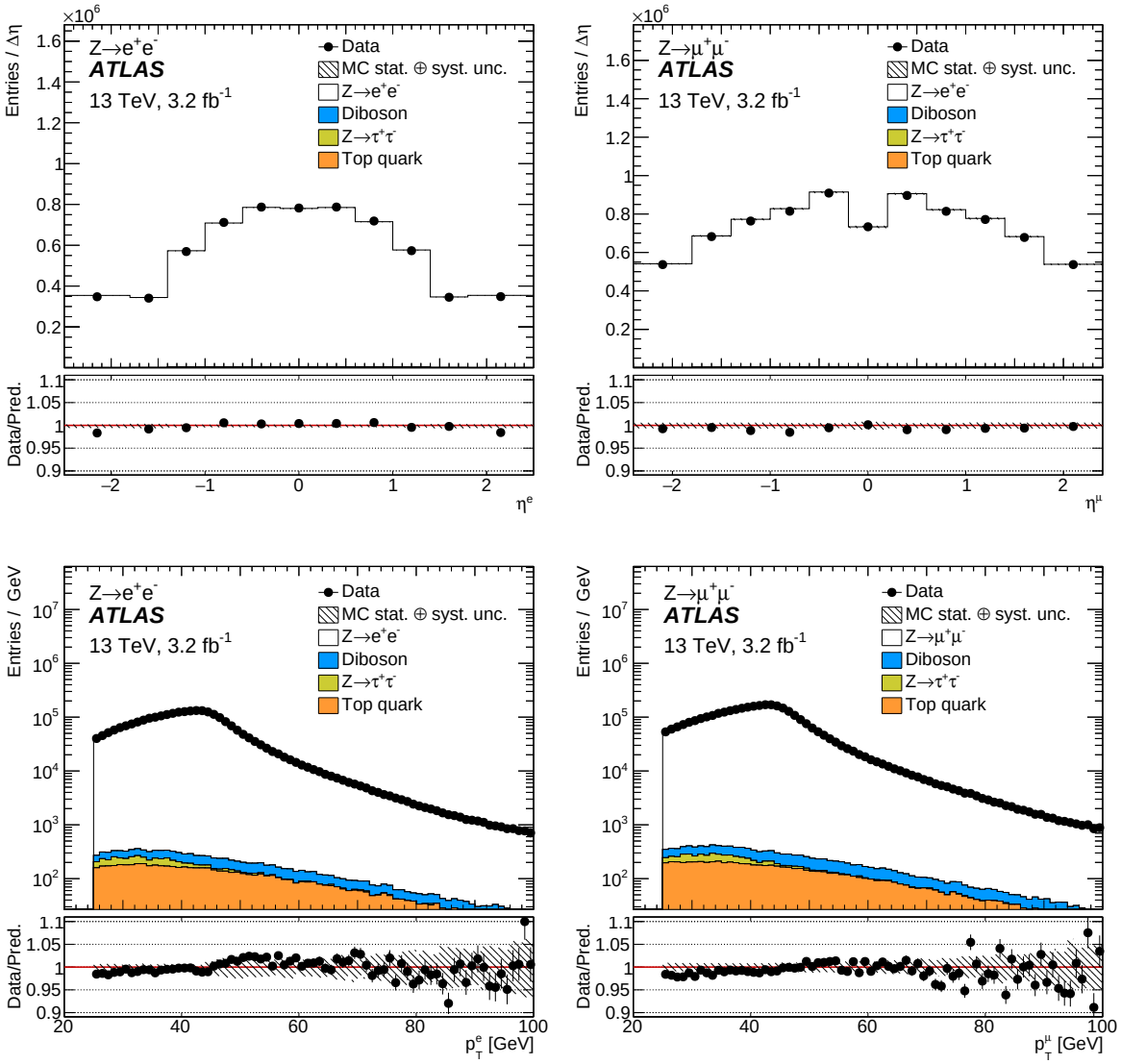

Figure 1: Lepton pseudorapidity (top) and transverse momentum (bottom) distributions from the $Z \to e^+e^-$ selection (left) and the $Z \to \mu^+\mu^-$ selection (right). Due to the unequal bin widths used in the lepton pseudorapidity distributions, these distributions are plotted divided by the bin width. The background processes are heavily suppressed and not visible on the linear scale. The systematic uncertainties for the signal and background distributions are combined in the shaded band, while the statistical uncertainty is shown on the data points. The luminosity uncertainties are not included. There are two lepton entries in the histogram for each candidate event.

are both employed and taken with the same weight in the ratio, i.e.

$$R_{t\bar{t}/Z} = \frac{\sigma_{t\bar{t}}}{0.5\left(\sigma_{Z\to ee} + \sigma_{Z\to\mu\mu}\right)} \tag{2}$$

since the $t\bar{t}$ production cross section is measured from the electron and muon pair final state topology. This ensures the best cancellation of important systematic uncertainties related to lepton reconstruction, identification, and trigger. For other ratios involving Z bosons, the $Z \to e^+e^-$ and $Z \to \mu^+\mu^-$ results are combined (Section 5.4.4 describes the results of the combination) using the code described in Refs. [74,

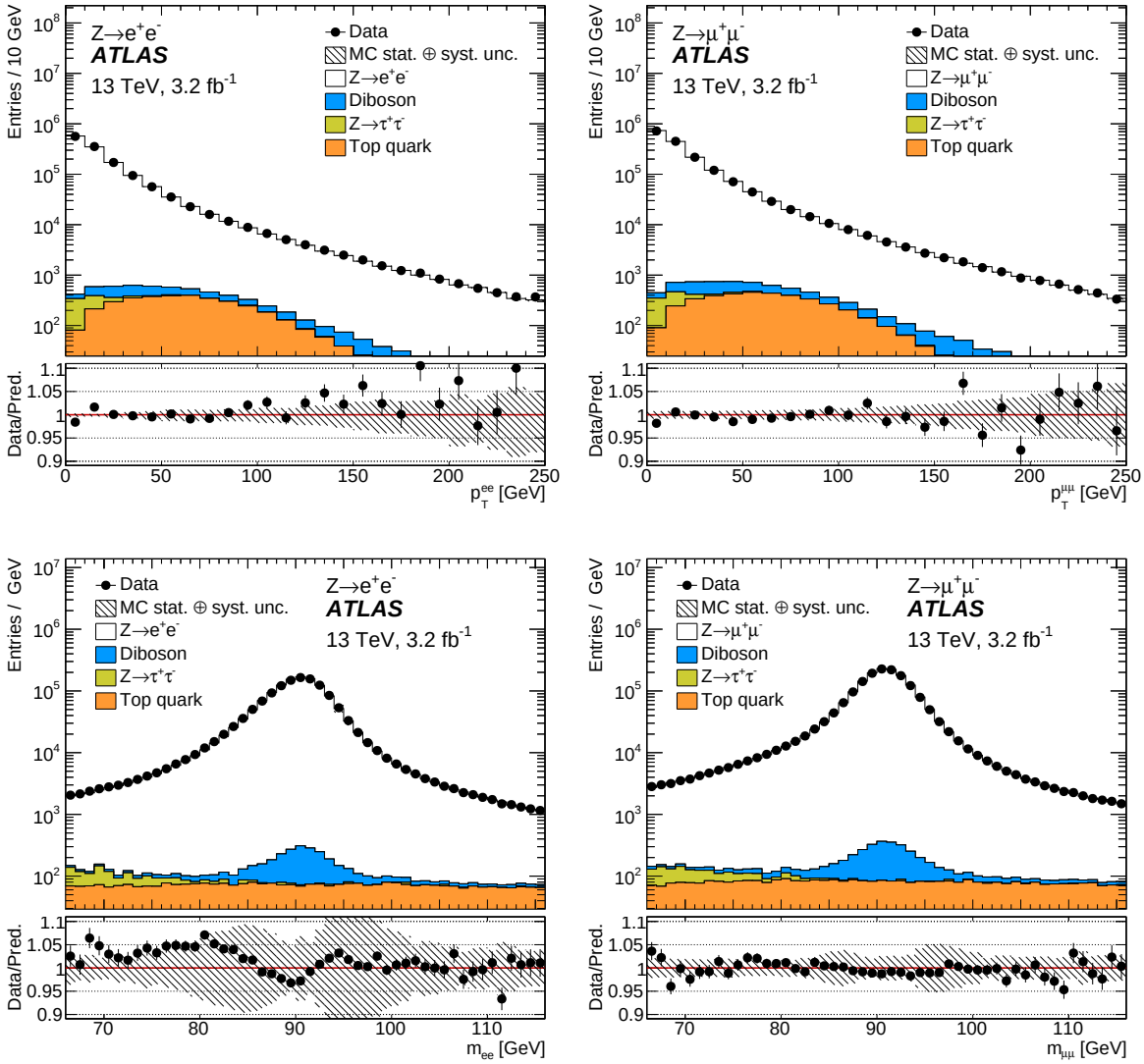

Figure 2: Dilepton transverse momentum (top) and invariant mass (bottom) distributions from the $Z \to e^+e^-$ selection (left) and the $Z \to \mu^+\mu^-$ selection (right). The systematic uncertainties for the signal and background distributions are combined in the shaded band, while the statistical uncertainty is shown on the data points. The luminosity uncertainties are not included.

75], taking into account correlations of systematic uncertainties across channels and $\sqrt{s}$.

5.2 Inputs to the ratios

The primary inputs to the ratios are the Z-boson and $t\bar{t}$ production cross sections at 13, 8, 7 TeV [1, 2, 8, 9], each obtained with its own experimental selection criteria, measured within an experimental phase space, and reported in a corresponding fiducial phase space or in the total phase space. The event topologies of the two processes are independent of the centre-of-mass energy. The Z-boson selections target two isolated, same-flavour, opposite-charge reconstructed leptons, identified as electrons or muons, whose

$\sqrt{s}$ [TeV]	13	8	7
$p_{\mathrm{T}}^{\ell} >$	25 GeV	20 GeV	20 GeV
$\lvert\eta_{\ell}\rvert <$	2.5	2.4	2.5
$\lvert y_{\ell\ell}\rvert <$	-	2.4	-
$m_{\ell\ell}$	66–116 GeV	66–116 GeV	66–116 GeV
Extrapolation E	-	0.941 ± 0.001 (PDF)	0.898 ± 0.001 (PDF)

Table 6: Z-boson fiducial definition at $\sqrt{s} = 13, 8, 7$ TeV. The ratios measured in this analysis are calculated in the 13 TeV phase space for all $\sqrt{s}$. The factor E is used to extrapolate the 7 and 8 TeV results to the common phase space defined by the 13 TeV results. The PDF uncertainty is obtained from the CT14 eigenvector set.

	$\sigma \pm$ stat $\pm$ syst [pb]		
$\sqrt{s}$ [TeV]	13	8	7
$\sigma^{\mathrm{fid}}_{Z\to ee}$	778.3 ± 0.7 ± 17.7	507.0 ± 0.2 ± 11.0	451.2 ± 0.5 ± 8.7
$\sigma^{\mathrm{fid}}_{Z\to \mu\mu}$	774.4 ± 0.6 ± 18.2	504.7 ± 0.2 ± 10.8	450.0 ± 0.3 ± 8.8
$\sigma^{\mathrm{fid}}_{t\bar{t}\to e\mu+X}$	9.94 ± 0.09 ± 0.37	3.04 ± 0.02 ± 0.10	2.30 ± 0.04 ± 0.08
$\sigma^{\mathrm{tot}}_{t\bar{t}}$	818 ± 8 ± 35	243 ± 2 ± 9	183 ± 3 ± 6

Table 7: Fiducial and total cross sections at $\sqrt{s} = 13, 8, 7$ TeV that form the primary input to the cross-section ratios. The Z-boson cross sections are provided in the common 13 TeV phase space. The systematic uncertainties include experimental, luminosity, beam-energy, and some theoretical uncertainties (see text).

dilepton invariant mass is consistent with that of a Z boson. The $t\bar{t}$ topology specific to this paper is that of an opposite-charge, isolated electron and muon pair, and additional jets tagged as containing b-hadrons. Although the $t\bar{t}$ fiducial phase space has remained unchanged at $13, 8, 7$ TeV (lepton $p_{\mathrm{T}} > 25$ GeV and $|\eta| < 2.5$), this has not been the case for the Z-boson measurements, in some part due to the evolution of the trigger requirements as the peak luminosity and the degree of pile-up from the LHC have increased with time. Table 6 reports the fiducial phase space used in the $13, 8, 7$ TeV measurements of the Z-boson fiducial cross sections. In this paper, all ratios involving Z bosons at 7 and 8 TeV are extrapolated to the 13 TeV phase space using the same methodology as reported in Section 3.1, i.e. computed using an optimised version of DYNNLO 1.5 and the NNLO parton distribution functions CT14. These 13-to-7 TeV and 13-to-8 TeV extrapolation factors, E, are multiplicative factors to the cross sections, and are also reported in Table 6.

Table 7 summarises the primary inputs, in the common 13 TeV phase space for the Z-boson measurements, that enter the cross-section ratios, including the statistical and total systematic uncertainties, the latter encompassing experimental, luminosity, beam-energy, and some theoretical uncertainties (as explained in Section 5.3). These results are taken directly from the publications and from Section 4, with one exception: since the publication of the 8 TeV Z-boson fiducial cross section [10], the 8 TeV luminosity values have been finalised [20], resulting in a slight shift of the integrated luminosity value from the published 20.3 fb^{-1} to 20.2 fb^{-1} and significantly reducing the uncertainty from 2.8% to 1.9%. The 8 TeV results presented here have been updated accordingly. The $t\bar{t}$ fiducial cross-section results in Table 7 are reported in the phase space defined by lepton $p_{\mathrm{T}} > 25$ GeV and $|\eta| < 2.5$ and for which the contribution from $W \to \tau \to \ell$ decay has been subtracted. The breakdown of the systematic uncertainties is presented in Table 8 while the correlation model for the uncertainties is elaborated in the next subsection.

Systematic [%] / $\sqrt{s}$ [TeV]	$\delta\,\sigma_Z^{\text{fid}}$			$\delta\,\sigma_{t\bar{t}}^{\text{tot}}$		
	13	8	7	13	8	7
Luminosity	2.1	1.9	1.8	2.3	2.1	2.0
Beam energy	0.7	0.6	0.6	1.5	1.7	1.8
Muon (lepton) trigger	0.1	0.6	0.1	0.1	0.2	0.2
Muon reconstruction/ID	0.7	0.5	0.3	0.4	0.4	0.3
Muon isolation	0.4	0.0	0.2	0.3	0.2	0.4
Muon momentum scale	0.1	0.0	0.0	0.0	0.0	0.1
Electron trigger	0.0	0.2	0.0	0.1	—	—
Electron reconstruction/ID	0.4	0.8	0.3	0.3	0.4	0.1
Electron isolation	0.1	0.0	—	0.4	0.3	0.6
Electron energy scale	0.3	0.1	0.1	0.2	0.5	0.2
Jet energy scale	—	—	—	0.4	0.7	0.4
b-tagging	—	—	—	0.5	0.4	0.5
Background	0.1	0.2	0.1	1.1	1.0	1.0
Signal modelling (incl. PDF)	0.1	0.1	0.3	3.0	1.7	1.8

Table 8: Systematic uncertainties in %, δ, for the measurement of Z-boson and $t\bar{t}$ production at $\sqrt{s} = 13, 8, 7$ TeV. Values listed as 0.0 are $< 0.05\%$. Values listed as "–" have no corresponding uncertainty. The entry "(lepton)" in "Muon (lepton) trigger" refers to the $t\bar{t}$ trigger for the 7 and 8 TeV data set which quotes a single uncertainty for the combined effects of the uncertainties in the electron and muon triggers and so there is a corresponding entry "–" for the electron trigger for the 7 and 8 TeV $t\bar{t}$ data set.

5.3 Correlation model

The correlation model used in this analysis is summarised in Table 9. The groups listed in the table may be represented by a single source, or by several individual sources of systematic uncertainties (nuisance parameters). The groups of sources are:

- *Luminosity* is considered to be correlated for the measurements performed at the same $\sqrt{s}$ but uncorrelated for data at different $\sqrt{s}$.
- *Beam energy* uncertainty is 0.66% of the beam-energy value [72] and is considered to be fully correlated for all data sets.
- *Muon trigger* is a small source of uncertainty for most analyses. It is considered to be correlated for all Z-boson measurements and for the $t\bar{t}$ measurement at 13 TeV, and separately between the two $t\bar{t}$ analyses at 7 and 8 TeV, following the prescription of Ref. [76].
- *Muon reconstruction/identification* is described by several nuisance parameters. The treatment is fully synchronised for the 13 TeV measurements. The Z-boson measurements at 7 and 8 TeV are considered uncorrelated with each other and with the $t\bar{t}$ measurements since different muon reconstruction algorithms were employed for these measurements. However, the measurements of $t\bar{t}$ at 7 and 8 TeV are assumed to be correlated since they use the same reconstruction algorithm.
- *Muon isolation* is a small and similar source of uncertainty for all Z-boson measurements and thus it is considered to be correlated amongst the measurements. For $t\bar{t}$ analyses, the muon isolation uncertainty is determined in situ, to account for different hadronic environments, and has significant

Source / $\sqrt{s}$ [TeV]	$\delta\,\sigma_Z^{\text{fid}}$ 13	8	7	$\delta\,\sigma_{t\bar{t}}^{\text{tot}}$ 13	8	7
Luminosity	A	B	C	A	B	C
Beam energy	A	A	A	A	A	A
Muon (lepton) trigger	A	A*	A	A	B	B
Muon reconstruction/ID	A	B	C	A	D	D
Muon isolation	A	A	A	B	C	D
Muon momentum scale	A	A	A	A	A	A
Electron trigger	A	A	A	A	—	—
Electron reconstruction/ID	A	B	C	A	D	D
Electron isolation	A	A	—	B	C	D
Electron energy scale	A	A	A	A	A	A
Jet energy scale	—	—	—	A	B	B
b-tagging	—	—	—	A	B	B
Background	A	A	A	B	B	B
Signal modelling (incl. PDF)	A	A	A	B*	B	B

Table 9: Correlation model for the systematic uncertainties, δ, of the measurements of Z-boson and $t\bar{t}$ production at $\sqrt{s} = 13, 8, 7$ TeV. Entries in different rows are uncorrelated with each other. Entries within a row with the same letter are fully correlated. Entries within a row with a starred letter are mostly correlated with the entries with the same letter (most of the individual sources of uncertainties within a group are taken as correlated). Entries with different letters within a row are either fully or mostly uncorrelated with each other. This table uses the same categories as Table 8.

statistical uncertainties. For these reasons, these uncertainties are considered to be uncorrelated with each other and with the Z-boson uncertainties.

- *Muon momentum scale* is a small source of uncertainty for all measurements. It is validated in situ by comparing the invariant mass distributions of muon pairs in data and simulation. Similar levels of agreement are observed for all data-taking periods, and thus all measurements are considered to be correlated.
- *Electron trigger* is a small source of uncertainty for all measurements and is considered to be fully correlated amongst all measurements.
- *Electron reconstruction/identification* is treated similarly to the muon reconstruction/identification.
- *Electron isolation* is treated similarly to the muon isolation.
- *Electron energy scale* is treated and validated similarly to the muon momentum scale.
- *Jet energy scale* only affects the $t\bar{t}$ measurements and is described by several nuisance parameters. The uncertainty is correlated for 7 and 8 TeV data, following the prescription of Ref. [76], and mostly uncorrelated with 13 TeV data, in part due to the in-situ corrections. The impact of this source on the $t\bar{t}$ measurements is small.
- *b-tagging* also only affects the $t\bar{t}$ measurements. The source is considered to be correlated for 7 and 8 TeV data but uncorrelated with 13 TeV data since the installation of the new insertable

B-layer in the inner detector and re-optimised b-tagging algorithms used at 13 TeV resulted in significantly improved b-tagging performance.

- *Background* is treated as fully correlated for all $\sqrt{s}$ within a given process. The main uncertainty for this source is driven by the theoretical uncertainties in the cross sections of the background processes, and the leading background sources are very different for the Z-boson and $t\bar{t}$ measurements.
- *Signal modelling* uncertainty is small for the fiducial Z-boson measurements. Signal modelling is the leading source of uncertainty for the $t\bar{t}$ measurements. Several sources of uncertainty, such as uncertainties related to signal and background MC generators and to PDFs, are considered to be correlated across the different $\sqrt{s}$ values. An additional source of uncertainty is included only for the $t\bar{t}$ measurement at 13 TeV, due to the level of agreement observed in events with at least three b-tagged jets [2].

The correlation model described above corresponds to a fully synchronised analysis of Z-boson and $t\bar{t}$ data at 13 TeV. It also follows the prescription given in Ref. [76] for the $t\bar{t}$ measurements at 7 and 8 TeV. The stability of the results relative to the correlation assumptions was verified by altering the model for the sources of uncertainty where the level of correlation is not precisely known, such as lepton reconstruction and identification at 7 and 8 TeV, resulting in only small changes in the uncertainties.

5.4 Results

In this section, a representative set of total $t\bar{t}$ and fiducial Z-boson cross sections and their ratios are compared to the theory predictions. The full set of single-ratio and double-ratio results for the various combinations of fiducial and total cross sections is given in Appendix C.

5.4.1 Single ratios at a given $\sqrt{s}$

The single ratios $R^{\text{tot/fid}}_{t\bar{t}/Z}$ are compared in Figure 3 to the theoretical predictions based on different PDF sets. For all centre-of-mass energies, the predictions follow a similar pattern for the following three groups of PDFs. The ABM12 set yields the lowest values. The three PDF sets used in the PDF4LHC prescription [77], CT14, NNPDF3.0, and MMHT14, predict the largest ratios. The HERA-based HERAPDF2.0 and ATLAS-epWZ12 sets are in the middle. The spread of the predictions is beyond the PDF uncertainties for the three groups of PDFs while the quoted PDF uncertainties are similar in size, with the HERAPDF2.0 errors being the largest and ABM12 the smallest. This pattern could be explained by the differences in the gluon density and the α_S value used in the PDF sets. The ABM12, HERAPDF2.0 and ATLAS-epWZ12 sets do not include collider jet data, which typically lead to a lower gluon density for the x values where the $t\bar{t}$ data at the LHC are sensitive. In addition, the ABM12 set uses a lower value of α_S. The size of the error bars depends on the data sets used in the PDF fits and also on the statistical model used for the analysis.

The ATLAS data are more precise than most of the theory predictions, suggesting the data have strong constraining power. The experimental uncertainties are the smallest for the 8 TeV measurement. The 7 TeV result has a sizeable statistical uncertainty, while the systematic uncertainty at 13 TeV is larger than at both 7 and 8 TeV, mostly due to a larger $t\bar{t}$ modelling uncertainty. For the most precise measurement, at 8 TeV, the data agree best with the HERAPDF2.0 and ATLAS-epWZ12 PDF sets while they deviate by 1.6–2.1σ from the PDF4LHC PDFs, where σ is the total experimental uncertainty plus the luminosity

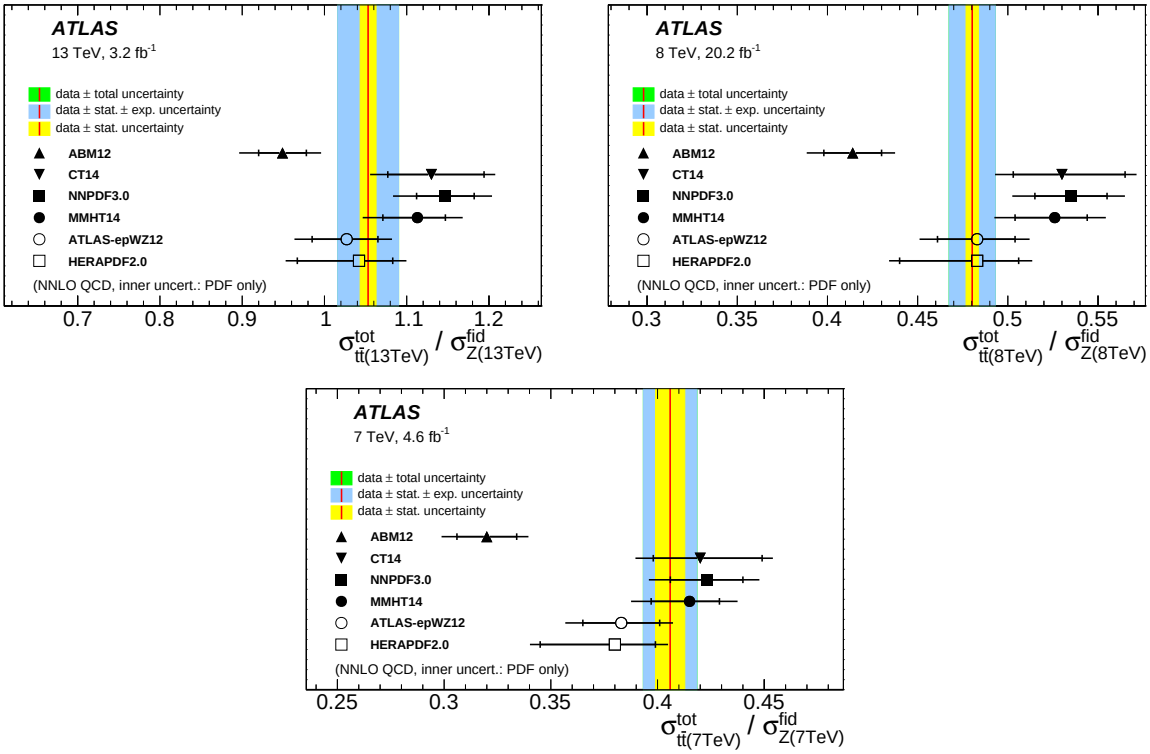

Figure 3: The ratios $R^{\mathrm{tot/fid}}_{t\bar{t}/Z}(i\ \mathrm{TeV})$, for $i = 13, 8, 7$ compared to predictions based on different PDF sets. The inner shaded band corresponds to the statistical uncertainty, the middle band to the statistical and experimental systematic uncertainties added in quadrature, while the outer band shows the total uncertainty, including the luminosity uncertainty. The latter is not visible since the the luminosity uncertainties almost entirely cancel in these ratios. The theory predictions are given with the corresponding PDF uncertainties shown as inner bars while the outer bars include all other uncertainties added in quadrature.

uncertainty (but agree well when including the respective prediction uncertainties), and by 2.6σ from the ABM12 PDF. A similar but less significant pattern is observed for the 13 TeV data. The 7 TeV data are most consistent with the MMHT14 PDF set. The data are between the predictions of the PDF4LHC PDFs and the HERA-based PDFs HERAPDF2.0 and ATLAS-epWZ12, deviating most from the ABM12 prediction. The difference between data and predictions for the 7 and 8 TeV results is consistent with the results published by ATLAS for the ratio of $t\bar{t}$ cross sections at these two energies [76], as is discussed in Section 5.4.2.

5.4.2 Single ratios at different $\sqrt{s}$

The ratios of the fiducial Z-boson cross sections at various $\sqrt{s}$ values are compared in Figure 4 to predictions employing different PDF sets. The uncertainty in these ratios is dominated by the luminosity uncertainty. Even though the total luminosity uncertainties are of comparable magnitude at 7, 8 and 13 TeV, they are mostly uncorrelated and therefore do not cancel in the cross-section ratios.

The measurements are consistent with the predictions for all PDF sets. Most of these predictions agree with the data within the experimental uncertainties, even omitting the luminosity uncertainty. This observation may indicate that the luminosity-determination uncertainty in the measured ratio is conservative.

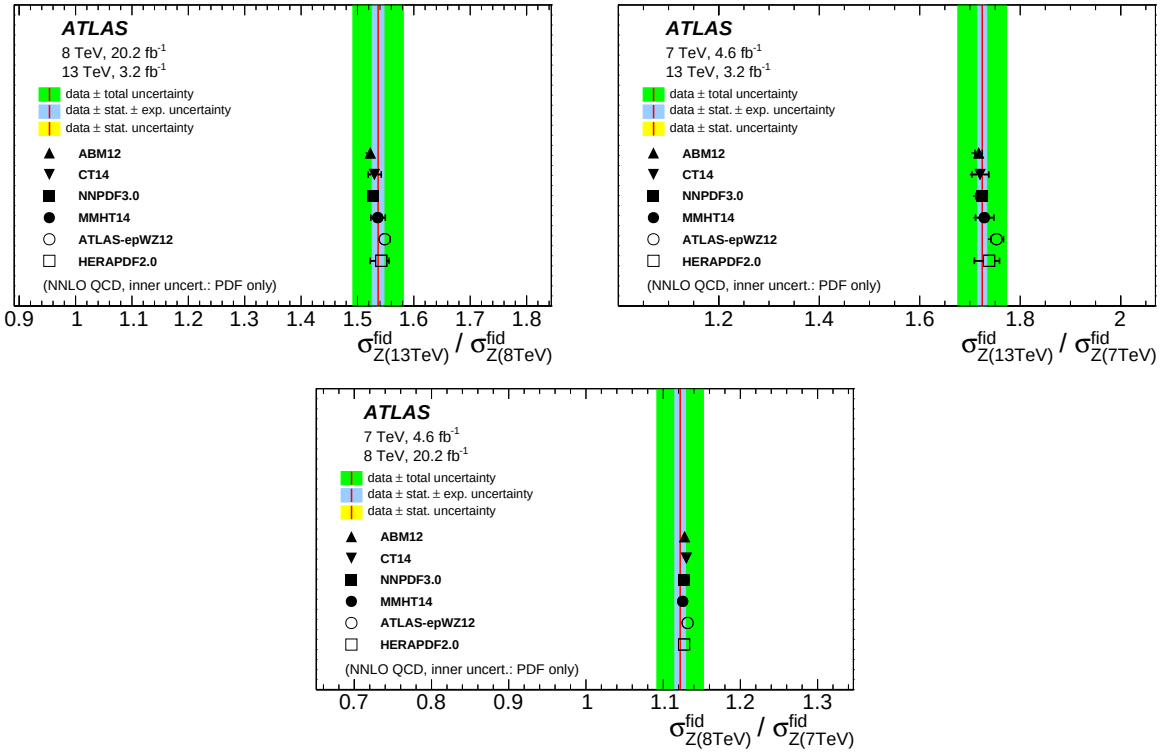

Figure 4: The ratios $R^{\text{fid}}_{Z_i/Z_j}$, for $i, j = 13, 8, 7$ compared to predictions based on different PDF sets. The inner shaded band (barely visible since it is small) corresponds to the statistical uncertainty, the middle band to the statistical and experimental systematic uncertainties added in quadrature, while the outer band shows the total uncertainty, including the luminosity uncertainty. The theory predictions are given with the corresponding PDF uncertainties shown as inner bars while the outer bars include all other uncertainties added in quadrature.

The smallness of the PDF uncertainties for different predictions and the overall small spread among them suggest that the measured Z-boson data could be used to cross-normalise the measurements at the different centre-of-mass energies, thereby avoiding the penalty associated with the combination of uncorrelated luminosity uncertainties. This aspect is explored in Section 5.4.3 by taking double ratios of $t\bar{t}$ to Z-boson cross sections, but this approach can be used for other processes as well.

The measured $t\bar{t}$ ratios for different pairs of $\sqrt{s}$ are compared to the predictions in Figure 5. These predictions follow a similar pattern for all ratios: the three predictions from PDF4LHC PDFs are the smallest, closely followed by ATLAS-epWZ12 and HERAPDF2.0, and the ABM12 prediction is the largest. This pattern could be explained by the PDFs having different gluon distributions as a function of x. At low x, all PDF sets have similar gluon content since the gluon PDF is primarily determined from a common source: scaling violations of the F_2 structure function measured at HERA. At high x, the ABM12 and HERA-based sets have a lower gluon density than other PDF sets. Thus, as the $\sqrt{s}$ increases, resulting in a decrease of the average value of x, the ABM12 and HERA-based sets exhibit a stronger $\sqrt{s}$ dependence than the PDF4LHC PDFs. Given the relative size of the experimental uncertainties and the spread of the theoretical predictions in these ratios, these measurements do not test the consistency of the luminosity calibrations at different centre-of-mass energies to the same precision as the Z-boson cross-section ratios.

The ratio of 13 TeV to 8 TeV cross sections agrees with all predictions within experimental uncertainties.

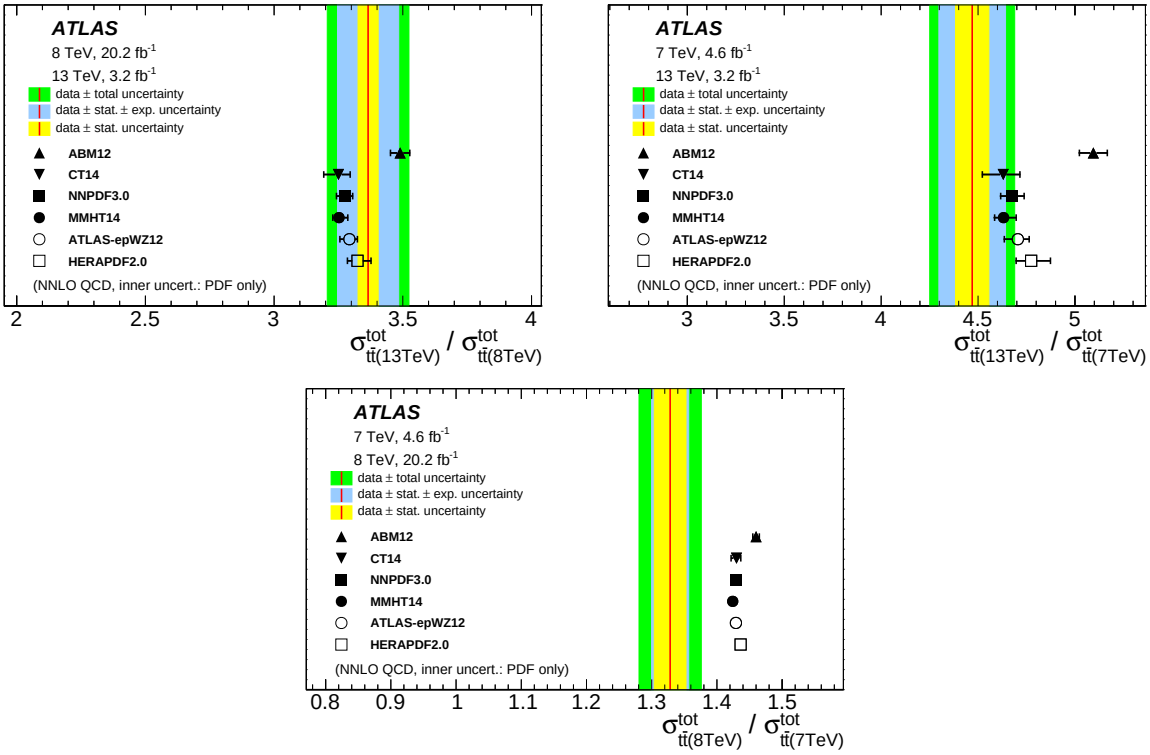

Figure 5: The ratios $R^{\text{tot}}_{t\bar{t}_i/t\bar{t}_j}$, for $i, j = 13, 8, 7$ compared to predictions based on different PDF sets. The inner shaded band corresponds to the statistical uncertainty, the middle band to the statistical and experimental systematic uncertainties added in quadrature, while the outer band shows the total uncertainty, including the luminosity uncertainty. For the 8-to-7 TeV ratio, the experimental systematic uncertainty band is too small to be clearly visible. The theory predictions are given with the corresponding PDF uncertainties shown as inner bars while the outer bars include all other uncertainties added in quadrature.

The central value is closest to the HERAPDF2.0 prediction. For the ratios involving 7 TeV data, the measured ratios have central values lower than predicted by all the PDFs. This is especially so for the 8 TeV to 7 TeV ratio, which deviates from all predictions by approximately two standard deviations. The deviation was observed previously by ATLAS [76] and the results of this analysis are consistent with those published values.

5.4.3 Double ratios

The double ratios of total $t\bar{t}$ to fiducial Z-boson cross sections at different $\sqrt{s}$ are compared to predictions in Figure 6. The total uncertainties are smaller than those in the $t\bar{t}$ cross-section ratios at different $\sqrt{s}$ due to the almost complete cancellation of the luminosity uncertainty, which more than compensates for the uncertainties that the Z-boson cross sections bring to these double ratios.

For the double ratios, the trends seen in comparisons between the data and the predictions are similar to those observed for the single ratios of the $t\bar{t}$ cross sections at different $\sqrt{s}$ values. The double ratio of 13 TeV to 8 TeV results is consistent with all predictions at the 1σ level. The tension between the measured 8 TeV to 7 TeV ratio and the predictions is increased, due to the reduced uncertainty in the measurement that this double ratio brings. This behaviour is difficult to ascribe to the x-dependence of

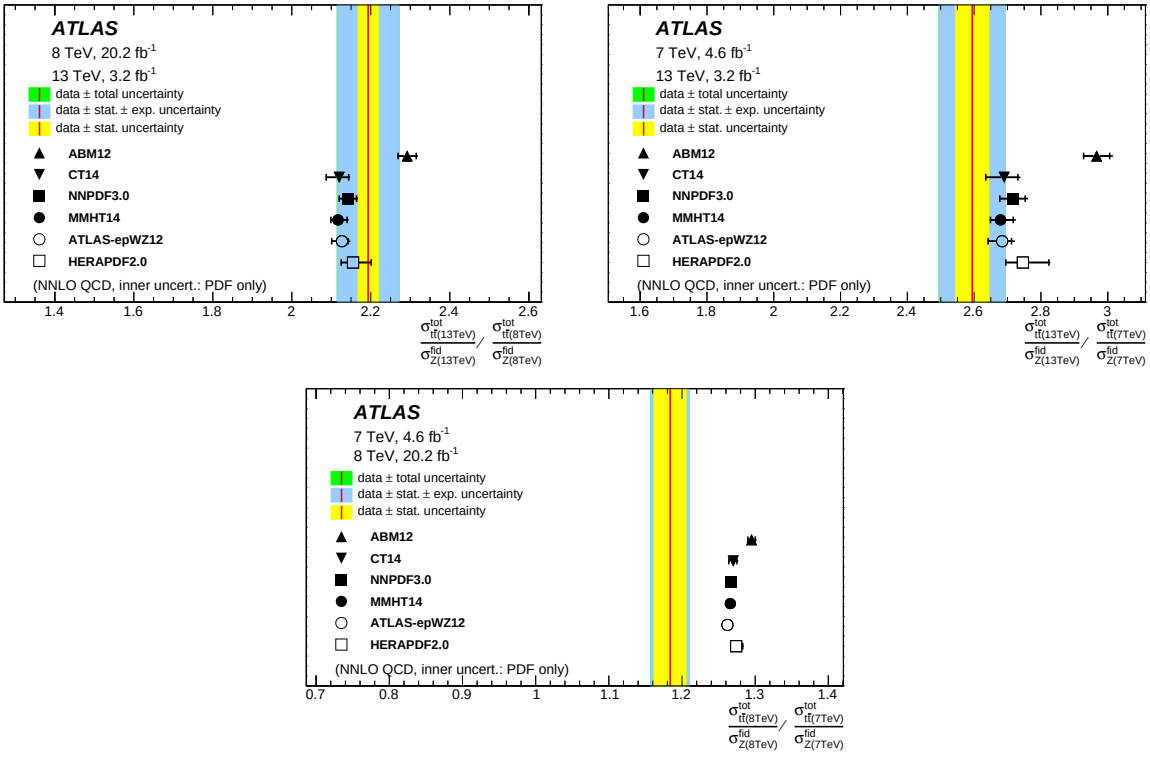

Figure 6: The ratios $R^{\mathrm{tot/fid}}_{t\bar{t}/Z}(i/j)$ where $i, j = 13, 8, 7$ compared to predictions based on different PDF sets. The inner shaded band corresponds to the statistical uncertainty, the middle band to the statistical and experimental systematic uncertainties added in quadrature, while the outer band shows the total uncertainty, including the luminosity uncertainty. The latter is not visible since the the luminosity uncertainties almost entirely cancel in these ratios. The theory predictions are given with the corresponding PDF uncertainties shown as inner bars while the outer bars include all other uncertainties added in quadrature.

the gluon distribution since the change in the average x is much larger for 13 TeV to 8 TeV than for 8 TeV to 7 TeV measurements. The deviation from the ABM12 PDFs is at the 4σ level while for all other PDFs they are at the 3σ level. The prediction closest to the observed ratio is obtained from the ATLAS-epWZ12 PDF set, which predicts a stronger variation of the fiducial Z-boson cross section as a function of $\sqrt{s}$.

5.4.4 Correlated cross-section measurements

As an alternative to taking ratios, the measured cross sections may be compared directly to theory, provided that the full correlation information amongst the experimental results is evaluated. The electron and muon channel σ_Z^{fid} are combined, accounting for the correlated systematic uncertainties, which as a result cause small shifts in all of the combined cross-sections values. The combination's χ^2 per degree of freedom is $\chi^2/\mathrm{NDF} = 0.6$ for $\mathrm{NDF} = 3$, indicating excellent compatibility of the $Z \to e^+e^-$ and $Z \to \mu^+\mu^-$ measured cross sections. The resulting Z-boson fiducial and $t\bar{t}$ total cross sections after combination are given in Table 10 with the correlation coefficients presented in Table 11. The correlations are large for the measurements at a given $\sqrt{s}$, due to the common luminosity uncertainty. The corresponding table omitting both the luminosity and beam-energy uncertainties is given in Appendix C. As expected from the ratio analysis, there is also a sizeable correlation between the $t\bar{t}$ results at 7 and 8 TeV. It is veri-

$\sqrt{s}$ [TeV]	Value ± stat ± syst ± beam ± lumi [pb]
	σ_Z^{fid}
13	777 ± 1 (0.1%) ± 3 (0.4%) ± 5 (0.7%) ± 16 (2.1%)
8	506 ± < 1 (< 0.1%) ± 3 (0.6%) ± 3 (0.6%) ± 10 (1.9%)
7	451 ± < 1 (0.1%) ± 1 (0.3%) ± 3 (0.6%) ± 8 (1.8%)
	$\sigma_{t\bar{t}}^{\text{tot}}$
13	818 ± 8 (0.9%) ± 27 (3.3%) ± 12 (1.5%) ± 19 (2.3%)
8	243 ± 2 (0.7%) ± 5 (2.3%) ± 4 (1.7%) ± 5 (2.1%)
7	183 ± 3 (1.7%) ± 4 (2.3%) ± 3 (1.8%) ± 4 (2.0%)

Table 10: Combined fiducial Z-boson and total $t\bar{t}$ cross sections for $\sqrt{s} = 13, 8, 7$ TeV. The uncertainties are listed as statistical, systematic, beam-energy, and luminosity.

	Z 13 TeV	$t\bar{t}$ 13 TeV	Z 8 TeV	$t\bar{t}$ 8 TeV	Z 7 TeV	$t\bar{t}$ 7 TeV
Z 13 TeV	1.00	0.61	0.10	0.16	0.10	0.15
$t\bar{t}$ 13 TeV	-	1.00	0.11	0.32	0.11	0.31
Z 8 TeV	-	-	1.00	0.68	0.10	0.14
$t\bar{t}$ 8 TeV	-	-	-	1.00	0.15	0.54
Z 7 TeV	-	-	-	-	1.00	0.62
$t\bar{t}$ 7 TeV	-	-	-	-	-	1.00

Table 11: The correlation coefficients amongst the combined Z-boson fiducial and $t\bar{t}$ total cross-section measurements at $\sqrt{s} = 13, 8, 7$ TeV.

fied that the uncertainties in the ratios are consistent with those of the direct evaluation of the combined cross section.

Figure 7 shows the results of this combination as two-dimensional 68% CL contours of σ_Z^{fid} vs. $\sigma_{t\bar{t}}^{\text{tot}}$ at the three $\sqrt{s}$ values, overlayed with the theoretical cross-section predictions calculated from the error sets associated with each specific PDF. The correlations of the measured cross sections are opposite in sign to those of the predicted cross sections (with exception of ABM12 set, which has a small positive correlation), providing discriminating input to the determination of the PDFs.

5.5 Quantitative comparison with predictions

The measured cross sections along with the complete correlation information are compared in a quantitative way to the predictions based on different PDF sets. The comparison is performed using the xFitter package [78], which allows PDF and other theoretical uncertainties to be included via asymmetric error propagation. The comparison is performed for the total $t\bar{t}$ and fiducial Z-boson cross sections, including their correlations, as reported in Section 5.4.4. The resulting χ^2 values corresponding to the different PDFs are given in Table 12. All comparisons give an acceptable χ^2 value except for the ABM12 PDF set, which is disfavoured by the data. The covariance matrix is decomposed so as to extract the uncorrelated component of the uncertainties. Figure 8 visually compares the measurements, with both the total and the uncorrelated components of the uncertainties, to the predictions. From Figure 8 and Table 12, it can be observed that the HERAPDF2.0 and ATLAS-epWZ12 sets have good compatibility with the ATLAS data and agreement is improved when the measurement of the $t\bar{t}$ cross section at 7 TeV is excluded.

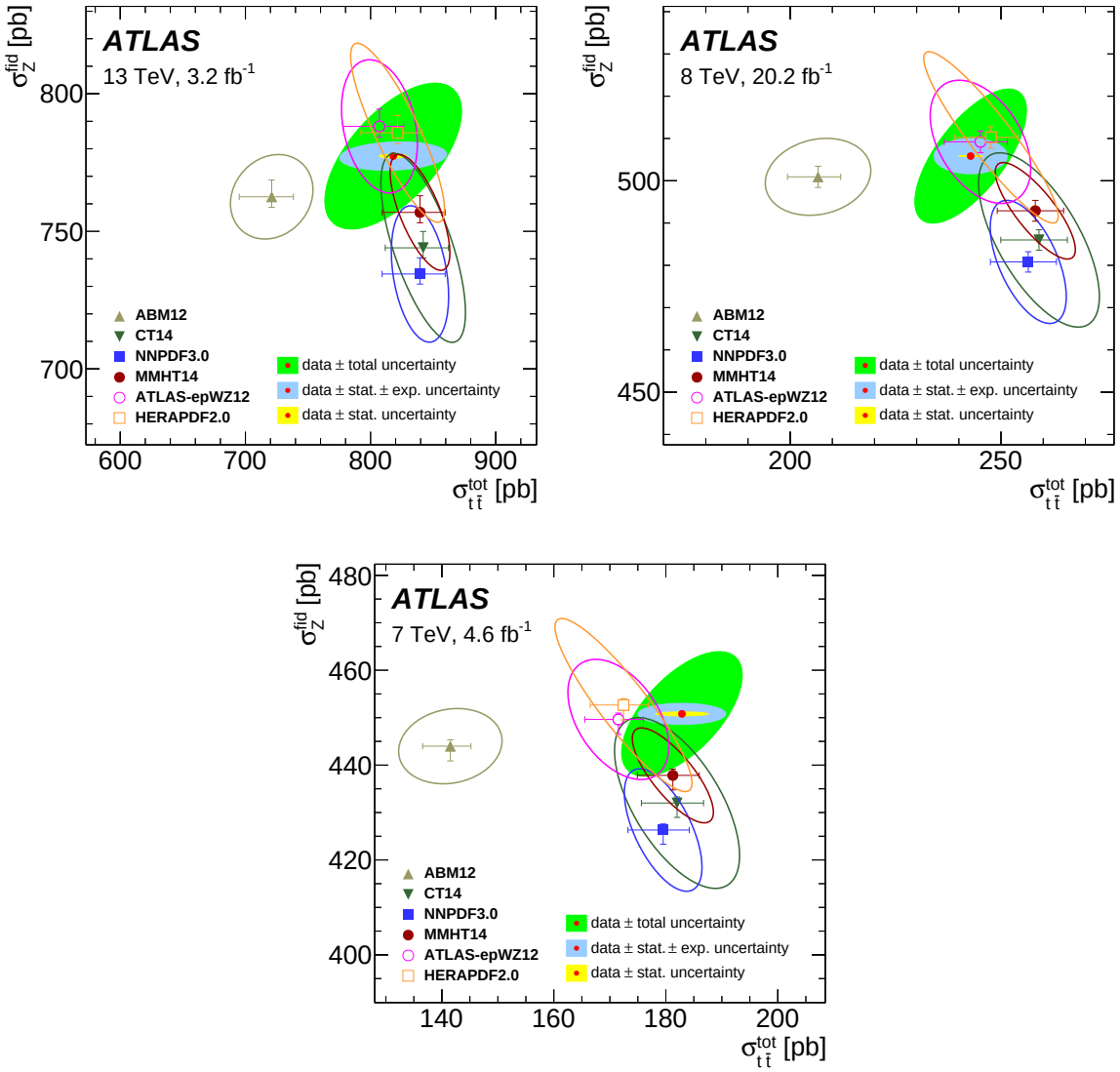

Figure 7: Two-dimensional 68% CL contours of σ_Z^{fid} vs. $\sigma_{t\bar{t}}^{\text{tot}}$ at 13 TeV (top, left), 8 TeV (top, right), and 7 TeV (bottom). The solid red circle shows the result of the combination, the yellow ellipse represents the statistical uncertainty, the blue ellipse adds the experimental uncertainty, while the green ellipse is the total uncertainty. The results are overlayed with the theoretical cross-section predictions calculated from the error sets associated with each specific PDF, also plotted at 68% CL. The ellipses correspond to the PDF uncertainties, the asymmetric error bars inside the ellipses represent the scale uncertainties, and the coloured markers are the central values.

The impact of the ATLAS data on the PDF uncertainties can be quantified by using the PDF profiling method [79, 80]. It is preferable to quantify the impact of the ATLAS data by using PDFs that do not include the cross-section data used in this analysis. Both the HERAPDF2.0 and ATLAS-epWZ12 sets satisfy these conditions. Given that the ATLAS-epWZ12 set provides smaller uncertainties for the predicted cross sections compared to HERAPDF2.0, it is chosen for this purpose. The profiling of the ATLAS-epWZ12 PDF set is performed only with the components related to the uncertainties of the HERA [75] and 2010 ATLAS [8] W, Z-boson data, to mimic the inclusion of the new ATLAS data in the PDF fit.

	ATLAS-epWZ12	CT14	MMHT14	NNPDF3.0	HERAPDF2.0	ABM12
χ^2/NDF	8.3 / 6	15 / 6	13 / 6	17 / 6	10 / 6	25 / 6
p-value	0.22	0.02	0.05	0.01	0.11	< 0.001

Table 12: χ^2 values for the comparisons of the ATLAS data to the predictions based on ATLAS-epWZ12, CT14, MMHT14, NNPDF3.0, HERAPDF2.0 and ABM12 PDF sets along with the probability of finding the observed value or larger.

The effect of additional uncertainties arising from model and PDF-parameterisation variations estimated in the ATLAS-epWZ12 PDF fit are not further investigated.

Figure 9 shows the light-quark sea $\Sigma = \bar{u} + \bar{d} + \bar{s}$ and gluon g distributions before and after the profiling, including their uncertainties, at the scales $Q^2 \approx m_Z^2$ and $Q^2 \approx m_t^2$, respectively. The upper plots show the profiled distributions divided by the central value of the ATLAS-epWZ12 PDF set and demonstrate that the central values of the profiled distributions agree very well with the original set. The lower plots show that the ATLAS $t\bar{t}$ and Z-boson cross-section data impose visible constraints on the light-quark sea distribution at $x < 0.02$ and on the gluon distribution at $x \sim 0.1$. These data constrain the least-well-understood component of the light-quark sea distribution, namely the strange-quark distribution while the other quark PDFs are not significantly constrained [9]. The lower plots also show the impact of the $t\bar{t}$ data only, which contribute significantly to the constraint on the gluon distribution, while the Z-boson data help to constrain both the light-quark-sea and gluon distributions.

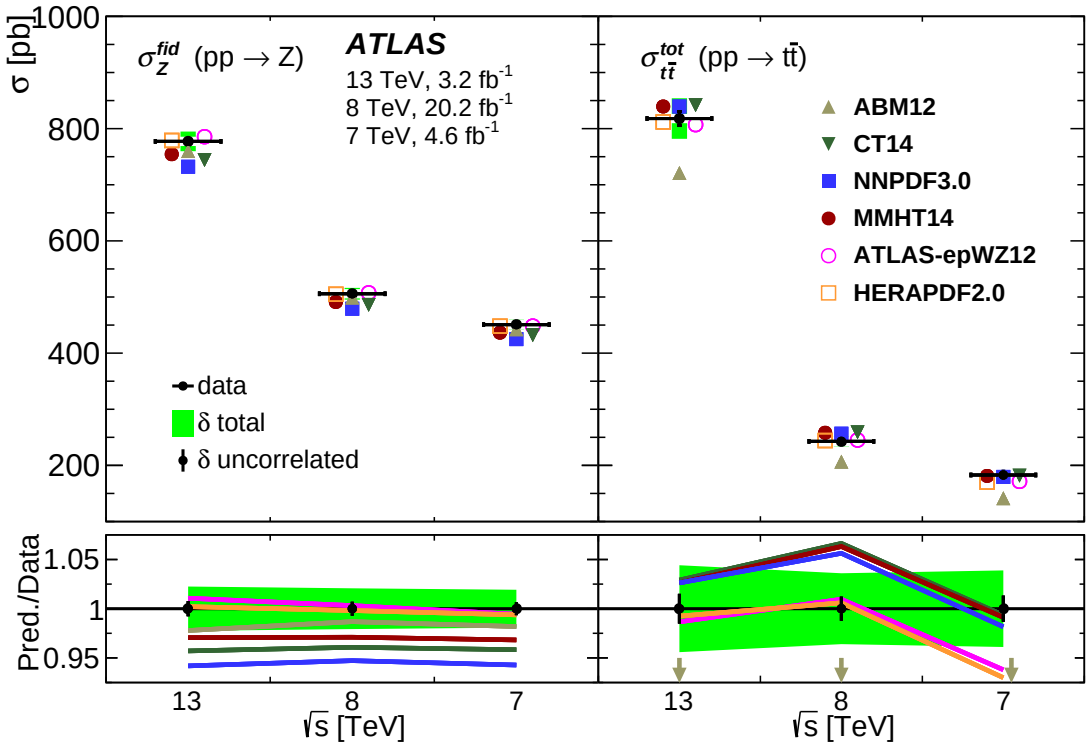

Figure 8: Comparison of the measured σ_Z^{fid} (left) and $\sigma_{t\bar{t}}^{\text{tot}}$ (right) to predictions based on different PDF sets. The lower panel shows the total and uncorrelated uncertainties, δ, associated with the ratios of the predictions to the data. In the lower-right panel, the $\sigma_{t\bar{t}}^{\text{tot}}$ ABM12 predictions are outside of the plot, as indicated by the arrows. The uncertainties in the Z-boson ($t\bar{t}$) predictions are typically 3% (6%).

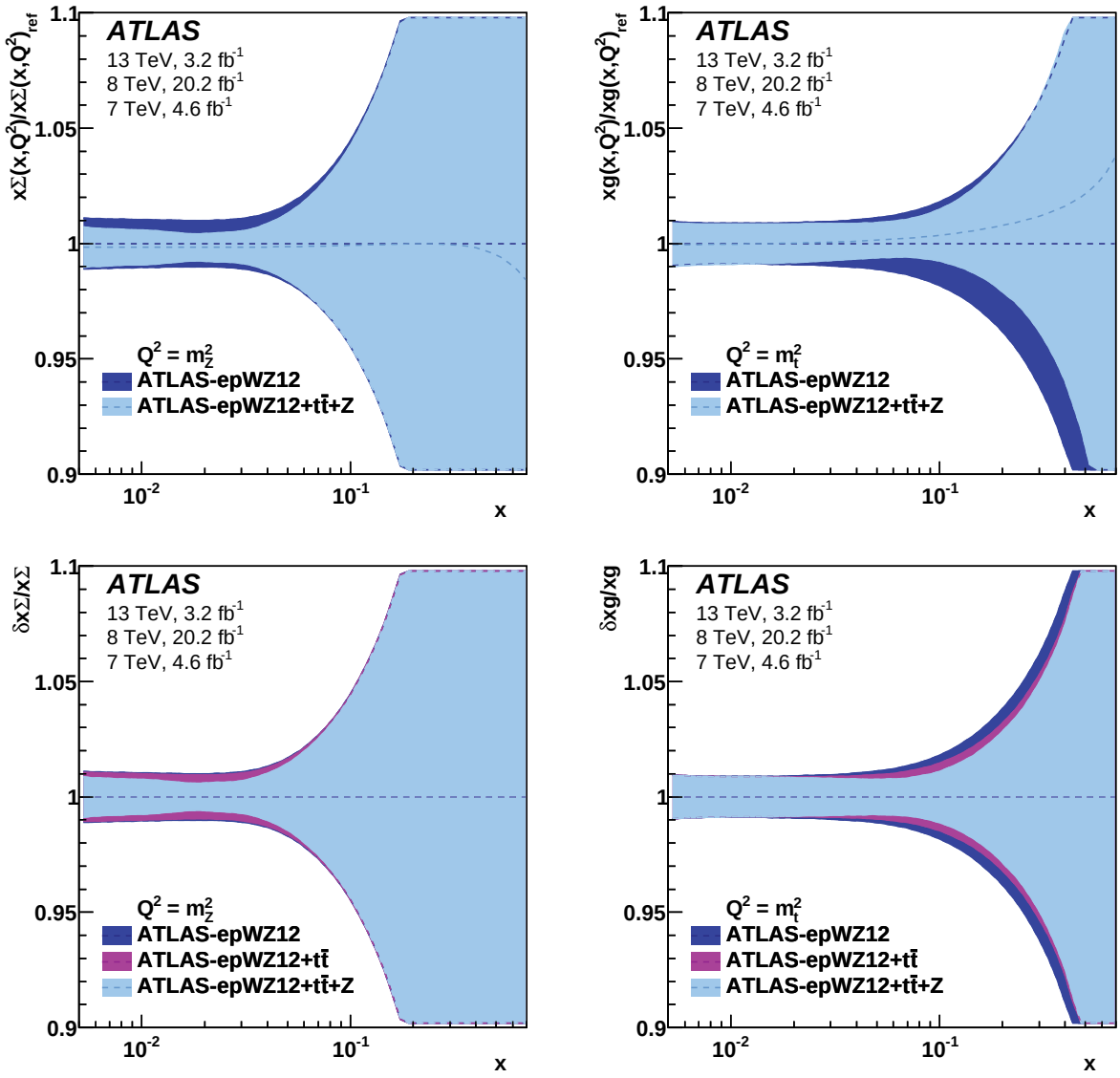

Figure 9: Impact of the ATLAS Z-boson and $t\bar{t}$ cross-section data on the determination of PDFs. The bands represent the uncertainty for the ATLAS-epWZ12 PDF set and the uncertainty of the profiled ATLAS-epWZ12 PDF set using $t\bar{t} + Z$ data as a function of x for the total light-quark-sea distribution, $x\Sigma$, at $Q^2 \approx m_Z^2$ (left) and for the gluon density, xg, at $Q^2 \approx m_t^2$ (right). In the upper plots, the profiled PDF set is divided by the central value of ATLAS-epWZ12 PDF set, "ref", while in the lower plots, the relative uncertainty, δ, is given. The lower plots also show the impact of only including the ATLAS $t\bar{t}$ data set. In the upper plots, the dashed blue curve represents the ratio of the central value of the profiled result to ATLAS-epWZ12 PDF set.

6 Conclusion

This paper reports a new measurement by the ATLAS Collaboration of the Z-boson production cross section at $\sqrt{s} = 13$ TeV using 3.2 fb^{-1}of pp collisions from the LHC, together with the evaluations of single and double ratios involving Z-boson and $t\bar{t}$ production cross sections, ($R^{\text{fid}}_{Z_i/Z_j}$, $R^{\text{tot}}_{t\bar{t}_i/t\bar{t}_j}$, $R^{\text{tot/fid}}_{t\bar{t}/Z}(i \text{ TeV})$, and $R^{\text{tot/fid}}_{t\bar{t}/Z}(i/j)$ where $i, j = 13, 8, 7$) using this new measurement and previously published cross-section measurements at $\sqrt{s} = 13, 8, 7$ TeV. The new measurement of Z-boson production at $\sqrt{s} = 13$ TeV is fully synchronised to the corresponding $t\bar{t}$ analysis, to improve the cancellation of the uncertainties in the ratios, while all other measurements also benefit significantly from the partial cancellation of uncertainties that evaluating ratios can bring.

The experimental results are compared to the state-of-the-art theoretical predictions, which are computed at NNLO (with NLO EW corrections) and NNLO+NNLL accuracy for Z-boson and $t\bar{t}$ production, respectively. Excellent agreement between data and predictions is observed in the Z-boson cross-section ratios at the various centre-of-mass energies, even omitting the luminosity uncertainties. These results indicate that such measurements could be used to normalise cross-section measurements at different $\sqrt{s}$, as well as provide stringent cross-checks on the corresponding ratios of absolute integrated luminosity values. The data are found to be in best agreement with the ATLAS-epWZ12 PDF set, closely followed by the HERAPDF2.0 set, while the CT14, NNPDF3.0, and MMHT14 PDF sets deviate from some of the ratio measurements at the 1–2σ level. The ABM12 PDF set is disfavoured by the data. A tension is observed between data and predictions of the double ratio between 8 TeV and 7 TeV, which is difficult to ascribe entirely to the $\sqrt{s}$ dependence of the PDFs.

The data presented here have significant power to constrain the gluon distribution function at Bjorken-$x \sim 0.1$ and the total light-quark sea at $x < 0.02$, as demonstrated from a profiling analysis involving the ATLAS-epWZ12 PDF set.

Acknowledgements

We thank CERN for the very successful operation of the LHC, as well as the support staff from our institutions without whom ATLAS could not be operated efficiently.

We acknowledge the support of ANPCyT, Argentina; YerPhI, Armenia; ARC, Australia; BMWFW and FWF, Austria; ANAS, Azerbaijan; SSTC, Belarus; CNPq and FAPESP, Brazil; NSERC, NRC and CFI, Canada; CERN; CONICYT, Chile; CAS, MOST and NSFC, China; COLCIENCIAS, Colombia; MSMT CR, MPO CR and VSC CR, Czech Republic; DNRF and DNSRC, Denmark; IN2P3-CNRS, CEA-DSM/IRFU, France; GNSF, Georgia; BMBF, HGF, and MPG, Germany; GSRT, Greece; RGC, Hong Kong SAR, China; ISF, I-CORE and Benoziyo Center, Israel; INFN, Italy; MEXT and JSPS, Japan; CNRST, Morocco; FOM and NWO, Netherlands; RCN, Norway; MNiSW and NCN, Poland; FCT, Portugal; MNE/IFA, Romania; MES of Russia and NRC KI, Russian Federation; JINR; MESTD, Serbia; MSSR, Slovakia; ARRS and MIZŠ, Slovenia; DST/NRF, South Africa; MINECO, Spain; SRC and Wallenberg Foundation, Sweden; SERI, SNSF and Cantons of Bern and Geneva, Switzerland; MOST, Taiwan; TAEK, Turkey; STFC, United Kingdom; DOE and NSF, United States of America. In addition, individual groups and members have received support from BCKDF, the Canada Council, CANARIE, CRC, Compute Canada, FQRNT, and the Ontario Innovation Trust, Canada; EPLANET, ERC, FP7, Horizon 2020 and Marie Skłodowska-Curie Actions, European Union; Investissements d'Avenir Labex and

Idex, ANR, Région Auvergne and Fondation Partager le Savoir, France; DFG and AvH Foundation, Germany; Herakleitos, Thales and Aristeia programmes co-financed by EU-ESF and the Greek NSRF; BSF, GIF and Minerva, Israel; BRF, Norway; Generalitat de Catalunya, Generalitat Valenciana, Spain; the Royal Society and Leverhulme Trust, United Kingdom.

The crucial computing support from all WLCG partners is acknowledged gratefully, in particular from CERN, the ATLAS Tier-1 facilities at TRIUMF (Canada), NDGF (Denmark, Norway, Sweden), CC-IN2P3 (France), KIT/GridKA (Germany), INFN-CNAF (Italy), NL-T1 (Netherlands), PIC (Spain), ASGC (Taiwan), RAL (UK) and BNL (USA), the Tier-2 facilities worldwide and large non-WLCG resource providers. Major contributors of computing resources are listed in Ref. [81].

Appendix

A Predictions involving Z-boson total cross sections

Tables 13 and 14 mirror the Z-boson information in Tables 1, 2 and 3, and use the same methodology as described in Section 3.1 except that the total Z-boson production cross sections times the branching ratio into a lepton pair of flavour $\ell^+\ell^-$ are given rather than the fiducial cross sections.

	$\sigma_Z^{\text{tot}}(i \text{ TeV})$			$R^{\text{tot}}_{Z_i/Z_j}$		
i or i/j	13	8	7	13/7	13/8	8/7
Central value [pb]	1 886	1 110	954	1.977	1.699	1.163
Uncertainties [%]						
PDF	$^{+2.4}_{-2.7}$	$^{+2.2}_{-2.5}$	$^{+2.2}_{-2.5}$	$^{+0.9}_{-0.8}$	$^{+0.7}_{-0.6}$	$^{+0.18}_{-0.17}$
α_S	$^{+1.0}_{-0.9}$	$^{+0.8}_{-0.8}$	$^{+0.8}_{-0.9}$	$^{+0.2}_{-0.1}$	$^{+0.2}_{-0.1}$	$^{-0.1}_{+0.1}$
Scale	$^{+0.7}_{-1.1}$	$^{+0.6}_{-0.9}$	$^{+0.5}_{-0.9}$	$^{+0.21}_{-0.30}$	$^{+0.20}_{-0.25}$	$^{+0.19}_{-0.05}$
Total	$^{+2.7}_{-3.0}$	$^{+2.4}_{-2.8}$	$^{+2.4}_{-2.8}$	$^{+0.9}_{-0.9}$	$^{+0.8}_{-0.7}$	$^{+0.27}_{-0.20}$

Table 13: Predictions of the total cross section σ_Z^{tot} at $\sqrt{s} = 13, 8, 7$ TeV (left) and of the cross-section ratio $R^{\text{tot}}_{Z_i/Z_j}$ where $i/j = 13/7, 13/8$, and $8/7$ (right) using the CT14 PDF. The uncertainties, given in %, correspond to variations of: CT14 eigenvector set at 68% CL, α_S, and QCD scale, as described in the text. The statistical uncertainties in the cross-section predictions are < 1 pb and are ≤ 0.002 for the ratio predictions, and are not given in the table.

	$R^{\text{tot/tot}}_{t\bar{t}/Z}(i \text{ TeV})$			$R^{\text{tot/tot}}_{t\bar{t}/Z}(i/j)$		
i or i/j	13	8	7	13/7	13/8	8/7
Central value	0.446	0.233	0.190	2.344	1.913	1.225
Uncertainties [%]						
PDF	$^{+5}_{-5}$	$^{+6}_{-5}$	$^{+6}_{-5}$	$^{+1.8}_{-2.2}$	$^{+1.4}_{-1.7}$	$^{+0.4}_{-0.6}$
α_S	$^{+0.9}_{-0.9}$	$^{+1.4}_{-1.3}$	$^{+1.4}_{-1.3}$	$^{-0.49}_{+0.36}$	$^{-0.49}_{+0.35}$	$^{-0.00}_{+0.01}$
Scale	$^{+2.7}_{-3.7}$	$^{+2.7}_{-3.6}$	$^{+2.8}_{-3.5}$	$^{+0.35}_{-0.34}$	$^{+0.38}_{-0.28}$	$^{+0.09}_{-0.21}$
m_t	$^{+2.8}_{-2.7}$	$^{+3.0}_{-2.9}$	$^{+3.1}_{-3.0}$	$^{+0.29}_{-0.29}$	$^{+0.22}_{-0.22}$	$^{+0.07}_{-0.07}$
Total	$^{+7}_{-7}$	$^{+7}_{-7}$	$^{+8}_{-7}$	$^{+1.9}_{-2.3}$	$^{+1.5}_{-1.8}$	$^{+0.4}_{-0.6}$

Table 14: Predictions of the cross-section ratios $R^{\text{tot/tot}}_{t\bar{t}/Z}(i \text{ TeV})$ and $R^{\text{tot/tot}}_{t\bar{t}/Z}(i/j)$ at the different $\sqrt{s}$ values where $i, j = 13, 8, 7$ using the CT14 PDF. The uncertainties, given in %, correspond to variations of: CT14 eigenvector set at 68% CL, α_S, QCD scale, intrinsic Z-boson prediction, and top-quark mass, as described in the text. The statistical uncertainties in the predictions are < 0.001 for $R^{\text{tot/tot}}_{t\bar{t}/Z}(i \text{ TeV})$ and ≤ 0.002 for $R^{\text{tot/tot}}_{t\bar{t}/Z}(i/j)$ and are not given in the table.

$\sqrt{s}$ [TeV]	$A \pm$ total uncertainty
13	0.395 ± 0.007
8	0.466 ± 0.008
7	0.505 ± 0.009

$\sqrt{s}$ [TeV]	$\sigma_Z^{\text{tot}} \pm$ stat $\pm$ syst $\pm$ beam $\pm$ lumi [pb]
13	$1\,969 \pm 1\ (0.1\%) \pm 36\ (1.8\%) \pm 14\ (0.7\%) \pm 41\ (2.1\%)$
8	$1\,154 \pm < 1\ (< 0.1\%) \pm 21\ (1.8\%) \pm 7\ (0.6\%) \pm 22\ (1.9\%)$
7	$995 \pm 1\ (0.1\%) \pm 18\ (1.8\%) \pm 6\ (0.6\%) \pm 18\ (1.8\%)$

Table 15: Acceptance factors A and combined total Z-boson cross sections times leptonic branching ratio within the invariant mass window $66 < m_{\ell\ell} < 116$ GeV for $\sqrt{s} = 13, 8, 7$ TeV. The uncertainties in the cross sections are listed as statistical, systematic, beam-energy, and luminosity while those for the A factor include the total uncertainty.

	Z 13 TeV	$t\bar{t}$ 13 TeV	Z 8 TeV	$t\bar{t}$ 8 TeV	Z 7 TeV	$t\bar{t}$ 7 TeV
Z 13 TeV	1.	0.13	0.09	0.08	0.12	0.03
$t\bar{t}$ 13 TeV	-	1.	0.01	0.32	0.00	0.27
Z 8 TeV	-	-	1.	0.01	0.09	0.00
$t\bar{t}$ 8 TeV	-	-	-	1.	0.00	0.67
Z 7 TeV	-	-	-	-	1.	0.00
$t\bar{t}$ 7 TeV	-	-	-	-	-	1.

Table 16: The correlation coefficients amongst the combined Z-boson fiducial and $t\bar{t}$ total cross-section measurements at $\sqrt{s} = 13, 8, 7$ TeV as in Table 11 but omitting the luminosity and beam-energy uncertainties.

B Acceptance factors and results in the Z-boson total phase space

The combined Z-boson fiducial cross sections in Section 5.4.4 are extrapolated to the full phase space within the dilepton invariant mass range $66 < m_{\ell\ell} < 116$ GeV in Table 15 by use of acceptance factors A, as described in Section 3. The acceptance factors A are expressed as the fraction of decays satisfying the fiducial acceptance at Monte Carlo generator level and are calculated using DYNNLO 1.5 with the CT14 PDF for the central value and for the variations reflecting the PDF set's systematic uncertainty. In addition, uncertainties due to parton showers and the hadronisation description are taken from a previous publication [8], after checking their validity for the 13 TeV result, and were derived as the differences between the acceptances calculated with Powheg-Box v1 but using different models for parton shower and hadronisation descriptions, namely the Herwig [82] or Pythia [63] programs. The acceptance factor used to extrapolate from fiducial to total cross sections, however, has a sizeable uncertainty which is treated as correlated in the ratio measurements for data at different $\sqrt{s}$ values.

C Tables of results

Table 16 presents the correlation coefficients matrix as in Table 11 but omitting both the luminosity and beam-energy uncertainties. Tables 17 and 18 summarise all of the single and double-ratio results for the $t\bar{t}$ and Z-boson production cross sections at $\sqrt{s} = 13, 8, 7$ TeV.

	$\sigma^{\text{tot}}/\sigma^{\text{tot}}$	$\sigma^{\text{tot}}/\sigma^{\text{fid}}$	$\sigma^{\text{fid}}/\sigma^{\text{fid}}$
	Value ± stat ± syst ± lumi	Value ± stat ± syst ± lumi	Value ± stat ± syst ± lumi
$t\bar{t}/Z(13)$	0.416 ± 0.004 (0.9%) ± 0.016 (3.8%) ± 0.001 (0.2%)	1.053 ± 0.010 (0.9%) ± 0.036 (3.4%) ± 0.002 (0.2%)	0.012 80 ± 0.000 12 (0.9%) ± 0.000 33 (2.6%) ± 0.000 03 (0.2%)
$t\bar{t}/Z(8)$	0.211 ± 0.001 (0.7%) ± 0.007 (3.1%) ± 0.000 (0.2%)	0.480 ± 0.003 (0.7%) ± 0.012 (2.6%) ± 0.001 (0.2%)	0.006 02 ± 0.000 04 (0.7%) ± 0.000 14 (2.4%) ± 0.000 01 (0.2%)
$t\bar{t}/Z(7)$	0.184 ± 0.003 (1.7%) ± 0.006 (3.1%) ± 0.000 (0.2%)	0.406 ± 0.007 (1.7%) ± 0.011 (2.6%)± 0.001 (0.2%)	0.005 11 ± 0.000 09 (1.7%) ± 0.000 13 (2.5%) ± 0.000 01 (0.2%)
$Z(13)/Z(8)$	1.707 ± 0.001 (0.1%) ± 0.013 (0.8%) ± 0.048 (2.8%)	-	1.537 ± 0.001 (0.1%) ± 0.010 (0.7%) ± 0.044 (2.8%)
$Z(13)/Z(7)$	1.979 ± 0.002 (0.1%) ± 0.014 (0.7%) ± 0.055 (2.8%)	-	1.724 ± 0.001 (0.1%) ± 0.009 (0.5%) ± 0.048 (2.8%)
$Z(8)/Z(7)$	1.160 ± 0.001 (0.1%) ± 0.007 (0.6%) ± 0.030 (2.6%)	-	1.122 ± 0.001 (0.1%) ± 0.007 (0.6%) ± 0.029 (2.6%)
$t\bar{t}(13)/t\bar{t}(8)$	3.365 ± 0.039 (1.2%) ± 0.112 (3.3%) ± 0.105 (3.1%)	-	3.270 ± 0.038 (1.2%) ± 0.086 (2.6%) ± 0.102 (3.1%)
$t\bar{t}(13)/t\bar{t}(7)$	4.470 ± 0.086 (1.9%) ± 0.149 (3.3%) ± 0.136 (3.0%)	-	4.322 ± 0.083 (1.9%) ± 0.116 (2.7%) ± 0.131 (3.0%)
$t\bar{t}(8)/t\bar{t}(7)$	1.328 ± 0.024 (1.8%) ± 0.015 (1.1%) ± 0.038 (2.9%)	-	1.322 ± 0.024 (1.8%) ± 0.015 (1.1%) ± 0.038 (2.9%)

Table 17: Summary of the Z-boson and $t\bar{t}$ production cross-section single ratios at 13, 8, 7 TeV. The beam-energy uncertainty, which largely cancels in the ratios, is included in the systematic uncertainty.

	$\left[\sigma^{\text{tot}}/\sigma^{\text{tot}}\right]/\left[\sigma^{\text{tot}}/\sigma^{\text{tot}}\right]$	$\left[\sigma^{\text{tot}}/\sigma^{\text{tot}}\right]/\left[\sigma^{\text{fid}}/\sigma^{\text{fid}}\right]$	$\left[\sigma^{\text{fid}}/\sigma^{\text{fid}}\right]/\left[\sigma^{\text{fid}}/\sigma^{\text{fid}}\right]$
	Value ± stat ± syst ± lumi	Value ± stat ± syst ± lumi	Value ± stat ± syst ± lumi
$t\bar{t}/Z(13/8)$	1.975 ± 0.023 (1.2%) ± 0.067 (3.4%) ± 0.006 (0.3%)	2.193 ± 0.026 (1.2%) ± 0.074 (3.4%) ± 0.008 (0.4%)	2.131 ± 0.025 (1.2%) ± 0.057 (2.7%) ± 0.006 (0.3%)
$t\bar{t}/Z(13/7)$	2.260 ± 0.044 (1.9%) ± 0.075 (3.3%) ± 0.007 (0.3%)	2.594 ± 0.050 (1.9%) ± 0.086 (3.3%) ± 0.008 (0.3%)	2.508 ± 0.048 (1.9%) ± 0.067 (2.7%) ± 0.008 (0.3%)
$t\bar{t}/Z(8/7)$	1.145 ± 0.021 (1.8%) ± 0.015 (1.3%) ± 0.003 (0.3%)	1.184 ± 0.022 (1.8%) ± 0.015 (1.3%) ± 0.003 (0.3%)	1.178 ± 0.022 (1.8%) ± 0.015 (1.3%) ± 0.003 (0.3%)

Table 18: Summary of the Z-boson and $t\bar{t}$ production cross-section double ratios at $13, 8, 7$ TeV. The beam-energy uncertainty, which largely cancels in the ratios, is included in the systematic uncertainty. The luminosity uncertainty mostly cancels in this ratio.

References

[1] ATLAS Collaboration, *Measurement of the $t\bar{t}$ production cross-section using $e\mu$ events with b-tagged jets in pp collisions at $\sqrt{s}$ = 7 and 8 TeV with the ATLAS detector*, Eur. Phys. J. C **74** (2014) 3109, arXiv:1406.5375 [hep-ex], and Addendum Eur. Phys. J. C **76** (2016) 642.

[2] ATLAS Collaboration, *Measurement of the $t\bar{t}$ production cross-section using $e\mu$ events with b-tagged jets in pp collisions at $\sqrt{s}$ = 13 TeV with the ATLAS detector*, Phys. Lett. B **761** (2016) 136, arXiv:1606.02699 [hep-ex].

[3] ATLAS Collaboration, *Measurement of the top quark pair production cross-section with ATLAS in the single lepton channel*, Phys. Lett. B **711** (2012) 244, arXiv:1201.1889 [hep-ex].

[4] CMS Collaboration, *Measurement of the $t\bar{t}$ production cross section in the $e\mu$ channel in proton–proton collisions at $\sqrt{s}$ = 7 and 8 TeV*, JHEP **08** (2016) 029, arXiv:1603.02303 [hep-ex].

[5] CMS Collaboration, *Measurements of the $t\bar{t}$ production cross section in lepton+jets final states in pp collisions at 8 TeV and ratio of 8 to 7 TeV cross sections*, (2016), arXiv:1602.09024 [hep-ex].

[6] CMS Collaboration, *Measurement of the $t\bar{t}$ production cross section in pp collisions at $\sqrt{s}$ = 7 TeV with lepton + jets final states*, Phys. Lett. B **720** (2013) 83, arXiv:1212.6682 [hep-ex].

[7] CMS Collaboration, *Measurement of the top quark pair production cross section in proton-proton collisions at $\sqrt{s}$ = 13 TeV*, Phys. Rev. Lett. **116** (2016) 052002, arXiv:1510.05302 [hep-ex].

[8] ATLAS Collaboration, *Measurement of the inclusive $W^{\pm}$ and Z/γ^{*} cross sections in the e and μ decay channels in pp collisions at $\sqrt{s}$ = 7 TeV with the ATLAS detector*, Phys. Rev. D **85** (2012) 072004, arXiv:1109.5141 [hep-ex].

[9] ATLAS Collaboration, *Precision measurement and interpretation of inclusive W^{+}, W^{-} and Z/γ^{*} production cross sections with the ATLAS detector*, (2016), arXiv:1612.03016 [hep-ex].

[10] ATLAS Collaboration, *Measurement of the transverse momentum and ϕ^{*}_{η} distributions of Drell-Yan lepton pairs in proton–proton collisions at $\sqrt{s}$ = 8 TeV with the ATLAS detector*, Eur. Phys. J. C **76** (2016) 291, arXiv:1512.02192 [hep-ex].

[11] ATLAS Collaboration, *Measurement of $W^{\pm}$ and Z-boson production cross sections in pp collisions at $\sqrt{s}$ = 13 TeV with the ATLAS detector*, Phys. Lett. B **759** (2016) 601–621, arXiv:1603.09222 [hep-ex].

[12] CMS Collaboration, *Measurement of the inclusive W and Z production cross sections in pp collisions at $\sqrt{s}$ = 7 TeV with the CMS experiment*, JHEP **10** (2011) 132, arXiv:1107.4789 [hep-ex].

[13] CMS Collaboration, *Measurement of inclusive W and Z boson production cross sections in pp collisions at $\sqrt{s}$ = 8 TeV*, Phys. Rev. Lett. **112** (2014) 191802, arXiv:1402.0923 [hep-ex].

[14] CMS Collaboration, *Measurement of the differential and double-differential Drell-Yan cross sections in proton-proton collisions at $\sqrt{s}$ = 7 TeV*, JHEP **12** (2013) 030, arXiv:1310.7291 [hep-ex].

[15] CMS Collaboration, *Measurements of differential and double-differential Drell-Yan cross sections in proton-proton collisions at 8 TeV*, Eur. Phys. J. C **75** (2015) 147, arXiv:1412.1115 [hep-ex].

[16] ATLAS Collaboration, *The ATLAS Experiment at the CERN Large Hadron Collider*, JINST **3** (2008) S08003.

[17] CMS Collaboration, *The CMS experiment at the CERN LHC*, JINST **3** (2008) S08004.

[18] L. Evans and P. Bryant, *LHC Machine*, JINST **3** (2008) S08001.

[19] ATLAS Collaboration, *Improved luminosity determination in pp collisions at $\sqrt{s} = 7$ TeV using the ATLAS detector at the LHC*, Eur. Phys. J. C **73** (2013) 2518, arXiv:1302.4393 [hep-ex].

[20] ATLAS Collaboration, *Luminosity determination in pp collisions at $\sqrt{s} = 8$ TeV using the ATLAS detector at the LHC*, Eur. Phys. J. C **76** (2016) 653, arXiv:1608.03953 [hep-ex].

[21] M. Czakon, P. Fiedler and A. Mitov, *Total Top-Quark Pair-Production Cross Section at Hadron Colliders Through $O(\alpha_S^4)$*, Phys. Rev. Lett. **110** (2013) 252004, arXiv:1303.6254 [hep-ph].

[22] M. Czakon and A. Mitov, *NNLO corrections to top pair production at hadron colliders: the quark-gluon reaction*, JHEP **01** (2013) 080, arXiv:1210.6832 [hep-ph].

[23] M. Czakon and A. Mitov, *NNLO corrections to top-pair production at hadron colliders: the all-fermionic scattering channels*, JHEP **12** (2012) 054, arXiv:1207.0236 [hep-ph].

[24] P. Baernreuther, M. Czakon and A. Mitov, *Percent Level Precision Physics at the Tevatron: First Genuine NNLO QCD Corrections to $q\bar{q} \to t\bar{t} + X$*, Phys. Rev. Lett. **109** (2012) 132001, arXiv:1204.5201 [hep-ph].

[25] M. Cacciari et al., *Top-pair production at hadron colliders with next-to-next-to-leading logarithmic soft-gluon resummation*, Phys. Lett. B **710** (2012) 612–622, arXiv:1111.5869 [hep-ph].

[26] M. Beneke et al., *Hadronic top-quark pair production with NNLL threshold resummation*, Nucl. Phys. B **855** (2012) 695–741, arXiv:1109.1536 [hep-ph].

[27] M. Czakon and A. Mitov, *Top++: A Program for the Calculation of the Top-Pair Cross-Section at Hadron Colliders*, Comput. Phys. Commun. **185** (2014) 2930, arXiv:1112.5675 [hep-ph].

[28] S. Catani and M. Grazzini, *An NNLO subtraction formalism in hadron collisions and its application to Higgs boson production at the LHC*, Phys. Rev. Lett. **98** (2007) 222002, arXiv:hep-ph/0703012 [hep-ph].

[29] S. Catani et al., *Vector boson production at hadron colliders: a fully exclusive QCD calculation at NNLO*, Phys. Rev. Lett. **103** (2009) 082001, arXiv:0903.2120 [hep-ph].

[30] C. Anastasiou et al., *High precision QCD at hadron colliders: Electroweak gauge boson rapidity distributions at NNLO*, Phys. Rev. D **69** (2004) 094008, arXiv:hep-ph/0312266 [hep-ph].

[31] R. Gavin et al., *FEWZ 2.0: A code for hadronic Z production at next-to-next-to-leading order*, Comput. Phys. Commun. **182** (2011) 2388, arXiv:1011.3540 [hep-ph].

[32] R. Gavin et al., *W Physics at the LHC with FEWZ 2.1*, Comput. Phys. Commun. **184** (2013) 209, arXiv:1201.5896 [hep-ph].

[33] Y. Li and F. Petriello,
Combining QCD and electroweak corrections to dilepton production in FEWZ,
Phys. Rev. D **86** (2012) 094034, arXiv:1208.5967 [hep-ph].

[34] D. Bardin et al., *SANC integrator in the progress: QCD and EW contributions*,
JETP Lett. **96** (2012) 285, arXiv:1207.4400 [hep-ph].

[35] A. B. Arbuzov, R. R. Sadykov and Z. Was,
QED Bremsstrahlung in decays of electroweak bosons, Eur. Phys. J. C **73** (2013) 2625,
arXiv:1212.6783 [hep-ph].

[36] J. Rojo et al.,
The PDF4LHC report on PDFs and LHC data: Results from Run I and preparation for Run II,
J. Phys. G **42** (2015) 103103, arXiv:1507.00556 [hep-ph].

[37] M. L. Mangano and J. Rojo, *Cross Section Ratios between different CM energies at the LHC: opportunities for precision measurements and BSM sensitivity*, JHEP **08** (2012) 010,
arXiv:1206.3557 [hep-ph].

[38] ATLAS Collaboration, *ATLAS Insertable B-Layer Technical Design Report*,
ATLAS-TDR-19 (2010), URL: https://cdsweb.cern.ch/record/1291633.

[39] ATLAS Collaboration, *2015 start-up trigger menu and initial performance assessment of the ATLAS trigger using Run-2 data*, ATL-DAQ-PUB-2016-001, 2016,
URL: https://cdsweb.cern.ch/record/2136007.

[40] W. F. L. Hollik, *Radiative Corrections in the Standard Model and their Role for Precision Tests of the Electroweak Theory*, Fortsch. Phys. **38** (1990) 165–260.

[41] S. Dittmaier and M. Huber, *Radiative corrections to the neutral-current Drell-Yan process in the Standard Model and its minimal supersymmetric extension*, JHEP **01** (2010) 060,
arXiv:0911.2329 [hep-ph].

[42] S. Dulat et al.,
New parton distribution functions from a global analysis of quantum chromodynamics,
Phys. Rev. D **93** (2016) 033006, arXiv:1506.07443 [hep-ph].

[43] R. D. Ball et al., *Parton distributions for the LHC Run II*, JHEP **04** (2015) 040,
arXiv:1410.8849 [hep-ph].

[44] L. A. Harland-Lang et al., *Parton distributions in the LHC era: MMHT 2014 PDFs*,
Eur. Phys. J. C **75** (2015) 204, arXiv:1412.3989 [hep-ph].

[45] S. Alekhin, J. Bluemlein and S. Moch, *The ABM parton distributions tuned to LHC data*,
Phys. Rev. D **89** (2014) 054028, arXiv:1310.3059 [hep-ph].

[46] H. Abramowicz et al., *Combination of measurements of inclusive deep inelastic $e^{\pm}p$ scattering cross sections and QCD analysis of HERA data*, Eur. Phys. J. C **75** (2015) 580,
arXiv:1506.06042 [hep-ex].

[47] ATLAS Collaboration, *Determination of the strange quark density of the proton from ATLAS measurements of the $W \to \ell\nu$ and $Z \to \ell\ell$ cross sections*, Phys. Rev. Lett. **109** (2012) 012001,
arXiv:1203.4051 [hep-ex].

[48] M. Aliev et al., *HATHOR: HAdronic Top and Heavy quarks crOss section calculatoR*,
Comput. Phys. Commun. **182** (2011) 1034–1046, arXiv:1007.1327 [hep-ph].

[49] S. Agostinelli et al., *GEANT4: A Simulation toolkit*, Nucl. Instrum. Meth. A **506** (2003) 250.

[50] ATLAS Collaboration, *The ATLAS Simulation Infrastructure*, Eur. Phys. J. C **70** (2010) 823, arXiv:1005.4568 [hep-ex].

[51] P. Nason, *A New method for combining NLO QCD with shower Monte Carlo algorithms*, JHEP **11** (2004) 040, arXiv:hep-ph/0409146 [hep-ph].

[52] S. Frixione, P. Nason and C. Oleari, *Matching NLO QCD computations with Parton Shower simulations: the POWHEG method*, JHEP **11** (2007) 070, arXiv:0709.2092 [hep-ph].

[53] S. Alioli et al., *A general framework for implementing NLO calculations in shower Monte Carlo programs: the POWHEG BOX*, JHEP **06** (2010) 043, arXiv:1002.2581 [hep-ph].

[54] S. Alioli et al., *NLO vector-boson production matched with shower in POWHEG*, JHEP **07** (2008) 060, arXiv:0805.4802 [hep-ph].

[55] S. Frixione, P. Nason and G. Ridolfi, *A Positive-weight next-to-leading-order Monte Carlo for heavy flavour hadroproduction*, JHEP **09** (2007) 126, arXiv:0707.3088 [hep-ph].

[56] T. Sjöstrand, S. Mrenna and P. Z. Skands, *A Brief Introduction to PYTHIA 8.1*, Comput. Phys. Commun. **178** (2008) 852, arXiv:0710.3820 [hep-ph].

[57] H.-L. Lai et al., *New parton distributions for collider physics*, Phys. Rev. D **82** (2010) 074024, arXiv:1007.2241 [hep-ph].

[58] ATLAS Collaboration, *Measurement of the Z/γ^* boson transverse momentum distribution in pp collisions at $\sqrt{s} = 7$ TeV with the ATLAS detector*, JHEP **09** (2014) 145, arXiv:1406.3660 [hep-ex].

[59] J. Pumplin et al., *New generation of parton distributions with uncertainties from global QCD analysis*, JHEP **07** (2002) 012, arXiv:hep-ph/0201195 [hep-ph].

[60] D. J. Lange, *The EvtGen particle decay simulation package*, Nucl. Instrum. Meth. A **462** (2001) 152.

[61] P. Golonka and Z. Was, *PHOTOS Monte Carlo: A Precision tool for QED corrections in Z and W decays*, Eur. Phys. J. C **45** (2006) 97, arXiv:hep-ph/0506026 [hep-ph].

[62] N. Davidson, T. Przedzinski and Z. Was, *PHOTOS Interface in C++: Technical and Physics Documentation*, Comput. Phys. Commun. **199** (2016) 86, arXiv:1011.0937 [hep-ph].

[63] T. Sjöstrand, S. Mrenna and P. Z. Skands, *PYTHIA 6.4 Physics and Manual*, JHEP **05** (2006) 026, arXiv:hep-ph/0603175 [hep-ph].

[64] P. Z. Skands, *Tuning Monte Carlo Generators: The Perugia Tunes*, Phys. Rev. D **82** (2010) 074018, arXiv:1005.3457 [hep-ph].

[65] T. Gleisberg et al., *Event generation with SHERPA 1.1*, JHEP **02** (2009) 007, arXiv:0811.4622 [hep-ph].

[66] ATLAS Collaboration, *Summary of ATLAS Pythia 8 tunes*, ATL-PHYS-PUB-2012-003, 2012, URL: https://cdsweb.cern.ch/record/1474107.

[67] A. D. Martin et al., *Parton distributions for the LHC*, Eur. Phys. J. C **63** (2009) 189, arXiv:0901.0002 [hep-ph].

[68] ATLAS Collaboration, *Electron efficiency measurements with the ATLAS detector using the 2015 LHC proton-proton collision data*, ATLAS-CONF-2016-024, 2016, URL: https://cdsweb.cern.ch/record/2157687.

[69] ATLAS Collaboration, *Muon reconstruction performance of the ATLAS detector in proton–proton collision data at $\sqrt{s}$ =13 TeV*, Eur. Phys. J. C **76** (2016) 292, arXiv:1603.05598 [hep-ex].

[70] ATLAS Collaboration, *Measurements of fiducial cross-sections for $t\bar{t}$ production with one or two additional b-jets in pp collisions at $\sqrt{s}$ = 8 TeV using the ATLAS detector*, Eur. Phys. J. C **76** (2016) 11, arXiv:1508.06868 [hep-ex].

[71] ATLAS Collaboration, *Measurements of fiducial and differential cross sections for Higgs boson production in the diphoton decay channel at $\sqrt{s}$ = 8 TeV with ATLAS*, JHEP **09** (2014) 112, arXiv:1407.4222 [hep-ex].

[72] J. Wenninger, *Energy Calibration of the LHC Beams at 4 TeV*, CERN-ATS-2013-040, 2013, URL: https://cdsweb.cern.ch/record/1546734.

[73] The source code of VRAP 0.9 may be found at http://www.slac.stanford.edu/~lance/Vrap/.

[74] A. Glazov, *Averaging of DIS cross section data*, AIP Conf. Proc. **792** (2005) 237.

[75] F. D. Aaron et al., *Measurement of the Inclusive ep Scattering Cross Section at Low Q^2 and x at HERA*, Eur. Phys. J. C **63** (2009) 625, arXiv:0904.0929 [hep-ex].

[76] ATLAS Collaboration, *Measurement of the $t\bar{t}$ production cross-section using $e\mu$ events with b-tagged jets in pp collisions at $\sqrt{s}$ = 7 and 8 TeV with the ATLAS detector*, Eur. Phys. J. C **74** (2014) 3109, arXiv:1406.5375 [hep-ex].

[77] J. Butterworth et al., *PDF4LHC recommendations for LHC Run II*, J. Phys. G **43** (2016) 023001, arXiv:1510.03865 [hep-ph].

[78] S. Alekhin et al., *HERAFitter, Open Source QCD Fit Project*, Eur. Phys. J. C **75** (2015) 304, arXiv:1410.4412 [hep-ph].

[79] H. Paukkunen and P. Zurita, *PDF reweighting in the Hessian matrix approach*, JHEP **12** (2014) 100, arXiv:1402.6623 [hep-ph].

[80] S. Camarda et al., *QCD analysis of W- and Z-boson production at Tevatron*, Eur. Phys. J. C **75** (2015) 458, arXiv:1503.05221 [hep-ph].

[81] ATLAS Collaboration, *ATLAS Computing Acknowledgements 2016–2017*, ATL-GEN-PUB-2016-002, 2016, URL: https://cdsweb.cern.ch/record/2202407.

[82] G. Corcella et al., *HERWIG 6: An Event generator for hadron emission reactions with interfering gluons (including supersymmetric processes)*, JHEP **01** (2001) 010, arXiv:hep-ph/0011363 [hep-ph].

The ATLAS Collaboration

M. Aaboud[137d], G. Aad[88], B. Abbott[115], J. Abdallah[8], O. Abdinov[12], B. Abeloos[119], S.H. Abidi[161], O.S. AbouZeid[139], N.L. Abraham[151], H. Abramowicz[155], H. Abreu[154], R. Abreu[118], Y. Abulaiti[148a,148b], B.S. Acharya[167a,167b,a], S. Adachi[157], L. Adamczyk[41a], D.L. Adams[27], J. Adelman[110], T. Adye[133], A.A. Affolder[139], T. Agatonovic-Jovin[14], C. Agheorghiesei[28b], J.A. Aguilar-Saavedra[128a,128f], S.P. Ahlen[24], F. Ahmadov[68,b], G. Aielli[135a,135b], S. Akatsuka[71], H. Akerstedt[148a,148b], T.P.A. Åkesson[84], A.V. Akimov[98], G.L. Alberghi[22a,22b], J. Albert[172], M.J. Alconada Verzini[74], M. Aleksa[32], I.N. Aleksandrov[68], C. Alexa[28b], G. Alexander[155], T. Alexopoulos[10], M. Alhroob[115], B. Ali[130], M. Aliev[76a,76b], G. Alimonti[94a], J. Alison[33], S.P. Alkire[38], B.M.M. Allbrooke[151], B.W. Allen[118], P.P. Allport[19], A. Aloisio[106a,106b], A. Alonso[39], F. Alonso[74], C. Alpigiani[140], A.A. Alshehri[56], M. Alstaty[88], B. Alvarez Gonzalez[32], D. Álvarez Piqueras[170], M.G. Alviggi[106a,106b], B.T. Amadio[16], Y. Amaral Coutinho[26a], C. Amelung[25], D. Amidei[92], S.P. Amor Dos Santos[128a,128c], A. Amorim[128a,128b], S. Amoroso[32], G. Amundsen[25], C. Anastopoulos[141], L.S. Ancu[52], N. Andari[19], T. Andeen[11], C.F. Anders[60b], J.K. Anders[77], K.J. Anderson[33], A. Andreazza[94a,94b], V. Andrei[60a], S. Angelidakis[9], I. Angelozzi[109], A. Angerami[38], F. Anghinolfi[32], A.V. Anisenkov[111,c], N. Anjos[13], A. Annovi[126a,126b], C. Antel[60a], M. Antonelli[50], A. Antonov[100,*], D.J. Antrim[166], F. Anulli[134a], M. Aoki[69], L. Aperio Bella[19], G. Arabidze[93], Y. Arai[69], J.P. Araque[128a], V. Araujo Ferraz[26a], A.T.H. Arce[48], F.A. Arduh[74], J-F. Arguin[97], S. Argyropoulos[66], M. Arik[20a], A.J. Armbruster[145], L.J. Armitage[79], O. Arnaez[32], H. Arnold[51], M. Arratia[30], O. Arslan[23], A. Artamonov[99], G. Artoni[122], S. Artz[86], S. Asai[157], N. Asbah[45], A. Ashkenazi[155], B. Åsman[148a,148b], L. Asquith[151], K. Assamagan[27], R. Astalos[146a], M. Atkinson[169], N.B. Atlay[143], K. Augsten[130], G. Avolio[32], B. Axen[16], M.K. Ayoub[119], G. Azuelos[97,d], A.E. Baas[60a], M.J. Baca[19], H. Bachacou[138], K. Bachas[76a,76b], M. Backes[122], M. Backhaus[32], P. Bagiacchi[134a,134b], P. Bagnaia[134a,134b], J.T. Baines[133], M. Bajic[39], O.K. Baker[179], E.M. Baldin[111,c], P. Balek[175], T. Balestri[150], F. Balli[138], W.K. Balunas[124], E. Banas[42], Sw. Banerjee[176,e], A.A.E. Bannoura[178], L. Barak[32], E.L. Barberio[91], D. Barberis[53a,53b], M. Barbero[88], T. Barillari[103], M-S Barisits[32], T. Barklow[145], N. Barlow[30], S.L. Barnes[87], B.M. Barnett[133], R.M. Barnett[16], Z. Barnovska-Blenessy[36a], A. Baroncelli[136a], G. Barone[25], A.J. Barr[122], L. Barranco Navarro[170], F. Barreiro[85], J. Barreiro Guimarães da Costa[35a], R. Bartoldus[145], A.E. Barton[75], P. Bartos[146a], A. Basalaev[125], A. Bassalat[119,f], R.L. Bates[56], S.J. Batista[161], J.R. Batley[30], M. Battaglia[139], M. Bauce[134a,134b], F. Bauer[138], H.S. Bawa[145,g], J.B. Beacham[113], M.D. Beattie[75], T. Beau[83], P.H. Beauchemin[165], P. Bechtle[23], H.P. Beck[18,h], K. Becker[122], M. Becker[86], M. Beckingham[173], C. Becot[112], A.J. Beddall[20e], A. Beddall[20b], V.A. Bednyakov[68], M. Bedognetti[109], C.P. Bee[150], L.J. Beemster[109], T.A. Beermann[32], M. Begel[27], J.K. Behr[45], A.S. Bell[81], G. Bella[155], L. Bellagamba[22a], A. Bellerive[31], M. Bellomo[89], K. Belotskiy[100], O. Beltramello[32], N.L. Belyaev[100], O. Benary[155,*], D. Benchekroun[137a], M. Bender[102], K. Bendtz[148a,148b], N. Benekos[10], Y. Benhammou[155], E. Benhar Noccioli[179], J. Benitez[66], D.P. Benjamin[48], M. Benoit[52], J.R. Bensinger[25], S. Bentvelsen[109], L. Beresford[122], M. Beretta[50], D. Berge[109], E. Bergeaas Kuutmann[168], N. Berger[5], J. Beringer[16], S. Berlendis[58], N.R. Bernard[89], G. Bernardi[83], C. Bernius[112], F.U. Bernlochner[23], T. Berry[80], P. Berta[131], C. Bertella[86], G. Bertoli[148a,148b], F. Bertolucci[126a,126b], I.A. Bertram[75], C. Bertsche[45], D. Bertsche[115], G.J. Besjes[39], O. Bessidskaia Bylund[148a,148b], M. Bessner[45], N. Besson[138], C. Betancourt[51], A. Bethani[58], S. Bethke[103], A.J. Bevan[79], R.M. Bianchi[127], M. Bianco[32], O. Biebel[102], D. Biedermann[17], R. Bielski[87], N.V. Biesuz[126a,126b], M. Biglietti[136a], J. Bilbao De Mendizabal[52], T.R.V. Billoud[97], H. Bilokon[50], M. Bindi[57], A. Bingul[20b], C. Bini[134a,134b], S. Biondi[22a,22b], T. Bisanz[57], C. Bittrich[47], D.M. Bjergaard[48], C.W. Black[152], J.E. Black[145], K.M. Black[24], D. Blackburn[140], R.E. Blair[6], T. Blazek[146a], I. Bloch[45], C. Blocker[25], A. Blue[56], W. Blum[86,*], U. Blumenschein[57],

S. Blunier[34a], G.J. Bobbink[109], V.S. Bobrovnikov[111,c], S.S. Bocchetta[84], A. Bocci[48], C. Bock[102], M. Boehler[51], D. Boerner[178], D. Bogavac[102], A.G. Bogdanchikov[111], C. Bohm[148a], V. Boisvert[80], P. Bokan[168], T. Bold[41a], A.S. Boldyrev[101], M. Bomben[83], M. Bona[79], M. Boonekamp[138], A. Borisov[132], G. Borissov[75], J. Bortfeldt[32], D. Bortoletto[122], V. Bortolotto[62a,62b,62c], K. Bos[109], D. Boscherini[22a], M. Bosman[13], J.D. Bossio Sola[29], J. Boudreau[127], J. Bouffard[2], E.V. Bouhova-Thacker[75], D. Boumediene[37], C. Bourdarios[119], S.K. Boutle[56], A. Boveia[113], J. Boyd[32], I.R. Boyko[68], J. Bracinik[19], A. Brandt[8], G. Brandt[57], O. Brandt[60a], U. Bratzler[158], B. Brau[89], J.E. Brau[118], W.D. Breaden Madden[56], K. Brendlinger[45], A.J. Brennan[91], L. Brenner[109], R. Brenner[168], S. Bressler[175], T.M. Bristow[49], D. Britton[56], D. Britzger[45], F.M. Brochu[30], I. Brock[23], R. Brock[93], G. Brooijmans[38], T. Brooks[80], W.K. Brooks[34b], J. Brosamer[16], E. Brost[110], J.H Broughton[19], P.A. Bruckman de Renstrom[42], D. Bruncko[146b], A. Bruni[22a], G. Bruni[22a], L.S. Bruni[109], BH Brunt[30], M. Bruschi[22a], N. Bruscino[23], P. Bryant[33], L. Bryngemark[84], T. Buanes[15], Q. Buat[144], P. Buchholz[143], A.G. Buckley[56], I.A. Budagov[68], F. Buehrer[51], M.K. Bugge[121], O. Bulekov[100], D. Bullock[8], H. Burckhart[32], S. Burdin[77], C.D. Burgard[51], A.M. Burger[5], B. Burghgrave[110], K. Burka[42], S. Burke[133], I. Burmeister[46], J.T.P. Burr[122], E. Busato[37], D. Büscher[51], V. Büscher[86], P. Bussey[56], J.M. Butler[24], C.M. Buttar[56], J.M. Butterworth[81], P. Butti[109], W. Buttinger[27], A. Buzatu[35c], A.R. Buzykaev[111,c], S. Cabrera Urbán[170], D. Caforio[130], V.M. Cairo[40a,40b], O. Cakir[4a], N. Calace[52], P. Calafiura[16], A. Calandri[88], G. Calderini[83], P. Calfayan[64], G. Callea[40a,40b], L.P. Caloba[26a], S. Calvente Lopez[85], D. Calvet[37], S. Calvet[37], T.P. Calvet[88], R. Camacho Toro[33], S. Camarda[32], P. Camarri[135a,135b], D. Cameron[121], R. Caminal Armadans[169], C. Camincher[58], S. Campana[32], M. Campanelli[81], A. Camplani[94a,94b], A. Campoverde[143], V. Canale[106a,106b], M. Cano Bret[36c], J. Cantero[116], T. Cao[155], M.D.M. Capeans Garrido[32], I. Caprini[28b], M. Caprini[28b], M. Capua[40a,40b], R.M. Carbone[38], R. Cardarelli[135a], F. Cardillo[51], I. Carli[131], T. Carli[32], G. Carlino[106a], B.T. Carlson[127], L. Carminati[94a,94b], R.M.D. Carney[148a,148b], S. Caron[108], E. Carquin[34b], G.D. Carrillo-Montoya[32], J.R. Carter[30], J. Carvalho[128a,128c], D. Casadei[19], M.P. Casado[13,i], M. Casolino[13], D.W. Casper[166], R. Castelijn[109], A. Castelli[109], V. Castillo Gimenez[170], N.F. Castro[128a,j], A. Catinaccio[32], J.R. Catmore[121], A. Cattai[32], J. Caudron[23], V. Cavaliere[169], E. Cavallaro[13], D. Cavalli[94a], M. Cavalli-Sforza[13], V. Cavasinni[126a,126b], F. Ceradini[136a,136b], L. Cerda Alberich[170], A.S. Cerqueira[26b], A. Cerri[151], L. Cerrito[135a,135b], F. Cerutti[16], A. Cervelli[18], S.A. Cetin[20d], A. Chafaq[137a], D. Chakraborty[110], S.K. Chan[59], W.S. Chan[62a], Y.L. Chan[62a], P. Chang[169], J.D. Chapman[30], D.G. Charlton[19], A. Chatterjee[52], C.C. Chau[161], C.A. Chavez Barajas[151], S. Che[113], S. Cheatham[167a,167c], A. Chegwidden[93], S. Chekanov[6], S.V. Chekulaev[163a], G.A. Chelkov[68,k], M.A. Chelstowska[32], C. Chen[67], H. Chen[27], S. Chen[35b], S. Chen[157], X. Chen[35c,l], Y. Chen[70], H.C. Cheng[92], H.J. Cheng[35a], Y. Cheng[33], A. Cheplakov[68], E. Cheremushkina[132], R. Cherkaoui El Moursli[137e], V. Chernyatin[27,*], E. Cheu[7], L. Chevalier[138], V. Chiarella[50], G. Chiarelli[126a,126b], G. Chiodini[76a], A.S. Chisholm[32], A. Chitan[28b], Y.H. Chiu[172], M.V. Chizhov[68], K. Choi[64], A.R. Chomont[37], S. Chouridou[9], B.K.B. Chow[102], V. Christodoulou[81], D. Chromek-Burckhart[32], J. Chudoba[129], A.J. Chuinard[90], J.J. Chwastowski[42], L. Chytka[117], A.K. Ciftci[4a], D. Cinca[46], V. Cindro[78], I.A. Cioara[23], C. Ciocca[22a,22b], A. Ciocio[16], F. Cirotto[106a,106b], Z.H. Citron[175], M. Citterio[94a], M. Ciubancan[28b], A. Clark[52], B.L. Clark[59], M.R. Clark[38], P.J. Clark[49], R.N. Clarke[16], C. Clement[148a,148b], Y. Coadou[88], M. Cobal[167a,167c], A. Coccaro[52], J. Cochran[67], L. Colasurdo[108], B. Cole[38], A.P. Colijn[109], J. Collot[58], T. Colombo[166], P. Conde Muiño[128a,128b], E. Coniavitis[51], S.H. Connell[147b], I.A. Connelly[80], V. Consorti[51], S. Constantinescu[28b], G. Conti[32], F. Conventi[106a,m], M. Cooke[16], B.D. Cooper[81], A.M. Cooper-Sarkar[122], F. Cormier[171], K.J.R. Cormier[161], T. Cornelissen[178], M. Corradi[134a,134b], F. Corriveau[90,n], A. Cortes-Gonzalez[32], G. Cortiana[103], G. Costa[94a], M.J. Costa[170], D. Costanzo[141], G. Cottin[30], G. Cowan[80], B.E. Cox[87], K. Cranmer[112], S.J. Crawley[56], R.A. Creager[124], G. Cree[31], S. Crépé-Renaudin[58], F. Crescioli[83], W.A. Cribbs[148a,148b], M. Crispin Ortuzar[122], M. Cristinziani[23], V. Croft[108], G. Crosetti[40a,40b], A. Cueto[85],

T. Cuhadar Donszelmann[141], J. Cummings[179], M. Curatolo[50], J. Cúth[86], H. Czirr[143], P. Czodrowski[3], G. D'amen[22a,22b], S. D'Auria[56], M. D'Onofrio[77], M.J. Da Cunha Sargedas De Sousa[128a,128b], C. Da Via[87], W. Dabrowski[41a], T. Dado[146a], T. Dai[92], O. Dale[15], F. Dallaire[97], C. Dallapiccola[89], M. Dam[39], J.R. Dandoy[124], N.P. Dang[51], A.C. Daniells[19], N.S. Dann[87], M. Danninger[171], M. Dano Hoffmann[138], V. Dao[51], G. Darbo[53a], S. Darmora[8], J. Dassoulas[3], A. Dattagupta[118], T. Daubney[45], W. Davey[23], C. David[45], T. Davidek[131], M. Davies[155], P. Davison[81], E. Dawe[91], I. Dawson[141], K. De[8], R. de Asmundis[106a], A. De Benedetti[115], S. De Castro[22a,22b], S. De Cecco[83], N. De Groot[108], P. de Jong[109], H. De la Torre[93], F. De Lorenzi[67], A. De Maria[57], D. De Pedis[134a], A. De Salvo[134a], U. De Sanctis[151], A. De Santo[151], J.B. De Vivie De Regie[119], W.J. Dearnaley[75], R. Debbe[27], C. Debenedetti[139], D.V. Dedovich[68], N. Dehghanian[3], I. Deigaard[109], M. Del Gaudio[40a,40b], J. Del Peso[85], T. Del Prete[126a,126b], D. Delgove[119], F. Deliot[138], C.M. Delitzsch[52], A. Dell'Acqua[32], L. Dell'Asta[24], M. Dell'Orso[126a,126b], M. Della Pietra[106a,m], D. della Volpe[52], M. Delmastro[5], P.A. Delsart[58], D.A. DeMarco[161], S. Demers[179], M. Demichev[68], A. Demilly[83], S.P. Denisov[132], D. Denysiuk[138], D. Derendarz[42], J.E. Derkaoui[137d], F. Derue[83], P. Dervan[77], K. Desch[23], C. Deterre[45], K. Dette[46], P.O. Deviveiros[32], A. Dewhurst[133], S. Dhaliwal[25], A. Di Ciaccio[135a,135b], L. Di Ciaccio[5], W.K. Di Clemente[124], C. Di Donato[106a,106b], A. Di Girolamo[32], B. Di Girolamo[32], B. Di Micco[136a,136b], R. Di Nardo[32], K.F. Di Petrillo[59], A. Di Simone[51], R. Di Sipio[161], D. Di Valentino[31], C. Diaconu[88], M. Diamond[161], F.A. Dias[49], M.A. Diaz[34a], E.B. Diehl[92], J. Dietrich[17], S. Díez Cornell[45], A. Dimitrievska[14], J. Dingfelder[23], P. Dita[28b], S. Dita[28b], F. Dittus[32], F. Djama[88], T. Djobava[54b], J.I. Djuvsland[60a], M.A.B. do Vale[26c], D. Dobos[32], M. Dobre[28b], C. Doglioni[84], J. Dolejsi[131], Z. Dolezal[131], M. Donadelli[26d], S. Donati[126a,126b], P. Dondero[123a,123b], J. Donini[37], J. Dopke[133], A. Doria[106a], M.T. Dova[74], A.T. Doyle[56], E. Drechsler[57], M. Dris[10], Y. Du[36b], J. Duarte-Campderros[155], E. Duchovni[175], G. Duckeck[102], O.A. Ducu[97,o], D. Duda[109], A. Dudarev[32], A.Chr. Dudder[86], E.M. Duffield[16], L. Duflot[119], M. Dührssen[32], M. Dumancic[175], A.K. Duncan[56], M. Dunford[60a], H. Duran Yildiz[4a], M. Düren[55], A. Durglishvili[54b], D. Duschinger[47], B. Dutta[45], M. Dyndal[45], C. Eckardt[45], K.M. Ecker[103], R.C. Edgar[92], T. Eifert[32], G. Eigen[15], K. Einsweiler[16], T. Ekelof[168], M. El Kacimi[137c], V. Ellajosyula[88], M. Ellert[168], S. Elles[5], F. Ellinghaus[178], A.A. Elliot[172], N. Ellis[32], J. Elmsheuser[27], M. Elsing[32], D. Emeliyanov[133], Y. Enari[157], O.C. Endner[86], J.S. Ennis[173], J. Erdmann[46], A. Ereditato[18], G. Ernis[178], J. Ernst[2], M. Ernst[27], S. Errede[169], E. Ertel[86], M. Escalier[119], H. Esch[46], C. Escobar[127], B. Esposito[50], A.I. Etienvre[138], E. Etzion[155], H. Evans[64], A. Ezhilov[125], M. Ezzi[137e], F. Fabbri[22a,22b], L. Fabbri[22a,22b], G. Facini[33], R.M. Fakhrutdinov[132], S. Falciano[134a], R.J. Falla[81], J. Faltova[32], Y. Fang[35a], M. Fanti[94a,94b], A. Farbin[8], A. Farilla[136a], C. Farina[127], E.M. Farina[123a,123b], T. Farooque[93], S. Farrell[16], S.M. Farrington[173], P. Farthouat[32], F. Fassi[137e], P. Fassnacht[32], D. Fassouliotis[9], M. Faucci Giannelli[80], A. Favareto[53a,53b], W.J. Fawcett[122], L. Fayard[119], O.L. Fedin[125,p], W. Fedorko[171], S. Feigl[121], L. Feligioni[88], C. Feng[36b], E.J. Feng[32], H. Feng[92], A.B. Fenyuk[132], L. Feremenga[8], P. Fernandez Martinez[170], S. Fernandez Perez[13], J. Ferrando[45], A. Ferrari[168], P. Ferrari[109], R. Ferrari[123a], D.E. Ferreira de Lima[60b], A. Ferrer[170], D. Ferrere[52], C. Ferretti[92], F. Fiedler[86], A. Filipčič[78], M. Filipuzzi[45], F. Filthaut[108], M. Fincke-Keeler[172], K.D. Finelli[152], M.C.N. Fiolhais[128a,128c], L. Fiorini[170], A. Fischer[2], C. Fischer[13], J. Fischer[178], W.C. Fisher[93], N. Flaschel[45], I. Fleck[143], P. Fleischmann[92], G.T. Fletcher[141], R.R.M. Fletcher[124], T. Flick[178], B.M. Flierl[102], L.R. Flores Castillo[62a], M.J. Flowerdew[103], G.T. Forcolin[87], A. Formica[138], A. Forti[87], A.G. Foster[19], D. Fournier[119], H. Fox[75], S. Fracchia[13], P. Francavilla[83], M. Franchini[22a,22b], D. Francis[32], L. Franconi[121], M. Franklin[59], M. Frate[166], M. Fraternali[123a,123b], D. Freeborn[81], S.M. Fressard-Batraneanu[32], D. Froidevaux[32], J.A. Frost[122], C. Fukunaga[158], E. Fullana Torregrosa[86], T. Fusayasu[104], J. Fuster[170], C. Gabaldon[58], O. Gabizon[154], A. Gabrielli[22a,22b], A. Gabrielli[16], G.P. Gach[41a], S. Gadatsch[32], G. Gagliardi[53a,53b], L.G. Gagnon[97], P. Gagnon[64], C. Galea[108], B. Galhardo[128a,128c], E.J. Gallas[122], B.J. Gallop[133], P. Gallus[130], G. Galster[39], K.K. Gan[113],

S. Ganguly[37], J. Gao[36a], Y. Gao[77], Y.S. Gao[145,g], F.M. Garay Walls[49], C. García[170], J.E. García Navarro[170], M. Garcia-Sciveres[16], R.W. Gardner[33], N. Garelli[145], V. Garonne[121], A. Gascon Bravo[45], K. Gasnikova[45], C. Gatti[50], A. Gaudiello[53a,53b], G. Gaudio[123a], L. Gauthier[97], I.L. Gavrilenko[98], C. Gay[171], G. Gaycken[23], E.N. Gazis[10], C.N.P. Gee[133], Ch. Geich-Gimbel[23], M. Geisen[86], M.P. Geisler[60a], K. Gellerstedt[148a,148b], C. Gemme[53a], M.H. Genest[58], C. Geng[36a,q], S. Gentile[134a,134b], C. Gentsos[156], S. George[80], D. Gerbaudo[13], A. Gershon[155], S. Ghasemi[143], M. Ghneimat[23], B. Giacobbe[22a], S. Giagu[134a,134b], P. Giannetti[126a,126b], S.M. Gibson[80], M. Gignac[171], M. Gilchriese[16], T.P.S. Gillam[30], D. Gillberg[31], G. Gilles[178], D.M. Gingrich[3,d], N. Giokaris[9,*], M.P. Giordani[167a,167c], F.M. Giorgi[22a], P.F. Giraud[138], P. Giromini[59], D. Giugni[94a], F. Giuli[122], C. Giuliani[103], M. Giulini[60b], B.K. Gjelsten[121], S. Gkaitatzis[156], I. Gkialas[9], E.L. Gkougkousis[139], L.K. Gladilin[101], C. Glasman[85], J. Glatzer[13], P.C.F. Glaysher[49], A. Glazov[45], M. Goblirsch-Kolb[25], J. Godlewski[42], S. Goldfarb[91], T. Golling[52], D. Golubkov[132], A. Gomes[128a,128b,128d], R. Gonçalo[128a], R. Goncalves Gama[26a], J. Goncalves Pinto Firmino Da Costa[138], G. Gonella[51], L. Gonella[19], A. Gongadze[68], S. González de la Hoz[170], S. Gonzalez-Sevilla[52], L. Goossens[32], P.A. Gorbounov[99], H.A. Gordon[27], I. Gorelov[107], B. Gorini[32], E. Gorini[76a,76b], A. Gorišek[78], A.T. Goshaw[48], C. Gössling[46], M.I. Gostkin[68], C.R. Goudet[119], D. Goujdami[137c], A.G. Goussiou[140], N. Govender[147b,r], E. Gozani[154], L. Graber[57], I. Grabowska-Bold[41a], P.O.J. Gradin[58], P. Grafström[22a,22b], J. Gramling[52], E. Gramstad[121], S. Grancagnolo[17], V. Gratchev[125], P.M. Gravila[28e], H.M. Gray[32], E. Graziani[136a], Z.D. Greenwood[82,s], C. Grefe[23], K. Gregersen[81], I.M. Gregor[45], P. Grenier[145], K. Grevtsov[5], J. Griffiths[8], A.A. Grillo[139], K. Grimm[75], S. Grinstein[13,t], Ph. Gris[37], J.-F. Grivaz[119], S. Groh[86], E. Gross[175], J. Grosse-Knetter[57], G.C. Grossi[82], Z.J. Grout[81], L. Guan[92], W. Guan[176], J. Guenther[65], F. Guescini[163a], D. Guest[166], O. Gueta[155], B. Gui[113], E. Guido[53a,53b], T. Guillemin[5], S. Guindon[2], U. Gul[56], C. Gumpert[32], J. Guo[36c], W. Guo[92], Y. Guo[36a], R. Gupta[43], S. Gupta[122], G. Gustavino[134a,134b], P. Gutierrez[115], N.G. Gutierrez Ortiz[81], C. Gutschow[81], C. Guyot[138], C. Gwenlan[122], C.B. Gwilliam[77], A. Haas[112], C. Haber[16], H.K. Hadavand[8], N. Haddad[137e], A. Hadef[88], S. Hageböck[23], M. Hagihara[164], H. Hakobyan[180,*], M. Haleem[45], J. Haley[116], G. Halladjian[93], G.D. Hallewell[88], K. Hamacher[178], P. Hamal[117], K. Hamano[172], A. Hamilton[147a], G.N. Hamity[141], P.G. Hamnett[45], L. Han[36a], S. Han[35a], K. Hanagaki[69,u], K. Hanawa[157], M. Hance[139], B. Haney[124], P. Hanke[60a], R. Hanna[138], J.B. Hansen[39], J.D. Hansen[39], M.C. Hansen[23], P.H. Hansen[39], K. Hara[164], A.S. Hard[176], T. Harenberg[178], F. Hariri[119], S. Harkusha[95], R.D. Harrington[49], P.F. Harrison[173], F. Hartjes[109], N.M. Hartmann[102], M. Hasegawa[70], Y. Hasegawa[142], A. Hasib[49], S. Hassani[138], S. Haug[18], R. Hauser[93], L. Hauswald[47], L.B. Havener[38], M. Havranek[130], C.M. Hawkes[19], R.J. Hawkings[32], D. Hayakawa[159], D. Hayden[93], C.P. Hays[122], J.M. Hays[79], H.S. Hayward[77], S.J. Haywood[133], S.J. Head[19], T. Heck[86], V. Hedberg[84], L. Heelan[8], S. Heim[45], T. Heim[16], B. Heinemann[45,v], J.J. Heinrich[102], L. Heinrich[112], C. Heinz[55], J. Hejbal[129], L. Helary[32], S. Hellman[148a,148b], C. Helsens[32], J. Henderson[122], R.C.W. Henderson[75], Y. Heng[176], S. Henkelmann[171], A.M. Henriques Correia[32], S. Henrot-Versille[119], G.H. Herbert[17], H. Herde[25], V. Herget[177], Y. Hernández Jiménez[147c], G. Herten[51], R. Hertenberger[102], L. Hervas[32], T.C. Herwig[124], G.G. Hesketh[81], N.P. Hessey[109], J.W. Hetherly[43], E. Higón-Rodriguez[170], E. Hill[172], J.C. Hill[30], K.H. Hiller[45], S.J. Hillier[19], I. Hinchliffe[16], E. Hines[124], M. Hirose[51], D. Hirschbuehl[178], O. Hladik[129], X. Hoad[49], J. Hobbs[150], N. Hod[163a], M.C. Hodgkinson[141], P. Hodgson[141], A. Hoecker[32], M.R. Hoeferkamp[107], F. Hoenig[102], D. Hohn[23], T.R. Holmes[16], M. Homann[46], S. Honda[164], T. Honda[69], T.M. Hong[127], B.H. Hooberman[169], W.H. Hopkins[118], Y. Horii[105], A.J. Horton[144], J-Y. Hostachy[58], S. Hou[153], A. Hoummada[137a], J. Howarth[45], J. Hoya[74], M. Hrabovsky[117], I. Hristova[17], J. Hrivnac[119], T. Hryn'ova[5], A. Hrynevich[96], P.J. Hsu[63], S.-C. Hsu[140], Q. Hu[36a], S. Hu[36c], Y. Huang[35a], Z. Hubacek[130], F. Hubaut[88], F. Huegging[23], T.B. Huffman[122], E.W. Hughes[38], G. Hughes[75], M. Huhtinen[32], P. Huo[150], N. Huseynov[68,b], J. Huston[93], J. Huth[59], G. Iacobucci[52], G. Iakovidis[27], I. Ibragimov[143], L. Iconomidou-Fayard[119], Z. Idrissi[137e], P. Iengo[32], O. Igonkina[109,w], T. Iizawa[174], Y. Ikegami[69],

M. Ikeno[69], Y. Ilchenko[11,x], D. Iliadis[156], N. Ilic[145], G. Introzzi[123a,123b], P. Ioannou[9,*], M. Iodice[136a], K. Iordanidou[38], V. Ippolito[59], N. Ishijima[120], M. Ishino[157], M. Ishitsuka[159], C. Issever[122], S. Istin[20a], F. Ito[164], J.M. Iturbe Ponce[87], R. Iuppa[162a,162b], H. Iwasaki[69], J.M. Izen[44], V. Izzo[106a], S. Jabbar[3], P. Jackson[1], V. Jain[2], K.B. Jakobi[86], K. Jakobs[51], S. Jakobsen[32], T. Jakoubek[129], D.O. Jamin[116], D.K. Jana[82], R. Jansky[65], J. Janssen[23], M. Janus[57], P.A. Janus[41a], G. Jarlskog[84], N. Javadov[68,b], T. Javůrek[51], M. Javurkova[51], F. Jeanneau[138], L. Jeanty[16], J. Jejelava[54a,y], P. Jenni[51,z], C. Jeske[173], S. Jézéquel[5], H. Ji[176], J. Jia[150], H. Jiang[67], Y. Jiang[36a], Z. Jiang[145], S. Jiggins[81], J. Jimenez Pena[170], S. Jin[35a], A. Jinaru[28b], O. Jinnouchi[159], H. Jivan[147c], P. Johansson[141], K.A. Johns[7], C.A. Johnson[64], W.J. Johnson[140], K. Jon-And[148a,148b], G. Jones[173], R.W.L. Jones[75], S. Jones[7], T.J. Jones[77], J. Jongmanns[60a], P.M. Jorge[128a,128b], J. Jovicevic[163a], X. Ju[176], A. Juste Rozas[13,t], M.K. Köhler[175], A. Kaczmarska[42], M. Kado[119], H. Kagan[113], M. Kagan[145], S.J. Kahn[88], T. Kaji[174], E. Kajomovitz[48], C.W. Kalderon[84], A. Kaluza[86], S. Kama[43], A. Kamenshchikov[132], N. Kanaya[157], S. Kaneti[30], L. Kanjir[78], V.A. Kantserov[100], J. Kanzaki[69], B. Kaplan[112], L.S. Kaplan[176], A. Kapliy[33], D. Kar[147c], K. Karakostas[10], A. Karamaoun[3], N. Karastathis[10], M.J. Kareem[57], E. Karentzos[10], S.N. Karpov[68], Z.M. Karpova[68], K. Karthik[112], V. Kartvelishvili[75], A.N. Karyukhin[132], K. Kasahara[164], L. Kashif[176], R.D. Kass[113], A. Kastanas[149], Y. Kataoka[157], C. Kato[157], A. Katre[52], J. Katzy[45], K. Kawade[105], K. Kawagoe[73], T. Kawamoto[157], G. Kawamura[57], V.F. Kazanin[111,c], R. Keeler[172], R. Kehoe[43], J.S. Keller[45], J.J. Kempster[80], H. Keoshkerian[161], O. Kepka[129], B.P. Kerševan[78], S. Kersten[178], R.A. Keyes[90], M. Khader[169], F. Khalil-zada[12], A. Khanov[116], A.G. Kharlamov[111,c], T. Kharlamova[111,c], T.J. Khoo[52], V. Khovanskiy[99], E. Khramov[68], J. Khubua[54b,aa], S. Kido[70], C.R. Kilby[80], H.Y. Kim[8], S.H. Kim[164], Y.K. Kim[33], N. Kimura[156], O.M. Kind[17], B.T. King[77], D. Kirchmeier[47], J. Kirk[133], A.E. Kiryunin[103], T. Kishimoto[157], D. Kisielewska[41a], K. Kiuchi[164], O. Kivernyk[138], E. Kladiva[146b], T. Klapdor-kleingrothaus[51], M.H. Klein[38], M. Klein[77], U. Klein[77], K. Kleinknecht[86], P. Klimek[110], A. Klimentov[27], R. Klingenberg[46], T. Klioutchnikova[32], E.-E. Kluge[60a], P. Kluit[109], S. Kluth[103], J. Knapik[42], E. Kneringer[65], E.B.F.G. Knoops[88], A. Knue[103], A. Kobayashi[157], D. Kobayashi[159], T. Kobayashi[157], M. Kobel[47], M. Kocian[145], P. Kodys[131], T. Koffas[31], E. Koffeman[109], N.M. Köhler[103], T. Koi[145], H. Kolanoski[17], M. Kolb[60b], I. Koletsou[5], A.A. Komar[98,*], Y. Komori[157], T. Kondo[69], N. Kondrashova[36c], K. Köneke[51], A.C. König[108], T. Kono[69,ab], R. Konoplich[112,ac], N. Konstantinidis[81], R. Kopeliansky[64], S. Koperny[41a], A.K. Kopp[51], K. Korcyl[42], K. Kordas[156], A. Korn[81], A.A. Korol[111,c], I. Korolkov[13], E.V. Korolkova[141], O. Kortner[103], S. Kortner[103], T. Kosek[131], V.V. Kostyukhin[23], A. Kotwal[48], A. Koulouris[10], A. Kourkoumeli-Charalampidi[123a,123b], C. Kourkoumelis[9], V. Kouskoura[27], A.B. Kowalewska[42], R. Kowalewski[172], T.Z. Kowalski[41a], C. Kozakai[157], W. Kozanecki[138], A.S. Kozhin[132], V.A. Kramarenko[101], G. Kramberger[78], D. Krasnopevtsev[100], M.W. Krasny[83], A. Krasznahorkay[32], A. Kravchenko[27], J.A. Kremer[41a], M. Kretz[60c], J. Kretzschmar[77], K. Kreutzfeldt[55], P. Krieger[161], K. Krizka[33], K. Kroeninger[46], H. Kroha[103], J. Kroll[124], J. Kroseberg[23], J. Krstic[14], U. Kruchonak[68], H. Krüger[23], N. Krumnack[67], M.C. Kruse[48], M. Kruskal[24], T. Kubota[91], H. Kucuk[81], S. Kuday[4b], J.T. Kuechler[178], S. Kuehn[51], A. Kugel[60c], F. Kuger[177], T. Kuhl[45], V. Kukhtin[68], R. Kukla[138], Y. Kulchitsky[95], S. Kuleshov[34b], M. Kuna[134a,134b], T. Kunigo[71], A. Kupco[129], O. Kuprash[155], H. Kurashige[70], L.L. Kurchaninov[163a], Y.A. Kurochkin[95], M.G. Kurth[35a], V. Kus[129], E.S. Kuwertz[172], M. Kuze[159], J. Kvita[117], T. Kwan[172], D. Kyriazopoulos[141], A. La Rosa[103], J.L. La Rosa Navarro[26d], L. La Rotonda[40a,40b], C. Lacasta[170], F. Lacava[134a,134b], J. Lacey[31], H. Lacker[17], D. Lacour[83], E. Ladygin[68], R. Lafaye[5], B. Laforge[83], T. Lagouri[179], S. Lai[57], S. Lammers[64], W. Lampl[7], E. Lançon[27], U. Landgraf[51], M.P.J. Landon[79], M.C. Lanfermann[52], V.S. Lang[60a], J.C. Lange[13], A.J. Lankford[166], F. Lanni[27], K. Lantzsch[23], A. Lanza[123a], A. Lapertosa[53a,53b], S. Laplace[83], J.F. Laporte[138], T. Lari[94a], F. Lasagni Manghi[22a,22b], M. Lassnig[32], P. Laurelli[50], W. Lavrijsen[16], A.T. Law[139], P. Laycock[77], T. Lazovich[59], M. Lazzaroni[94a,94b], B. Le[91], O. Le Dortz[83], E. Le Guirriec[88], E.P. Le Quilleuc[138], M. LeBlanc[172], T. LeCompte[6], F. Ledroit-Guillon[58], C.A. Lee[27], S.C. Lee[153],

L. Lee[1], B. Lefebvre[90], G. Lefebvre[83], M. Lefebvre[172], F. Legger[102], C. Leggett[16], A. Lehan[77], G. Lehmann Miotto[32], X. Lei[7], W.A. Leight[31], A.G. Leister[179], M.A.L. Leite[26d], R. Leitner[131], D. Lellouch[175], B. Lemmer[57], K.J.C. Leney[81], T. Lenz[23], B. Lenzi[32], R. Leone[7], S. Leone[126a,126b], C. Leonidopoulos[49], S. Leontsinis[10], G. Lerner[151], C. Leroy[97], A.A.J. Lesage[138], C.G. Lester[30], M. Levchenko[125], J. Levêque[5], D. Levin[92], L.J. Levinson[175], M. Levy[19], D. Lewis[79], M. Leyton[44], B. Li[36a,q], C. Li[36a], H. Li[150], L. Li[48], L. Li[36c], Q. Li[35a], S. Li[48], X. Li[87], Y. Li[143], Z. Liang[35a], B. Liberti[135a], A. Liblong[161], K. Lie[169], J. Liebal[23], W. Liebig[15], A. Limosani[152], S.C. Lin[153,ad], T.H. Lin[86], B.E. Lindquist[150], A.E. Lionti[52], E. Lipeles[124], A. Lipniacka[15], M. Lisovyi[60b], T.M. Liss[169], A. Lister[171], A.M. Litke[139], B. Liu[153,ae], H. Liu[92], H. Liu[27], J. Liu[36b], J.B. Liu[36a], K. Liu[88], L. Liu[169], M. Liu[36a], Y.L. Liu[36a], Y. Liu[36a], M. Livan[123a,123b], A. Lleres[58], J. Llorente Merino[35a], S.L. Lloyd[79], F. Lo Sterzo[153], E.M. Lobodzinska[45], P. Loch[7], F.K. Loebinger[87], K.M. Loew[25], A. Loginov[179,*], T. Lohse[17], K. Lohwasser[45], M. Lokajicek[129], B.A. Long[24], J.D. Long[169], R.E. Long[75], L. Longo[76a,76b], K.A. Looper[113], J.A. Lopez[34b], D. Lopez Mateos[59], B. Lopez Paredes[141], I. Lopez Paz[13], A. Lopez Solis[83], J. Lorenz[102], N. Lorenzo Martinez[64], M. Losada[21], P.J. Lösel[102], X. Lou[35a], A. Lounis[119], J. Love[6], P.A. Love[75], H. Lu[62a], N. Lu[92], H.J. Lubatti[140], C. Luci[134a,134b], A. Lucotte[58], C. Luedtke[51], F. Luehring[64], W. Lukas[65], L. Luminari[134a], O. Lundberg[148a,148b], B. Lund-Jensen[149], P.M. Luzi[83], D. Lynn[27], R. Lysak[129], E. Lytken[84], V. Lyubushkin[68], H. Ma[27], L.L. Ma[36b], Y. Ma[36b], G. Maccarrone[50], A. Macchiolo[103], C.M. Macdonald[141], B. Maček[78], J. Machado Miguens[124,128b], D. Madaffari[88], R. Madar[37], H.J. Maddocks[168], W.F. Mader[47], A. Madsen[45], J. Maeda[70], S. Maeland[15], T. Maeno[27], A. Maevskiy[101], E. Magradze[57], J. Mahlstedt[109], C. Maiani[119], C. Maidantchik[26a], A.A. Maier[103], T. Maier[102], A. Maio[128a,128b,128d], S. Majewski[118], Y. Makida[69], N. Makovec[119], B. Malaescu[83], Pa. Malecki[42], V.P. Maleev[125], F. Malek[58], U. Mallik[66], D. Malon[6], C. Malone[30], S. Maltezos[10], S. Malyukov[32], J. Mamuzic[170], G. Mancini[50], L. Mandelli[94a], I. Mandić[78], J. Maneira[128a,128b], L. Manhaes de Andrade Filho[26b], J. Manjarres Ramos[163b], A. Mann[102], A. Manousos[32], B. Mansoulie[138], J.D. Mansour[35a], R. Mantifel[90], M. Mantoani[57], S. Manzoni[94a,94b], L. Mapelli[32], G. Marceca[29], L. March[52], G. Marchiori[83], M. Marcisovsky[129], M. Marjanovic[14], D.E. Marley[92], F. Marroquim[26a], S.P. Marsden[87], Z. Marshall[16], M.U.F Martensson[168], S. Marti-Garcia[170], T.A. Martin[173], V.J. Martin[49], B. Martin dit Latour[15], M. Martinez[13,t], V.I. Martinez Outschoorn[169], S. Martin-Haugh[133], V.S. Martoiu[28b], A.C. Martyniuk[81], A. Marzin[32], L. Masetti[86], T. Mashimo[157], R. Mashinistov[98], J. Masik[87], A.L. Maslennikov[111,c], L. Massa[135a,135b], P. Mastrandrea[5], A. Mastroberardino[40a,40b], T. Masubuchi[157], P. Mättig[178], J. Mattmann[86], J. Maurer[28b], S.J. Maxfield[77], D.A. Maximov[111,c], R. Mazini[153], I. Maznas[156], S.M. Mazza[94a,94b], N.C. Mc Fadden[107], G. Mc Goldrick[161], S.P. Mc Kee[92], A. McCarn[92], R.L. McCarthy[150], T.G. McCarthy[103], L.I. McClymont[81], E.F. McDonald[91], J.A. Mcfayden[81], G. Mchedlidze[57], S.J. McMahon[133], P.C. McNamara[91], R.A. McPherson[172,n], S. Meehan[140], S. Mehlhase[102], A. Mehta[77], K. Meier[60a], C. Meineck[102], B. Meirose[44], D. Melini[170,af], B.R. Mellado Garcia[147c], M. Melo[146a], F. Meloni[18], S.B. Menary[87], L. Meng[77], X.T. Meng[92], A. Mengarelli[22a,22b], S. Menke[103], E. Meoni[165], S. Mergelmeyer[17], P. Mermod[52], L. Merola[106a,106b], C. Meroni[94a], F.S. Merritt[33], A. Messina[134a,134b], J. Metcalfe[6], A.S. Mete[166], C. Meyer[124], J-P. Meyer[138], J. Meyer[109], H. Meyer Zu Theenhausen[60a], F. Miano[151], R.P. Middleton[133], S. Miglioranzi[53a,53b], L. Mijović[49], G. Mikenberg[175], M. Mikestikova[129], M. Mikuž[78], M. Milesi[91], A. Milic[27], D.W. Miller[33], C. Mills[49], A. Milov[175], D.A. Milstead[148a,148b], A.A. Minaenko[132], Y. Minami[157], I.A. Minashvili[68], A.I. Mincer[112], B. Mindur[41a], M. Mineev[68], Y. Minegishi[157], Y. Ming[176], L.M. Mir[13], K.P. Mistry[124], T. Mitani[174], J. Mitrevski[102], V.A. Mitsou[170], A. Miucci[18], P.S. Miyagawa[141], A. Mizukami[69], J.U. Mjörnmark[84], M. Mlynarikova[131], T. Moa[148a,148b], K. Mochizuki[97], P. Mogg[51], S. Mohapatra[38], S. Molander[148a,148b], R. Moles-Valls[23], R. Monden[71], M.C. Mondragon[93], K. Mönig[45], J. Monk[39], E. Monnier[88], A. Montalbano[150], J. Montejo Berlingen[32], F. Monticelli[74], S. Monzani[94a,94b], R.W. Moore[3], N. Morange[119], D. Moreno[21], M. Moreno Llácer[57],

P. Morettini[53a], S. Morgenstern[32], D. Mori[144], T. Mori[157], M. Morii[59], M. Morinaga[157], V. Morisbak[121], S. Moritz[86], A.K. Morley[152], G. Mornacchi[32], J.D. Morris[79], L. Morvaj[150], P. Moschovakos[10], M. Mosidze[54b], H.J. Moss[141], J. Moss[145,ag], K. Motohashi[159], R. Mount[145], E. Mountricha[27], E.J.W. Moyse[89], S. Muanza[88], R.D. Mudd[19], F. Mueller[103], J. Mueller[127], R.S.P. Mueller[102], T. Mueller[30], D. Muenstermann[75], P. Mullen[56], G.A. Mullier[18], F.J. Munoz Sanchez[87], J.A. Murillo Quijada[19], W.J. Murray[173,133], H. Musheghyan[57], M. Muškinja[78], A.G. Myagkov[132,ah], M. Myska[130], B.P. Nachman[16], O. Nackenhorst[52], K. Nagai[122], R. Nagai[69,ab], K. Nagano[69], Y. Nagasaka[61], K. Nagata[164], M. Nagel[51], E. Nagy[88], A.M. Nairz[32], Y. Nakahama[105], K. Nakamura[69], T. Nakamura[157], I. Nakano[114], R.F. Naranjo Garcia[45], R. Narayan[11], D.I. Narrias Villar[60a], I. Naryshkin[125], T. Naumann[45], G. Navarro[21], R. Nayyar[7], H.A. Neal[92], P.Yu. Nechaeva[98], T.J. Neep[87], A. Negri[123a,123b], M. Negrini[22a], S. Nektarijevic[108], C. Nellist[119], A. Nelson[166], S. Nemecek[129], P. Nemethy[112], A.A. Nepomuceno[26a], M. Nessi[32,ai], M.S. Neubauer[169], M. Neumann[178], R.M. Neves[112], P. Nevski[27], P.R. Newman[19], T. Nguyen Manh[97], R.B. Nickerson[122], R. Nicolaidou[138], J. Nielsen[139], V. Nikolaenko[132,ah], I. Nikolic-Audit[83], K. Nikolopoulos[19], J.K. Nilsen[121], P. Nilsson[27], Y. Ninomiya[157], A. Nisati[134a], R. Nisius[103], T. Nobe[157], Y. Noguchi[71], M. Nomachi[120], I. Nomidis[31], T. Nooney[79], M. Nordberg[32], N. Norjoharuddeen[122], O. Novgorodova[47], S. Nowak[103], M. Nozaki[69], L. Nozka[117], K. Ntekas[166], E. Nurse[81], F. Nuti[91], D.C. O'Neil[144], A.A. O'Rourke[45], V. O'Shea[56], F.G. Oakham[31,d], H. Oberlack[103], T. Obermann[23], J. Ocariz[83], A. Ochi[70], I. Ochoa[38], J.P. Ochoa-Ricoux[34a], S. Oda[73], S. Odaka[69], H. Ogren[64], A. Oh[87], S.H. Oh[48], C.C. Ohm[16], H. Ohman[168], H. Oide[53a,53b], H. Okawa[164], Y. Okumura[157], T. Okuyama[69], A. Olariu[28b], L.F. Oleiro Seabra[128a], S.A. Olivares Pino[49], D. Oliveira Damazio[27], A. Olszewski[42], J. Olszowska[42], A. Onofre[128a,128e], K. Onogi[105], P.U.E. Onyisi[11,x], M.J. Oreglia[33], Y. Oren[155], D. Orestano[136a,136b], N. Orlando[62b], R.S. Orr[161], B. Osculati[53a,53b,*], R. Ospanov[87], G. Otero y Garzon[29], H. Otono[73], M. Ouchrif[137d], F. Ould-Saada[121], A. Ouraou[138], K.P. Oussoren[109], Q. Ouyang[35a], M. Owen[56], R.E. Owen[19], V.E. Ozcan[20a], N. Ozturk[8], K. Pachal[144], A. Pacheco Pages[13], L. Pacheco Rodriguez[138], C. Padilla Aranda[13], S. Pagan Griso[16], M. Paganini[179], F. Paige[27], P. Pais[89], G. Palacino[64], S. Palazzo[40a,40b], S. Palestini[32], M. Palka[41b], D. Pallin[37], E.St. Panagiotopoulou[10], I. Panagoulias[10], C.E. Pandini[83], J.G. Panduro Vazquez[80], P. Pani[148a,148b], S. Panitkin[27], D. Pantea[28b], L. Paolozzi[52], Th.D. Papadopoulou[10], K. Papageorgiou[9], A. Paramonov[6], D. Paredes Hernandez[179], A.J. Parker[75], M.A. Parker[30], K.A. Parker[45], F. Parodi[53a,53b], J.A. Parsons[38], U. Parzefall[51], V.R. Pascuzzi[161], E. Pasqualucci[134a], S. Passaggio[53a], Fr. Pastore[80], S. Pataraia[178], J.R. Pater[87], T. Pauly[32], J. Pearce[172], B. Pearson[115], L.E. Pedersen[39], S. Pedraza Lopez[170], R. Pedro[128a,128b], S.V. Peleganchuk[111,c], O. Penc[129], C. Peng[35a], H. Peng[36a], J. Penwell[64], B.S. Peralva[26b], M.M. Perego[138], D.V. Perepelitsa[27], L. Perini[94a,94b], H. Pernegger[32], S. Perrella[106a,106b], R. Peschke[45], V.D. Peshekhonov[68], K. Peters[45], R.F.Y. Peters[87], B.A. Petersen[32], T.C. Petersen[39], E. Petit[58], A. Petridis[1], C. Petridou[156], P. Petroff[119], E. Petrolo[134a], M. Petrov[122], F. Petrucci[136a,136b], N.E. Pettersson[89], A. Peyaud[138], R. Pezoa[34b], P.W. Phillips[133], G. Piacquadio[150], E. Pianori[173], A. Picazio[89], E. Piccaro[79], M.A. Pickering[122], R. Piegaia[29], J.E. Pilcher[33], A.D. Pilkington[87], A.W.J. Pin[87], M. Pinamonti[167a,167c,aj], J.L. Pinfold[3], S. Pires[83], H. Pirumov[45], M. Pitt[175], L. Plazak[146a], M.-A. Pleier[27], V. Pleskot[86], E. Plotnikova[68], D. Pluth[67], P. Podberezko[111], R. Poettgen[148a,148b], L. Poggioli[119], D. Pohl[23], G. Polesello[123a], A. Poley[45], A. Policicchio[40a,40b], R. Polifka[32], A. Polini[22a], C.S. Pollard[56], V. Polychronakos[27], K. Pommès[32], L. Pontecorvo[134a], B.G. Pope[93], G.A. Popeneciu[28c], A. Poppleton[32], S. Pospisil[130], K. Potamianos[16], I.N. Potrap[68], C.J. Potter[30], C.T. Potter[118], G. Poulard[32], J. Poveda[32], V. Pozdnyakov[68], M.E. Pozo Astigarraga[32], P. Pralavorio[88], A. Pranko[16], S. Prell[67], D. Price[87], L.E. Price[6], M. Primavera[76a], S. Prince[90], K. Prokofiev[62c], F. Prokoshin[34b], S. Protopopescu[27], J. Proudfoot[6], M. Przybycien[41a], D. Puddu[136a,136b], M. Purohit[27,ak], P. Puzo[119], J. Qian[92], G. Qin[56], Y. Qin[87], A. Quadt[57], W.B. Quayle[167a,167b], M. Queitsch-Maitland[45], D. Quilty[56], S. Raddum[121], V. Radeka[27], V. Radescu[122], S.K. Radhakrishnan[150], P. Radloff[118], P. Rados[91],

F. Ragusa[94a,94b], G. Rahal[181], J.A. Raine[87], S. Rajagopalan[27], M. Rammensee[32], C. Rangel-Smith[168], M.G. Ratti[94a,94b], D.M. Rauch[45], F. Rauscher[102], S. Rave[86], T. Ravenscroft[56], I. Ravinovich[175], M. Raymond[32], A.L. Read[121], N.P. Readioff[77], M. Reale[76a,76b], D.M. Rebuzzi[123a,123b], A. Redelbach[177], G. Redlinger[27], R. Reece[139], R.G. Reed[147c], K. Reeves[44], L. Rehnisch[17], J. Reichert[124], A. Reiss[86], C. Rembser[32], H. Ren[35a], M. Rescigno[134a], S. Resconi[94a], E.D. Resseguie[124], O.L. Rezanova[111,c], P. Reznicek[131], R. Rezvani[97], R. Richter[103], S. Richter[81], E. Richter-Was[41b], O. Ricken[23], M. Ridel[83], P. Rieck[103], C.J. Riegel[178], J. Rieger[57], O. Rifki[115], M. Rijssenbeek[150], A. Rimoldi[123a,123b], M. Rimoldi[18], L. Rinaldi[22a], B. Ristić[52], E. Ritsch[32], I. Riu[13], F. Rizatdinova[116], E. Rizvi[79], C. Rizzi[13], R.T. Roberts[87], S.H. Robertson[90,n], A. Robichaud-Veronneau[90], D. Robinson[30], J.E.M. Robinson[45], A. Robson[56], C. Roda[126a,126b], Y. Rodina[88,al], A. Rodriguez Perez[13], D. Rodriguez Rodriguez[170], S. Roe[32], C.S. Rogan[59], O. Røhne[121], J. Roloff[59], A. Romaniouk[100], M. Romano[22a,22b], S.M. Romano Saez[37], E. Romero Adam[170], N. Rompotis[77], M. Ronzani[51], L. Roos[83], E. Ros[170], S. Rosati[134a], K. Rosbach[51], P. Rose[139], N.-A. Rosien[57], V. Rossetti[148a,148b], E. Rossi[106a,106b], L.P. Rossi[53a], J.H.N. Rosten[30], R. Rosten[140], M. Rotaru[28b], I. Roth[175], J. Rothberg[140], D. Rousseau[119], A. Rozanov[88], Y. Rozen[154], X. Ruan[147c], F. Rubbo[145], F. Rühr[51], A. Ruiz-Martinez[31], Z. Rurikova[51], N.A. Rusakovich[68], A. Ruschke[102], H.L. Russell[140], J.P. Rutherfoord[7], N. Ruthmann[32], Y.F. Ryabov[125], M. Rybar[169], G. Rybkin[119], S. Ryu[6], A. Ryzhov[132], G.F. Rzehorz[57], A.F. Saavedra[152], G. Sabato[109], S. Sacerdoti[29], H.F-W. Sadrozinski[139], R. Sadykov[68], F. Safai Tehrani[134a], P. Saha[110], M. Sahinsoy[60a], M. Saimpert[138], T. Saito[157], H. Sakamoto[157], Y. Sakurai[174], G. Salamanna[136a,136b], J.E. Salazar Loyola[34b], D. Salek[109], P.H. Sales De Bruin[140], D. Salihagic[103], A. Salnikov[145], J. Salt[170], D. Salvatore[40a,40b], F. Salvatore[151], A. Salvucci[62a,62b,62c], A. Salzburger[32], D. Sammel[51], D. Sampsonidis[156], J. Sánchez[170], V. Sanchez Martinez[170], A. Sanchez Pineda[106a,106b], H. Sandaker[121], R.L. Sandbach[79], M. Sandhoff[178], C. Sandoval[21], D.P.C. Sankey[133], M. Sannino[53a,53b], A. Sansoni[50], C. Santoni[37], R. Santonico[135a,135b], H. Santos[128a], I. Santoyo Castillo[151], K. Sapp[127], A. Sapronov[68], J.G. Saraiva[128a,128d], B. Sarrazin[23], O. Sasaki[69], K. Sato[164], E. Sauvan[5], G. Savage[80], P. Savard[161,d], N. Savic[103], C. Sawyer[133], L. Sawyer[82,s], J. Saxon[33], C. Sbarra[22a], A. Sbrizzi[22a,22b], T. Scanlon[81], D.A. Scannicchio[166], M. Scarcella[152], V. Scarfone[40a,40b], J. Schaarschmidt[140], P. Schacht[103], B.M. Schachtner[102], D. Schaefer[32], L. Schaefer[124], R. Schaefer[45], J. Schaeffer[86], S. Schaepe[23], S. Schaetzel[60b], U. Schäfer[86], A.C. Schaffer[119], D. Schaile[102], R.D. Schamberger[150], V. Scharf[60a], V.A. Schegelsky[125], D. Scheirich[131], M. Schernau[166], C. Schiavi[53a,53b], S. Schier[139], C. Schillo[51], M. Schioppa[40a,40b], S. Schlenker[32], K.R. Schmidt-Sommerfeld[103], K. Schmieden[32], C. Schmitt[86], S. Schmitt[45], S. Schmitz[86], B. Schneider[163a], U. Schnoor[51], L. Schoeffel[138], A. Schoening[60b], B.D. Schoenrock[93], E. Schopf[23], M. Schott[86], J.F.P. Schouwenberg[108], J. Schovancova[8], S. Schramm[52], M. Schreyer[177], N. Schuh[86], A. Schulte[86], M.J. Schultens[23], H.-C. Schultz-Coulon[60a], H. Schulz[17], M. Schumacher[51], B.A. Schumm[139], Ph. Schune[138], A. Schwartzman[145], T.A. Schwarz[92], H. Schweiger[87], Ph. Schwemling[138], R. Schwienhorst[93], J. Schwindling[138], T. Schwindt[23], G. Sciolla[25], F. Scuri[126a,126b], F. Scutti[91], J. Searcy[92], P. Seema[23], S.C. Seidel[107], A. Seiden[139], J.M. Seixas[26a], G. Sekhniaidze[106a], K. Sekhon[92], S.J. Sekula[43], N. Semprini-Cesari[22a,22b], C. Serfon[121], L. Serin[119], L. Serkin[167a,167b], M. Sessa[136a,136b], R. Seuster[172], H. Severini[115], T. Sfiligoj[78], F. Sforza[32], A. Sfyrla[52], E. Shabalina[57], N.W. Shaikh[148a,148b], L.Y. Shan[35a], R. Shang[169], J.T. Shank[24], M. Shapiro[16], P.B. Shatalov[99], K. Shaw[167a,167b], S.M. Shaw[87], A. Shcherbakova[148a,148b], C.Y. Shehu[151], Y. Shen[115], P. Sherwood[81], L. Shi[153,am], S. Shimizu[70], C.O. Shimmin[166], M. Shimojima[104], S. Shirabe[73], M. Shiyakova[68,an], J. Shlomi[175], A. Shmeleva[98], D. Shoaleh Saadi[97], M.J. Shochet[33], S. Shojaii[94a], D.R. Shope[115], S. Shrestha[113], E. Shulga[100], M.A. Shupe[7], P. Sicho[129], A.M. Sickles[169], P.E. Sidebo[149], E. Sideras Haddad[147c], O. Sidiropoulou[177], D. Sidorov[116], A. Sidoti[22a,22b], F. Siegert[47], Dj. Sijacki[14], J. Silva[128a,128d], S.B. Silverstein[148a], V. Simak[130], Lj. Simic[14], S. Simion[119], E. Simioni[86], B. Simmons[81], M. Simon[86], P. Sinervo[161], N.B. Sinev[118], M. Sioli[22a,22b], G. Siragusa[177], I. Siral[92],

S.Yu. Sivoklokov[101], J. Sjölin[148a,148b], M.B. Skinner[75], P. Skubic[115], M. Slater[19], T. Slavicek[130], M. Slawinska[109], K. Sliwa[165], R. Slovak[131], V. Smakhtin[175], B.H. Smart[5], L. Smestad[15], J. Smiesko[146a], S.Yu. Smirnov[100], Y. Smirnov[100], L.N. Smirnova[101,ao], O. Smirnova[84], J.W. Smith[57], M.N.K. Smith[38], R.W. Smith[38], M. Smizanska[75], K. Smolek[130], A.A. Snesarev[98], I.M. Snyder[118], S. Snyder[27], R. Sobie[172,n], F. Socher[47], A. Soffer[155], D.A. Soh[153], G. Sokhrannyi[78], C.A. Solans Sanchez[32], M. Solar[130], E.Yu. Soldatov[100], U. Soldevila[170], A.A. Solodkov[132], A. Soloshenko[68], O.V. Solovyanov[132], V. Solovyev[125], P. Sommer[51], H. Son[165], H.Y. Song[36a,ap], A. Sopczak[130], V. Sorin[13], D. Sosa[60b], C.L. Sotiropoulou[126a,126b], R. Soualah[167a,167c], A.M. Soukharev[111,c], D. South[45], B.C. Sowden[80], S. Spagnolo[76a,76b], M. Spalla[126a,126b], M. Spangenberg[173], F. Spanò[80], D. Sperlich[17], F. Spettel[103], T.M. Spieker[60a], R. Spighi[22a], G. Spigo[32], L.A. Spiller[91], M. Spousta[131], R.D. St. Denis[56,*], A. Stabile[94a], R. Stamen[60a], S. Stamm[17], E. Stanecka[42], R.W. Stanek[6], C. Stanescu[136a], M.M. Stanitzki[45], S. Stapnes[121], E.A. Starchenko[132], G.H. Stark[33], J. Stark[58], S.H Stark[39], P. Staroba[129], P. Starovoitov[60a], S. Stärz[32], R. Staszewski[42], P. Steinberg[27], B. Stelzer[144], H.J. Stelzer[32], O. Stelzer-Chilton[163a], H. Stenzel[55], G.A. Stewart[56], J.A. Stillings[23], M.C. Stockton[90], M. Stoebe[90], G. Stoicea[28b], P. Stolte[57], S. Stonjek[103], A.R. Stradling[8], A. Straessner[47], M.E. Stramaglia[18], J. Strandberg[149], S. Strandberg[148a,148b], A. Strandlie[121], M. Strauss[115], P. Strizenec[146b], R. Ströhmer[177], D.M. Strom[118], R. Stroynowski[43], A. Strubig[108], S.A. Stucci[27], B. Stugu[15], N.A. Styles[45], D. Su[145], J. Su[127], S. Suchek[60a], Y. Sugaya[120], M. Suk[130], V.V. Sulin[98], S. Sultansoy[4c], T. Sumida[71], S. Sun[59], X. Sun[3], K. Suruliz[151], C.J.E. Suster[152], M.R. Sutton[151], S. Suzuki[69], M. Svatos[129], M. Swiatlowski[33], S.P. Swift[2], I. Sykora[146a], T. Sykora[131], D. Ta[51], K. Tackmann[45], J. Taenzer[155], A. Taffard[166], R. Tafirout[163a], N. Taiblum[155], H. Takai[27], R. Takashima[72], T. Takeshita[142], Y. Takubo[69], M. Talby[88], A.A. Talyshev[111,c], J. Tanaka[157], M. Tanaka[159], R. Tanaka[119], S. Tanaka[69], R. Tanioka[70], B.B. Tannenwald[113], S. Tapia Araya[34b], S. Tapprogge[86], S. Tarem[154], G.F. Tartarelli[94a], P. Tas[131], M. Tasevsky[129], T. Tashiro[71], E. Tassi[40a,40b], A. Tavares Delgado[128a,128b], Y. Tayalati[137e], A.C. Taylor[107], G.N. Taylor[91], P.T.E. Taylor[91], W. Taylor[163b], P. Teixeira-Dias[80], K.K. Temming[51], D. Temple[144], H. Ten Kate[32], P.K. Teng[153], J.J. Teoh[120], F. Tepel[178], S. Terada[69], K. Terashi[157], J. Terron[85], S. Terzo[13], M. Testa[50], R.J. Teuscher[161,n], T. Theveneaux-Pelzer[88], J.P. Thomas[19], J. Thomas-Wilsker[80], P.D. Thompson[19], A.S. Thompson[56], L.A. Thomsen[179], E. Thomson[124], M.J. Tibbetts[16], R.E. Ticse Torres[88], V.O. Tikhomirov[98,aq], Yu.A. Tikhonov[111,c], S. Timoshenko[100], P. Tipton[179], S. Tisserant[88], K. Todome[159], S. Todorova-Nova[5], J. Tojo[73], S. Tokár[146a], K. Tokushuku[69], E. Tolley[59], L. Tomlinson[87], M. Tomoto[105], L. Tompkins[145,ar], K. Toms[107], B. Tong[59], P. Tornambe[51], E. Torrence[118], H. Torres[144], E. Torró Pastor[140], J. Toth[88,as], F. Touchard[88], D.R. Tovey[141], C.J. Treado[112], T. Trefzger[177], A. Tricoli[27], I.M. Trigger[163a], S. Trincaz-Duvoid[83], M.F. Tripiana[13], W. Trischuk[161], B. Trocmé[58], A. Trofymov[45], C. Troncon[94a], M. Trottier-McDonald[16], M. Trovatelli[172], L. Truong[167a,167c], M. Trzebinski[42], A. Trzupek[42], K.W. Tsang[62a], J.C-L. Tseng[122], P.V. Tsiareshka[95], G. Tsipolitis[10], N. Tsirintanis[9], S. Tsiskaridze[13], V. Tsiskaridze[51], E.G. Tskhadadze[54a], K.M. Tsui[62a], I.I. Tsukerman[99], V. Tsulaia[16], S. Tsuno[69], D. Tsybychev[150], Y. Tu[62b], A. Tudorache[28b], V. Tudorache[28b], T.T. Tulbure[28a], A.N. Tuna[59], S.A. Tupputi[22a,22b], S. Turchikhin[68], D. Turgeman[175], I. Turk Cakir[4b,at], R. Turra[94a,94b], P.M. Tuts[38], G. Ucchielli[22a,22b], I. Ueda[69], M. Ughetto[148a,148b], F. Ukegawa[164], G. Unal[32], A. Undrus[27], G. Unel[166], F.C. Ungaro[91], Y. Unno[69], C. Unverdorben[102], J. Urban[146b], P. Urquijo[91], P. Urrejola[86], G. Usai[8], J. Usui[69], L. Vacavant[88], V. Vacek[130], B. Vachon[90], C. Valderanis[102], E. Valdes Santurio[148a,148b], N. Valencic[109], S. Valentinetti[22a,22b], A. Valero[170], L. Valery[13], S. Valkar[131], J.A. Valls Ferrer[170], W. Van Den Wollenberg[109], P.C. Van Der Deijl[109], H. van der Graaf[109], N. van Eldik[154], P. van Gemmeren[6], J. Van Nieuwkoop[144], I. van Vulpen[109], M.C. van Woerden[109], M. Vanadia[134a,134b], W. Vandelli[32], R. Vanguri[124], A. Vaniachine[160], P. Vankov[109], G. Vardanyan[180], R. Vari[134a], E.W. Varnes[7], C. Varni[53a,53b], T. Varol[43], D. Varouchas[83], A. Vartapetian[8], K.E. Varvell[152], J.G. Vasquez[179], G.A. Vasquez[34b], F. Vazeille[37],

T. Vazquez Schroeder[90], J. Veatch[57], V. Veeraraghavan[7], L.M. Veloce[161], F. Veloso[128a,128c], S. Veneziano[134a], A. Ventura[76a,76b], M. Venturi[172], N. Venturi[161], A. Venturini[25], V. Vercesi[123a], M. Verducci[136a,136b], W. Verkerke[109], J.C. Vermeulen[109], M.C. Vetterli[144,d], O. Viazlo[84], I. Vichou[169,*], T. Vickey[141], O.E. Vickey Boeriu[141], G.H.A. Viehhauser[122], S. Viel[16], L. Vigani[122], M. Villa[22a,22b], M. Villaplana Perez[94a,94b], E. Vilucchi[50], M.G. Vincter[31], V.B. Vinogradov[68], A. Vishwakarma[45], C. Vittori[22a,22b], I. Vivarelli[151], S. Vlachos[10], M. Vlasak[130], M. Vogel[178], P. Vokac[130], G. Volpi[126a,126b], M. Volpi[91], H. von der Schmitt[103], E. von Toerne[23], V. Vorobel[131], K. Vorobev[100], M. Vos[170], R. Voss[32], J.H. Vossebeld[77], N. Vranjes[14], M. Vranjes Milosavljevic[14], V. Vrba[130], M. Vreeswijk[109], R. Vuillermet[32], I. Vukotic[33], P. Wagner[23], W. Wagner[178], H. Wahlberg[74], S. Wahrmund[47], J. Wakabayashi[105], J. Walder[75], R. Walker[102], W. Walkowiak[143], V. Wallangen[148a,148b], C. Wang[35b], C. Wang[36b,au], F. Wang[176], H. Wang[16], H. Wang[3], J. Wang[45], J. Wang[152], Q. Wang[115], R. Wang[6], S.M. Wang[153], T. Wang[38], W. Wang[36a], C. Wanotayaroj[118], A. Warburton[90], C.P. Ward[30], D.R. Wardrope[81], A. Washbrook[49], P.M. Watkins[19], A.T. Watson[19], M.F. Watson[19], G. Watts[140], S. Watts[87], B.M. Waugh[81], S. Webb[86], M.S. Weber[18], S.W. Weber[177], S.A. Weber[31], J.S. Webster[6], A.R. Weidberg[122], B. Weinert[64], J. Weingarten[57], C. Weiser[51], H. Weits[109], P.S. Wells[32], T. Wenaus[27], T. Wengler[32], S. Wenig[32], N. Wermes[23], M.D. Werner[67], P. Werner[32], M. Wessels[60a], J. Wetter[165], K. Whalen[118], N.L. Whallon[140], A.M. Wharton[75], A. White[8], M.J. White[1], R. White[34b], D. Whiteson[166], F.J. Wickens[133], W. Wiedenmann[176], M. Wielers[133], C. Wiglesworth[39], L.A.M. Wiik-Fuchs[23], A. Wildauer[103], F. Wilk[87], H.G. Wilkens[32], H.H. Williams[124], S. Williams[109], C. Willis[93], S. Willocq[89], J.A. Wilson[19], I. Wingerter-Seez[5], F. Winklmeier[118], O.J. Winston[151], B.T. Winter[23], M. Wittgen[145], M. Wobisch[82,s], T.M.H. Wolf[109], R. Wolff[88], M.W. Wolter[42], H. Wolters[128a,128c], S.D. Worm[133], B.K. Wosiek[42], J. Wotschack[32], M.J. Woudstra[87], K.W. Wozniak[42], M. Wu[58], M. Wu[33], S.L. Wu[176], X. Wu[52], Y. Wu[92], T.R. Wyatt[87], B.M. Wynne[49], S. Xella[39], Z. Xi[92], L. Xia[35c], D. Xu[35a], L. Xu[27], B. Yabsley[152], S. Yacoob[147a], D. Yamaguchi[159], Y. Yamaguchi[120], A. Yamamoto[69], S. Yamamoto[157], T. Yamanaka[157], K. Yamauchi[105], Y. Yamazaki[70], Z. Yan[24], H. Yang[36c], H. Yang[176], Y. Yang[153], Z. Yang[15], W-M. Yao[16], Y.C. Yap[83], Y. Yasu[69], E. Yatsenko[5], K.H. Yau Wong[23], J. Ye[43], S. Ye[27], I. Yeletskikh[68], E. Yildirim[86], K. Yorita[174], R. Yoshida[6], K. Yoshihara[124], C. Young[145], C.J.S. Young[32], S. Youssef[24], D.R. Yu[16], J. Yu[8], J. Yu[67], L. Yuan[70], S.P.Y. Yuen[23], I. Yusuff[30,av], B. Zabinski[42], G. Zacharis[10], R. Zaidan[13], A.M. Zaitsev[132,ah], N. Zakharchuk[45], J. Zalieckas[15], A. Zaman[150], S. Zambito[59], D. Zanzi[91], C. Zeitnitz[178], M. Zeman[130], A. Zemla[41a], J.C. Zeng[169], Q. Zeng[145], O. Zenin[132], T. Ženiš[146a], D. Zerwas[119], D. Zhang[92], F. Zhang[176], G. Zhang[36a,ap], H. Zhang[35b], J. Zhang[6], L. Zhang[51], L. Zhang[36a], M. Zhang[169], R. Zhang[23], R. Zhang[36a,au], X. Zhang[36b], Y. Zhang[35a], Z. Zhang[119], X. Zhao[43], Y. Zhao[36b,aw], Z. Zhao[36a], A. Zhemchugov[68], J. Zhong[122], B. Zhou[92], C. Zhou[176], L. Zhou[43], M. Zhou[35a], M. Zhou[150], N. Zhou[35c], C.G. Zhu[36b], H. Zhu[35a], J. Zhu[92], Y. Zhu[36a], X. Zhuang[35a], K. Zhukov[98], A. Zibell[177], D. Zieminska[64], N.I. Zimine[68], C. Zimmermann[86], S. Zimmermann[51], Z. Zinonos[103], M. Zinser[86], M. Ziolkowski[143], L. Živković[14], G. Zobernig[176], A. Zoccoli[22a,22b], M. zur Nedden[17], L. Zwalinski[32].

[1] Department of Physics, University of Adelaide, Adelaide, Australia
[2] Physics Department, SUNY Albany, Albany NY, United States of America
[3] Department of Physics, University of Alberta, Edmonton AB, Canada
[4] [(a)] Department of Physics, Ankara University, Ankara; [(b)] Istanbul Aydin University, Istanbul; [(c)] Division of Physics, TOBB University of Economics and Technology, Ankara, Turkey
[5] LAPP, CNRS/IN2P3 and Université Savoie Mont Blanc, Annecy-le-Vieux, France
[6] High Energy Physics Division, Argonne National Laboratory, Argonne IL, United States of America
[7] Department of Physics, University of Arizona, Tucson AZ, United States of America
[8] Department of Physics, The University of Texas at Arlington, Arlington TX, United States of America

[9] Physics Department, National and Kapodistrian University of Athens, Athens, Greece
[10] Physics Department, National Technical University of Athens, Zografou, Greece
[11] Department of Physics, The University of Texas at Austin, Austin TX, United States of America
[12] Institute of Physics, Azerbaijan Academy of Sciences, Baku, Azerbaijan
[13] Institut de Física d'Altes Energies (IFAE), The Barcelona Institute of Science and Technology, Barcelona, Spain
[14] Institute of Physics, University of Belgrade, Belgrade, Serbia
[15] Department for Physics and Technology, University of Bergen, Bergen, Norway
[16] Physics Division, Lawrence Berkeley National Laboratory and University of California, Berkeley CA, United States of America
[17] Department of Physics, Humboldt University, Berlin, Germany
[18] Albert Einstein Center for Fundamental Physics and Laboratory for High Energy Physics, University of Bern, Bern, Switzerland
[19] School of Physics and Astronomy, University of Birmingham, Birmingham, United Kingdom
[20] [(a)] Department of Physics, Bogazici University, Istanbul; [(b)] Department of Physics Engineering, Gaziantep University, Gaziantep; [(d)] Istanbul Bilgi University, Faculty of Engineering and Natural Sciences, Istanbul,Turkey; [(e)] Bahcesehir University, Faculty of Engineering and Natural Sciences, Istanbul, Turkey, Turkey
[21] Centro de Investigaciones, Universidad Antonio Narino, Bogota, Colombia
[22] [(a)] INFN Sezione di Bologna; [(b)] Dipartimento di Fisica e Astronomia, Università di Bologna, Bologna, Italy
[23] Physikalisches Institut, University of Bonn, Bonn, Germany
[24] Department of Physics, Boston University, Boston MA, United States of America
[25] Department of Physics, Brandeis University, Waltham MA, United States of America
[26] [(a)] Universidade Federal do Rio De Janeiro COPPE/EE/IF, Rio de Janeiro; [(b)] Electrical Circuits Department, Federal University of Juiz de Fora (UFJF), Juiz de Fora; [(c)] Federal University of Sao Joao del Rei (UFSJ), Sao Joao del Rei; [(d)] Instituto de Fisica, Universidade de Sao Paulo, Sao Paulo, Brazil
[27] Physics Department, Brookhaven National Laboratory, Upton NY, United States of America
[28] [(a)] Transilvania University of Brasov, Brasov, Romania; [(b)] Horia Hulubei National Institute of Physics and Nuclear Engineering, Bucharest; [(c)] National Institute for Research and Development of Isotopic and Molecular Technologies, Physics Department, Cluj Napoca; [(d)] University Politehnica Bucharest, Bucharest; [(e)] West University in Timisoara, Timisoara, Romania
[29] Departamento de Física, Universidad de Buenos Aires, Buenos Aires, Argentina
[30] Cavendish Laboratory, University of Cambridge, Cambridge, United Kingdom
[31] Department of Physics, Carleton University, Ottawa ON, Canada
[32] CERN, Geneva, Switzerland
[33] Enrico Fermi Institute, University of Chicago, Chicago IL, United States of America
[34] [(a)] Departamento de Física, Pontificia Universidad Católica de Chile, Santiago; [(b)] Departamento de Física, Universidad Técnica Federico Santa María, Valparaíso, Chile
[35] [(a)] Institute of High Energy Physics, Chinese Academy of Sciences, Beijing; [(b)] Department of Physics, Nanjing University, Jiangsu; [(c)] Physics Department, Tsinghua University, Beijing 100084, China
[36] [(a)] Department of Modern Physics, University of Science and Technology of China, Anhui; [(b)] School of Physics, Shandong University, Shandong; [(c)] Department of Physics and Astronomy, Key Laboratory for Particle Physics, Astrophysics and Cosmology, Ministry of Education; Shanghai Key Laboratory for Particle Physics and Cosmology (SKLPPC), Shanghai Jiao Tong University, Shanghai;, China
[37] Laboratoire de Physique Corpusculaire, Université Clermont Auvergne, Université Blaise Pascal,

CNRS/IN2P3, Clermont-Ferrand, France
[38] Nevis Laboratory, Columbia University, Irvington NY, United States of America
[39] Niels Bohr Institute, University of Copenhagen, Kobenhavn, Denmark
[40] [(a)] INFN Gruppo Collegato di Cosenza, Laboratori Nazionali di Frascati; [(b)] Dipartimento di Fisica, Università della Calabria, Rende, Italy
[41] [(a)] AGH University of Science and Technology, Faculty of Physics and Applied Computer Science, Krakow; [(b)] Marian Smoluchowski Institute of Physics, Jagiellonian University, Krakow, Poland
[42] Institute of Nuclear Physics Polish Academy of Sciences, Krakow, Poland
[43] Physics Department, Southern Methodist University, Dallas TX, United States of America
[44] Physics Department, University of Texas at Dallas, Richardson TX, United States of America
[45] DESY, Hamburg and Zeuthen, Germany
[46] Lehrstuhl für Experimentelle Physik IV, Technische Universität Dortmund, Dortmund, Germany
[47] Institut für Kern- und Teilchenphysik, Technische Universität Dresden, Dresden, Germany
[48] Department of Physics, Duke University, Durham NC, United States of America
[49] SUPA - School of Physics and Astronomy, University of Edinburgh, Edinburgh, United Kingdom
[50] INFN Laboratori Nazionali di Frascati, Frascati, Italy
[51] Fakultät für Mathematik und Physik, Albert-Ludwigs-Universität, Freiburg, Germany
[52] Departement de Physique Nucleaire et Corpusculaire, Université de Genève, Geneva, Switzerland
[53] [(a)] INFN Sezione di Genova; [(b)] Dipartimento di Fisica, Università di Genova, Genova, Italy
[54] [(a)] E. Andronikashvili Institute of Physics, Iv. Javakhishvili Tbilisi State University, Tbilisi; [(b)] High Energy Physics Institute, Tbilisi State University, Tbilisi, Georgia
[55] II Physikalisches Institut, Justus-Liebig-Universität Giessen, Giessen, Germany
[56] SUPA - School of Physics and Astronomy, University of Glasgow, Glasgow, United Kingdom
[57] II Physikalisches Institut, Georg-August-Universität, Göttingen, Germany
[58] Laboratoire de Physique Subatomique et de Cosmologie, Université Grenoble-Alpes, CNRS/IN2P3, Grenoble, France
[59] Laboratory for Particle Physics and Cosmology, Harvard University, Cambridge MA, United States of America
[60] [(a)] Kirchhoff-Institut für Physik, Ruprecht-Karls-Universität Heidelberg, Heidelberg; [(b)] Physikalisches Institut, Ruprecht-Karls-Universität Heidelberg, Heidelberg; [(c)] ZITI Institut für technische Informatik, Ruprecht-Karls-Universität Heidelberg, Mannheim, Germany
[61] Faculty of Applied Information Science, Hiroshima Institute of Technology, Hiroshima, Japan
[62] [(a)] Department of Physics, The Chinese University of Hong Kong, Shatin, N.T., Hong Kong; [(b)] Department of Physics, The University of Hong Kong, Hong Kong; [(c)] Department of Physics and Institute for Advanced Study, The Hong Kong University of Science and Technology, Clear Water Bay, Kowloon, Hong Kong, China
[63] Department of Physics, National Tsing Hua University, Taiwan, Taiwan
[64] Department of Physics, Indiana University, Bloomington IN, United States of America
[65] Institut für Astro- und Teilchenphysik, Leopold-Franzens-Universität, Innsbruck, Austria
[66] University of Iowa, Iowa City IA, United States of America
[67] Department of Physics and Astronomy, Iowa State University, Ames IA, United States of America
[68] Joint Institute for Nuclear Research, JINR Dubna, Dubna, Russia
[69] KEK, High Energy Accelerator Research Organization, Tsukuba, Japan
[70] Graduate School of Science, Kobe University, Kobe, Japan
[71] Faculty of Science, Kyoto University, Kyoto, Japan
[72] Kyoto University of Education, Kyoto, Japan
[73] Department of Physics, Kyushu University, Fukuoka, Japan

[74] Instituto de Física La Plata, Universidad Nacional de La Plata and CONICET, La Plata, Argentina
[75] Physics Department, Lancaster University, Lancaster, United Kingdom
[76] [(a)] INFN Sezione di Lecce; [(b)] Dipartimento di Matematica e Fisica, Università del Salento, Lecce, Italy
[77] Oliver Lodge Laboratory, University of Liverpool, Liverpool, United Kingdom
[78] Department of Experimental Particle Physics, Jožef Stefan Institute and Department of Physics, University of Ljubljana, Ljubljana, Slovenia
[79] School of Physics and Astronomy, Queen Mary University of London, London, United Kingdom
[80] Department of Physics, Royal Holloway University of London, Surrey, United Kingdom
[81] Department of Physics and Astronomy, University College London, London, United Kingdom
[82] Louisiana Tech University, Ruston LA, United States of America
[83] Laboratoire de Physique Nucléaire et de Hautes Energies, UPMC and Université Paris-Diderot and CNRS/IN2P3, Paris, France
[84] Fysiska institutionen, Lunds universitet, Lund, Sweden
[85] Departamento de Fisica Teorica C-15, Universidad Autonoma de Madrid, Madrid, Spain
[86] Institut für Physik, Universität Mainz, Mainz, Germany
[87] School of Physics and Astronomy, University of Manchester, Manchester, United Kingdom
[88] CPPM, Aix-Marseille Université and CNRS/IN2P3, Marseille, France
[89] Department of Physics, University of Massachusetts, Amherst MA, United States of America
[90] Department of Physics, McGill University, Montreal QC, Canada
[91] School of Physics, University of Melbourne, Victoria, Australia
[92] Department of Physics, The University of Michigan, Ann Arbor MI, United States of America
[93] Department of Physics and Astronomy, Michigan State University, East Lansing MI, United States of America
[94] [(a)] INFN Sezione di Milano; [(b)] Dipartimento di Fisica, Università di Milano, Milano, Italy
[95] B.I. Stepanov Institute of Physics, National Academy of Sciences of Belarus, Minsk, Republic of Belarus
[96] Research Institute for Nuclear Problems of Byelorussian State University, Minsk, Republic of Belarus
[97] Group of Particle Physics, University of Montreal, Montreal QC, Canada
[98] P.N. Lebedev Physical Institute of the Russian Academy of Sciences, Moscow, Russia
[99] Institute for Theoretical and Experimental Physics (ITEP), Moscow, Russia
[100] National Research Nuclear University MEPhI, Moscow, Russia
[101] D.V. Skobeltsyn Institute of Nuclear Physics, M.V. Lomonosov Moscow State University, Moscow, Russia
[102] Fakultät für Physik, Ludwig-Maximilians-Universität München, München, Germany
[103] Max-Planck-Institut für Physik (Werner-Heisenberg-Institut), München, Germany
[104] Nagasaki Institute of Applied Science, Nagasaki, Japan
[105] Graduate School of Science and Kobayashi-Maskawa Institute, Nagoya University, Nagoya, Japan
[106] [(a)] INFN Sezione di Napoli; [(b)] Dipartimento di Fisica, Università di Napoli, Napoli, Italy
[107] Department of Physics and Astronomy, University of New Mexico, Albuquerque NM, United States of America
[108] Institute for Mathematics, Astrophysics and Particle Physics, Radboud University Nijmegen/Nikhef, Nijmegen, Netherlands
[109] Nikhef National Institute for Subatomic Physics and University of Amsterdam, Amsterdam, Netherlands
[110] Department of Physics, Northern Illinois University, DeKalb IL, United States of America
[111] Budker Institute of Nuclear Physics, SB RAS, Novosibirsk, Russia

[112] Department of Physics, New York University, New York NY, United States of America
[113] Ohio State University, Columbus OH, United States of America
[114] Faculty of Science, Okayama University, Okayama, Japan
[115] Homer L. Dodge Department of Physics and Astronomy, University of Oklahoma, Norman OK, United States of America
[116] Department of Physics, Oklahoma State University, Stillwater OK, United States of America
[117] Palacký University, RCPTM, Olomouc, Czech Republic
[118] Center for High Energy Physics, University of Oregon, Eugene OR, United States of America
[119] LAL, Univ. Paris-Sud, CNRS/IN2P3, Université Paris-Saclay, Orsay, France
[120] Graduate School of Science, Osaka University, Osaka, Japan
[121] Department of Physics, University of Oslo, Oslo, Norway
[122] Department of Physics, Oxford University, Oxford, United Kingdom
[123] [(a)] INFN Sezione di Pavia; [(b)] Dipartimento di Fisica, Università di Pavia, Pavia, Italy
[124] Department of Physics, University of Pennsylvania, Philadelphia PA, United States of America
[125] National Research Centre "Kurchatov Institute" B.P.Konstantinov Petersburg Nuclear Physics Institute, St. Petersburg, Russia
[126] [(a)] INFN Sezione di Pisa; [(b)] Dipartimento di Fisica E. Fermi, Università di Pisa, Pisa, Italy
[127] Department of Physics and Astronomy, University of Pittsburgh, Pittsburgh PA, United States of America
[128] [(a)] Laboratório de Instrumentação e Física Experimental de Partículas - LIP, Lisboa; [(b)] Faculdade de Ciências, Universidade de Lisboa, Lisboa; [(c)] Department of Physics, University of Coimbra, Coimbra; [(d)] Centro de Física Nuclear da Universidade de Lisboa, Lisboa; [(e)] Departamento de Fisica, Universidade do Minho, Braga; [(f)] Departamento de Fisica Teorica y del Cosmos and CAFPE, Universidad de Granada, Granada (Spain); [(g)] Dep Fisica and CEFITEC of Faculdade de Ciencias e Tecnologia, Universidade Nova de Lisboa, Caparica, Portugal
[129] Institute of Physics, Academy of Sciences of the Czech Republic, Praha, Czech Republic
[130] Czech Technical University in Prague, Praha, Czech Republic
[131] Charles University, Faculty of Mathematics and Physics, Prague, Czech Republic
[132] State Research Center Institute for High Energy Physics (Protvino), NRC KI, Russia
[133] Particle Physics Department, Rutherford Appleton Laboratory, Didcot, United Kingdom
[134] [(a)] INFN Sezione di Roma; [(b)] Dipartimento di Fisica, Sapienza Università di Roma, Roma, Italy
[135] [(a)] INFN Sezione di Roma Tor Vergata; [(b)] Dipartimento di Fisica, Università di Roma Tor Vergata, Roma, Italy
[136] [(a)] INFN Sezione di Roma Tre; [(b)] Dipartimento di Matematica e Fisica, Università Roma Tre, Roma, Italy
[137] [(a)] Faculté des Sciences Ain Chock, Réseau Universitaire de Physique des Hautes Energies - Université Hassan II, Casablanca; [(b)] Centre National de l'Energie des Sciences Techniques Nucleaires, Rabat; [(c)] Faculté des Sciences Semlalia, Université Cadi Ayyad, LPHEA-Marrakech; [(d)] Faculté des Sciences, Université Mohamed Premier and LPTPM, Oujda; [(e)] Faculté des sciences, Université Mohammed V, Rabat, Morocco
[138] DSM/IRFU (Institut de Recherches sur les Lois Fondamentales de l'Univers), CEA Saclay (Commissariat à l'Energie Atomique et aux Energies Alternatives), Gif-sur-Yvette, France
[139] Santa Cruz Institute for Particle Physics, University of California Santa Cruz, Santa Cruz CA, United States of America
[140] Department of Physics, University of Washington, Seattle WA, United States of America
[141] Department of Physics and Astronomy, University of Sheffield, Sheffield, United Kingdom
[142] Department of Physics, Shinshu University, Nagano, Japan

[143] Fachbereich Physik, Universität Siegen, Siegen, Germany
[144] Department of Physics, Simon Fraser University, Burnaby BC, Canada
[145] SLAC National Accelerator Laboratory, Stanford CA, United States of America
[146] [(a)] Faculty of Mathematics, Physics & Informatics, Comenius University, Bratislava; [(b)] Department of Subnuclear Physics, Institute of Experimental Physics of the Slovak Academy of Sciences, Kosice, Slovak Republic
[147] [(a)] Department of Physics, University of Cape Town, Cape Town; [(b)] Department of Physics, University of Johannesburg, Johannesburg; [(c)] School of Physics, University of the Witwatersrand, Johannesburg, South Africa
[148] [(a)] Department of Physics, Stockholm University; [(b)] The Oskar Klein Centre, Stockholm, Sweden
[149] Physics Department, Royal Institute of Technology, Stockholm, Sweden
[150] Departments of Physics & Astronomy and Chemistry, Stony Brook University, Stony Brook NY, United States of America
[151] Department of Physics and Astronomy, University of Sussex, Brighton, United Kingdom
[152] School of Physics, University of Sydney, Sydney, Australia
[153] Institute of Physics, Academia Sinica, Taipei, Taiwan
[154] Department of Physics, Technion: Israel Institute of Technology, Haifa, Israel
[155] Raymond and Beverly Sackler School of Physics and Astronomy, Tel Aviv University, Tel Aviv, Israel
[156] Department of Physics, Aristotle University of Thessaloniki, Thessaloniki, Greece
[157] International Center for Elementary Particle Physics and Department of Physics, The University of Tokyo, Tokyo, Japan
[158] Graduate School of Science and Technology, Tokyo Metropolitan University, Tokyo, Japan
[159] Department of Physics, Tokyo Institute of Technology, Tokyo, Japan
[160] Tomsk State University, Tomsk, Russia, Russia
[161] Department of Physics, University of Toronto, Toronto ON, Canada
[162] [(a)] INFN-TIFPA; [(b)] University of Trento, Trento, Italy, Italy
[163] [(a)] TRIUMF, Vancouver BC; [(b)] Department of Physics and Astronomy, York University, Toronto ON, Canada
[164] Faculty of Pure and Applied Sciences, and Center for Integrated Research in Fundamental Science and Engineering, University of Tsukuba, Tsukuba, Japan
[165] Department of Physics and Astronomy, Tufts University, Medford MA, United States of America
[166] Department of Physics and Astronomy, University of California Irvine, Irvine CA, United States of America
[167] [(a)] INFN Gruppo Collegato di Udine, Sezione di Trieste, Udine; [(b)] ICTP, Trieste; [(c)] Dipartimento di Chimica, Fisica e Ambiente, Università di Udine, Udine, Italy
[168] Department of Physics and Astronomy, University of Uppsala, Uppsala, Sweden
[169] Department of Physics, University of Illinois, Urbana IL, United States of America
[170] Instituto de Fisica Corpuscular (IFIC) and Departamento de Fisica Atomica, Molecular y Nuclear and Departamento de Ingeniería Electrónica and Instituto de Microelectrónica de Barcelona (IMB-CNM), University of Valencia and CSIC, Valencia, Spain
[171] Department of Physics, University of British Columbia, Vancouver BC, Canada
[172] Department of Physics and Astronomy, University of Victoria, Victoria BC, Canada
[173] Department of Physics, University of Warwick, Coventry, United Kingdom
[174] Waseda University, Tokyo, Japan
[175] Department of Particle Physics, The Weizmann Institute of Science, Rehovot, Israel
[176] Department of Physics, University of Wisconsin, Madison WI, United States of America

[177] Fakultät für Physik und Astronomie, Julius-Maximilians-Universität, Würzburg, Germany
[178] Fakultät für Mathematik und Naturwissenschaften, Fachgruppe Physik, Bergische Universität Wuppertal, Wuppertal, Germany
[179] Department of Physics, Yale University, New Haven CT, United States of America
[180] Yerevan Physics Institute, Yerevan, Armenia
[181] Centre de Calcul de l'Institut National de Physique Nucléaire et de Physique des Particules (IN2P3), Villeurbanne, France
[a] Also at Department of Physics, King's College London, London, United Kingdom
[b] Also at Institute of Physics, Azerbaijan Academy of Sciences, Baku, Azerbaijan
[c] Also at Novosibirsk State University, Novosibirsk, Russia
[d] Also at TRIUMF, Vancouver BC, Canada
[e] Also at Department of Physics & Astronomy, University of Louisville, Louisville, KY, United States of America
[f] Also at Physics Department, An-Najah National University, Nablus, Palestine
[g] Also at Department of Physics, California State University, Fresno CA, United States of America
[h] Also at Department of Physics, University of Fribourg, Fribourg, Switzerland
[i] Also at Departament de Fisica de la Universitat Autonoma de Barcelona, Barcelona, Spain
[j] Also at Departamento de Fisica e Astronomia, Faculdade de Ciencias, Universidade do Porto, Portugal
[k] Also at Tomsk State University, Tomsk, Russia, Russia
[l] Also at The Collaborative Innovation Center of Quantum Matter (CICQM), Beijing, China
[m] Also at Universita di Napoli Parthenope, Napoli, Italy
[n] Also at Institute of Particle Physics (IPP), Canada
[o] Also at Horia Hulubei National Institute of Physics and Nuclear Engineering, Bucharest, Romania
[p] Also at Department of Physics, St. Petersburg State Polytechnical University, St. Petersburg, Russia
[q] Also at Department of Physics, The University of Michigan, Ann Arbor MI, United States of America
[r] Also at Centre for High Performance Computing, CSIR Campus, Rosebank, Cape Town, South Africa
[s] Also at Louisiana Tech University, Ruston LA, United States of America
[t] Also at Institucio Catalana de Recerca i Estudis Avancats, ICREA, Barcelona, Spain
[u] Also at Graduate School of Science, Osaka University, Osaka, Japan
[v] Also at Fakultät für Mathematik und Physik, Albert-Ludwigs-Universität, Freiburg, Germany
[w] Also at Institute for Mathematics, Astrophysics and Particle Physics, Radboud University Nijmegen/Nikhef, Nijmegen, Netherlands
[x] Also at Department of Physics, The University of Texas at Austin, Austin TX, United States of America
[y] Also at Institute of Theoretical Physics, Ilia State University, Tbilisi, Georgia
[z] Also at CERN, Geneva, Switzerland
[aa] Also at Georgian Technical University (GTU),Tbilisi, Georgia
[ab] Also at Ochadai Academic Production, Ochanomizu University, Tokyo, Japan
[ac] Also at Manhattan College, New York NY, United States of America
[ad] Also at Academia Sinica Grid Computing, Institute of Physics, Academia Sinica, Taipei, Taiwan
[ae] Also at School of Physics, Shandong University, Shandong, China
[af] Also at Departamento de Fisica Teorica y del Cosmos and CAFPE, Universidad de Granada, Granada (Spain), Portugal
[ag] Also at Department of Physics, California State University, Sacramento CA, United States of America
[ah] Also at Moscow Institute of Physics and Technology State University, Dolgoprudny, Russia
[ai] Also at Departement de Physique Nucleaire et Corpusculaire, Université de Genève, Geneva, Switzerland

[aj] Also at International School for Advanced Studies (SISSA), Trieste, Italy
[ak] Also at Department of Physics and Astronomy, University of South Carolina, Columbia SC, United States of America
[al] Also at Institut de Física d'Altes Energies (IFAE), The Barcelona Institute of Science and Technology, Barcelona, Spain
[am] Also at School of Physics, Sun Yat-sen University, Guangzhou, China
[an] Also at Institute for Nuclear Research and Nuclear Energy (INRNE) of the Bulgarian Academy of Sciences, Sofia, Bulgaria
[ao] Also at Faculty of Physics, M.V.Lomonosov Moscow State University, Moscow, Russia
[ap] Also at Institute of Physics, Academia Sinica, Taipei, Taiwan
[aq] Also at National Research Nuclear University MEPhI, Moscow, Russia
[ar] Also at Department of Physics, Stanford University, Stanford CA, United States of America
[as] Also at Institute for Particle and Nuclear Physics, Wigner Research Centre for Physics, Budapest, Hungary
[at] Also at Giresun University, Faculty of Engineering, Turkey
[au] Also at CPPM, Aix-Marseille Université and CNRS/IN2P3, Marseille, France
[av] Also at University of Malaya, Department of Physics, Kuala Lumpur, Malaysia
[aw] Also at LAL, Univ. Paris-Sud, CNRS/IN2P3, Université Paris-Saclay, Orsay, France
[*] Deceased